UNIVERSITÀ DEGLI STUDI DI MILANO

DOCTORAL PROGRAMME IN

INTEGRATED BIOMEDICAL RESEARCH – XXXIII CYCLE

DEPARTMENT OF BIOMEDICAL SCIENCES FOR HEALTH

Scientific Disciplinary Sector ING-INF/06 – Electronic Bioengineering and Informatics

Estimating cardiorespiratory coupling from spontaneous variability in health and pathology

PhD candidate:

Beatrice Cairo

Supervisor: Prof. Alberto Porta

Doctoral Programme Chair: Prof. Chiarella Sforza

Academic Year

2019-2020

UNIVERSITÀ DEGLI STUDI DI MILANO

DOTTORATO DI RICERCA IN

RICERCA BIOMEDICA INTEGRATA – CICLO XXXIII

DIPARTIMENTO DI SCIENZE BIOMEDICHE PER LA SALUTE

Settore Scientifico-Disciplinare ING-INF/06 - Bioingegneria Elettronica e Informatica

Misurare l'accoppiamento cardiorespiratorio dalla variabilità spontanea in soggetti sani e patologici

Dottoranda:

Beatrice Cairo

Supervisore: Prof. Alberto Porta

Coordinatore del Corso di Dottorato: Prof. Chiarella Sforza

A.A.

2019-2020

Abstract

Several mechanisms are responsible for cardiorespiratory interactions observed in humans. The action of these mechanisms results in specific patterns in heart rate variability (HRV) and affects the interaction between heart and respiratory activities. The four main types of phenomena resulting from the interactions between heart and respiratory system are: i) respiratory sinus arrhythmia (RSA); ii) cardioventilatory coupling; iii) cardiorespiratory phase synchronization; iv) cardiorespiratory frequency synchronization.

The aim of this thesis is to describe and quantify different aspects of cardiorespiratory interactions employing a variety of methods from literature, adapted and optimized for the usual experimental settings in which HRV and respiratory signal are commonly acquired. Six analytical methods were exploited for this purpose assessing transfer entropy (TE), cross-conditional entropy via normalized corrected cross-conditional entropy (NCCCE), squared coherence (K^2), cardioventilatory coupling via normalized Shannon entropy (NSE) of the time interval between QRS complex and inspiratory, or expiratory, onsets, phase synchronization via a synchronization index (SYNC%) and pulse-respiration quotient (PRQ). These approaches were employed with the goal of testing the effects of a sympathetic challenge, namely postural stimuli like head-up tilt (TILT) and active standing (STAND), on cardiorespiratory interactions.

The proposed approaches were tested on three protocols: i) amateur athletes undergoing an inspiratory muscle training (IMT) during supine rest (REST) and STAND; ii) healthy volunteers undergoing a prolonged bed rest deconditioning (HDBR), during REST and TILT; iii) patients suffering from postural orthostatic tachycardia syndrome (POTS), during REST and TILT, at baseline and at one-year follow-up.

The most important findings of the present doctoral thesis concern the effect of postural stimuli on cardiorespiratory interactions in health and disease. Indeed, all proposed indexes gave a coherent view of cardiorespiratory interaction strength in response to the orthostatic challenge, as it decreased in all protocols. However, the statistical power of the indexes was different. TE and K^2 appeared to be particularly weak in detecting the effect of postural challenge on cardiorespiratory interactions. NCCCE, NSE and SYNC% exhibited much stronger ability in this regard, while PRQ seemed too closely related to heart rate, in presence of no significant modification of the respiratory rate. Conversely, all indexes appeared to be weak in detecting the chronic effects of IMT and HDBR on a healthy population and the long-term consequences of the clinical management in POTS patients. The thesis concludes that the different aspects of cardiorespiratory interactions can be modified acutely but the chronic effects of a long-term treatment or intervention on the magnitude of cardiorespiratory interactions are negligible and/or could be confused with the variability of markers.

Considerations about the methodological dissimilarities and differences in effectiveness of the proposed indexes suggest that the simultaneous exploitation of all bivariate methodologies in cardiorespiratory studies is advantageous, as different aspects of cardiorespiratory interactions can be evaluated concurrently. This simultaneous evaluation can be carried out with a relatively negligible computational cost and in applicative contexts when only an ECG signal is available.

Sommario

Molteplici meccanismi sono responsabili delle interazioni cardiorespiratorie osservate nell'uomo. L'azione di questi meccanismi risulta in specifici ritmi di variabilità cardiaca (HRV) e ha effetti sulle interazioni tra attività cardiaca e respiratoria. I quattro principali tipi di fenomeni che derivano dalle interazioni tra cuore e sistema respiratorio sono: i) aritmia respiratoria sinusale (RSA); ii) accoppiamento cardioventilatorio; iii) sincronizzazione cardiorespiratoria in fase; iv) sincronizzazione cardiorespiratoria in frequenza.

L'obiettivo di questa tesi è la descrizione e quantificazione di diversi aspetti delle interazioni cardiorespiratorie tramite l'utilizzo di una varietà di metodologie derivate dalla letteratura, adattate e ottimizzate per i tipici contesti sperimentali in cui HRV e segnale respiratorio sono comunemente acquisiti. Sei metodi analitici sono stati sfruttati a questo scopo per valutare l'entropia di trasferimento (TE), l'entropia cross-condizionata tramite entropia corretta cross-condizionata normalizzata (NCCCE), la coerenza quadratica (K^2), l'accoppiamento cardioventilatorio tramite entropia normalizzata di Shannon (NSE) dell'intervallo temporale tra complesso QRS e inizio di fase inspiratoria o espiratoria, la sincronizzazione in fase tramite un indice di sincronizzazione (SYNC%) e il quoziente pulsazione-respirazione (PRQ). Questi approcci sono stati utilizzati con la finalità di testare gli effetti di uno stimolo simpatico, ovvero stimoli posturali quali l'head-up tilt (TILT) e l'ortostatismo attivo (STAND) sulle interazioni cardiorespiratorie.

Gli approcci proposti sono stati testati in tre protocolli: i) atleti amatoriali sottoposti a un allenamento muscolare inspiratorio (IMT) durante clinostatismo supino (REST) e STAND; ii) volontari sani sottoposti a un decondizionamento da allettamento prolungato (HDBR), durante REST e TILT; iii) pazienti affetti da sindrome da tachicardia posturale ortostatica (POTS), durante REST e TILT, in condizione basale e durante approfondimento un anno dopo.

I risultati principali della presente tesi di dottorato concernono l'effetto degli stimoli posturali sulle interazioni cardiorespiratorie in soggetti sani e patologici. Infatti, tutti gli indici proposti danno una visione coerente dell'intensità dell'interazione cardiorespiratoria in risposta a uno stimolo ortostatico, in quanto essa diminuisce in tutti i protocolli. Tuttavia, il potere statistico degli indici è differente. TE e K^2 appaiono essere particolarmente deboli nell'identificare l'effetto dello stimolo posturale sulle interazioni cardiorespiratorie. NCCCE, NSE, e SYNC% dimostrano una capacità molto maggiore a tale riguardo, mentre PRQ appare troppo intimamente collegata alla frequenza cardiaca, in assenza di cambiamenti significativi della frequenza respiratoria. Per contro, tutti gli indici appaiono deboli nell'identificare gli effetti cronici di IMT e HDBR in una popolazione sana o le conseguenze croniche della gestione clinica in pazienti POTS. La tesi conclude che diversi aspetti delle interazioni cardiorespiratorie possono essere modificati in modo acuto ma gli effetti cronici di un trattamento o intervento a lungo termine sono irrisori sulla magnitudine delle interazioni cardiorespiratorie e/o possono essere confusi con la variabilità intrinseca degli indici.

Considerazioni sulle differenze metodologiche e sull'efficacia degli indici proposti suggeriscono che un utilizzo simultaneo di molteplici metodi bivariati è vantaggiosa negli studi cardiorespiratori, in quanto diversi aspetti delle interazioni cardiorespiratorie possono essere valutati contemporaneamente. Questa valutazione simultanea può essere effettuata a un costo computazionale trascurabile e in contesti applicativi in cui il solo segnale ECG è disponibile.

List of Content

List of Figures

List of Tables

List of Abbreviations

ANS = autonomic nervous system

AR = autoregressive model

ARX = autoregressive model with exogenous input

BASELINE = recording after recruitment

bpm = beats per minute

CCCE = corrected CCE

CCE = cross-CE

CE = conditional entropy

CIP = critical inspiratory pressure

E = epinephrine

ECG = electrocardiogram

EXP = expiratory onset

FOLLOW-UP = recording one year after recruitment

HDBR = head-down bed rest

HF = high frequency

HP = heart period

HR = heart rate

HRV = heart rate variability

IMT = inspiratory muscle training

INSP = inspiratory onset

K^2 = squared coherence

MEP = maximal expiratory pressure

MIP = maximal inspiratory pressure

MIP60 = 60% of MIP

NCCCE = normalized CCCE

NCI = normalized complexity index

NE = norepinephrine

NSE = normalized SE

POST = after intervention

POTS = postural orthostatic tachycardia syndrome

PRE = before intervention

PRQ = pulse-respiration quotient

R = respiration

RE = intervals between the R-wave detected on the ECG and the expiratory onset

REST = supine rest

RI = interval between the R-wave detected on the ECG and the inspiratory onset

RR = interval between consecutive ECG R-peaks

RSA = respiratory sinus arrhythmia

SE = Shannon entropy

SHAM = sham inspiratory muscle training

STAND = active standing

SYNC% = synchronization index

TE = transfer entropy

TILT = head-up tilt test

VO_2 = oxygen uptake

CHAPTER 1 - Background

1.1 Introduction

The following chapter begins with a description of the physiological mechanisms governing the interactions between heart and respiratory system (Sect.1.2). The mechanisms are responsible for the phenomena of respiratory sinus arrhythmia, cardioventilatory coupling, cardiorespiratory phase synchronization and frequency synchronization, explained in Sect.1.3. The assessment of these interactions is typically carried out via several signal processing tools which can be defined in various domains. Sect.1.4 describing the known effects of sympathetic modulation on the cardiorespiratory system is also present. The following Sect.1.5 provides a description of orthostatic manoeuvres that can be employed to activate sympathetic control, which in turns dampens or enhances cardiorespiratory interactions: head-up tilt test and active standing. Subsequent sections define protocols and autonomic disorders with chronic effects on cardiovascular control. Specifically, Sect.1.6 describes inspiratory muscle training (IMT), which might have some impact on vagal control, Sect.1.7 exemplifies long-term head-down bed rest (HDBR) as a form of autonomic deconditioning, and Sect.1.8 describes postural orthostatic tachycardia syndrome (POTS), which leads to an important derangement of the sympathetic control. The chapter ends with Sect.1.9, which defines the aims of this doctoral thesis.

1.2 Mechanisms of Cardiorespiratory Interactions

Several mechanisms are responsible for cardiorespiratory interactions observed in humans (Figure 1.1).

The central respiratory drive and the sympathetic and parasympathetic neural activity are generated in the brainstem. In particular, the parasympathetic activity modulates heart rate (HR), while the sympathetic outflow modifies HR, contractility and blood pressure. The modulation of HR and contractility directly affect stroke volume, which in turns influences blood flow to the body and the lungs. Pulmonary blood flow, together with respiration, determines the partial pressures of oxygen and carbon dioxide, which influence the central respiratory drive via peripheral and central chemoreceptors. Systemic blood flow, together with the peripheral resistances, determines arterial blood pressure. In turn, changes in arterial blood pressure sensed through the arterial baroreceptors modulate sympathetic and parasympathetic activity. Furthermore, the central respiratory drive has an inhibitory effect on the parasympathetic nerves during inspiration, specifically the cardiac vagal nerve. The central respiratory drive also directs inspiration, affecting breathing amplitude and frequency through changes in pleural pressure. Respiration in turn influences pulmonary stretch receptor activity, with a direct negative feedback to the parasympathetic nerves via the afferent neural pathway (Elstad et al., 2018).

The action of these mechanisms results in specific patterns in heart rate variability (HRV) and affects the interaction between heart and respiratory activities. In the following sections, this

chapter will focus on four main types of dynamics resulting from the interactions between heart and respiratory system: i) respiratory sinus arrhythmia (RSA), i.e. the respiratory-gated component of HRV (Eckberg, 2003); ii) cardioventilatory coupling, which defines the mutual influence of the respiratory and cardiac cycles onset on each other, leading to a constant temporal relationship between the two (Galletly & Larsen, 1997; Moser et al., 1995); iii) cardiorespiratory phase synchronization, in which the relative phase between heartbeat and inspiratory onset remains constant over brief periods of time (Schäfer et al., 1998); iv) cardiorespiratory frequency synchronization, which occurs when an integer, stable number of heartbeats is present in each respiratory cycle leading to a constant ratio between cardiac and respiratory frequency (Lotrič & Stefanovska, 2000; Moser et al., 1995).

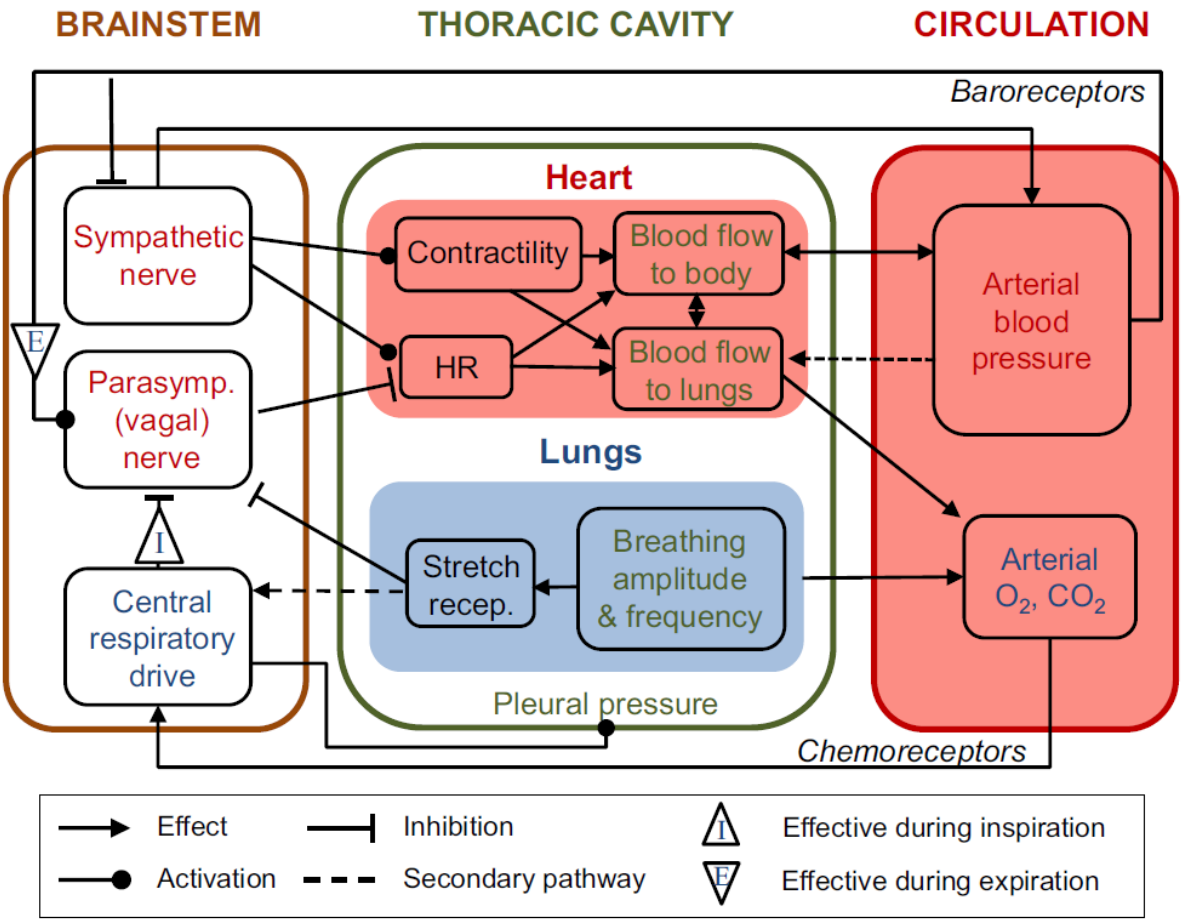

Figure 1.1 Main known mechanisms of cardiorespiratory interaction, from (Elstad et al., 2015).

1.3 Cardiorespiratory Interactions

1.3.1 Respiratory Sinus Arrhythmia

RSA was first observed in terms of increases in HR during inspiration and decreases during expiration, but only with the advent of the computerized cardiology this phenomenon was fully quantified. A graphical representation of this phenomenon is presented in Figure 1.2, which reports the instantaneous variation of HR with respect to its mean as a function of the respiratory phase in a subject during deep sleep. In humans, RSA accounts for a sizeable portion of short-

term HRV at rest (Montano et al., 1994) and is known to be dependent on ageing (Hellman & Stacy, 1976) and physical conditioning (de Abreu et al., 2019; de Meersman, 1992). RSA can also be exaggerated with deep, slow breathing and is related to changes in tidal volume and respiratory frequency (Hirsch & Bishop, 1981). Finally, RSA is closely linked to vagal modulation (Eckberg, 1983; Katona & Jih, 1975), whose magnitude depends on both the tone set by central neural pattern generators and feedback from periphery.

The increase in HR observed during late inspiration is partially the result of the central inspiratory drive which is known to inhibit vagal bradycardia. For example, in rats, severing the efferent pathways from the pontine nuclei supporting the respiratory cycle resulted in the elimination of RSA (Baekey et al., 2008). More specifically, it was recently demonstrated (Farmer et al., 2016) that the Kolliker-Fuse, a nucleus active post-inspiration, has a critical role in the phasic activity of the RSA-driving cardiac vagal motoneurons. Central neural circuits (in particular, those linked to cardiac vagal motoneurons) are also subject to respiratory gating (Baekey et al., 2008; Lopes & Palmer, 1976). However, peripheral feedback circuits must also be taken into account: the activation of pulmonary stretch receptors (mechanoreceptors located in the bronchial smooth muscle) is directly proportional to lung volume. The afferent pathways activated by pulmonary stretch inhibit inspiratory discharge and cause a slowing of respiratory frequency by increasing expiratory time (Hering-Breuer reflex). This mechanism could maintain a considerable portion of the RSA amplitude in humans (Taha et al., 1995). Furthermore, atrial stretch receptors in the right atrium are activated by increases in systemic venous return, which coincide with inspiration. This mechanism causes tachycardia and vasodilatation (Bainbridge reflex). Finally, an indirect, baroreflex-mediated coupling has also been postulated. Indeed, RSA might be partially due to the response of HR to the modulation of arterial pressure by respiration (Karemaker, 2009). More recent studies (Porta et al., 2012) have suggested that the contribution of reflex and baroreflex mediated cardiorespiratory coupling to the overall coupling is significantly smaller than that of the central drive.

Just as the physiological origin of RSA is still being debated, its function is also still under study. While RSA has been traditionally been considered an effect of complex interactions between systems, it has also been postulated to enhance pulmonary gas exchange (Hayano et al., 1996; Hayano & Yasuma, 2003). Other than this physiological function (which is the most studied, if not without controversy (Ben-Tal et al., 2012)), studies have also proposed RSA as a mechanism to improve cardiac efficiency while maintaining physiological levels of arterial carbon dioxide (Ben-Tal et al., 2012) and to stabilize arterial blood pressure and systemic blood flow (Elstad et al., 2001, 2015).

It is however without a doubt that RSA and HRV are marker of cardiovascular health that should be carefully examined in pathological situations and, if possible, restored.

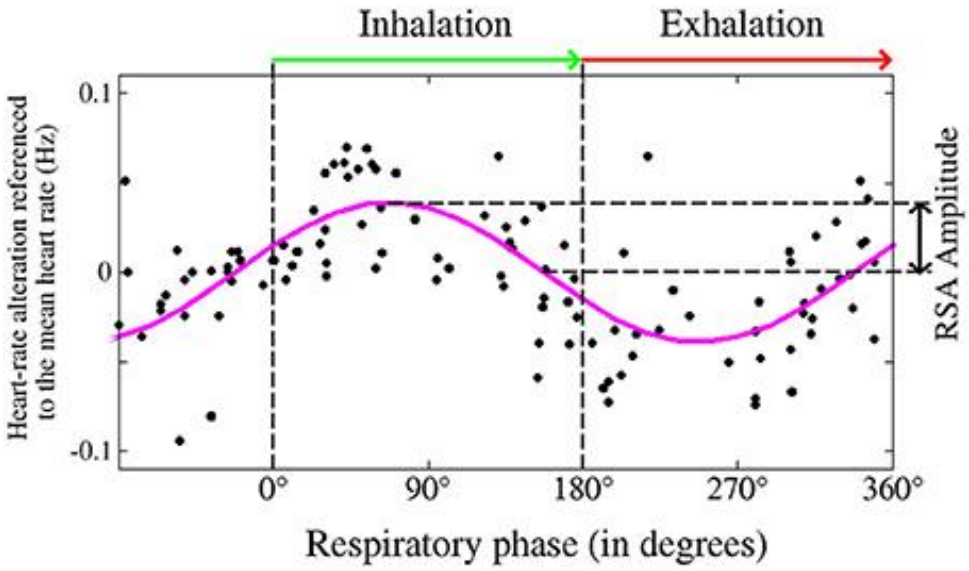

Figure 1.2 The graph, taken from a subject during deep sleep, reports the instantaneous variation of heart rate (HR) with respect to its mean as a function of the respiratory phase (0° = inspiration onset; 180° = expiration onset). The HR trend (magenta plot) shows respiratory sinus arrhythmia (RSA), namely the increase of HR during inspiration (green) and a decrease of HR during expiration (red). Taken from (Penzel et al., 2016).

1.3.2 Cardioventilatory Coupling

Experimental studies have observed that systole usually precedes inspiration onset by 0.15–0.5 seconds (Friedman et al., 2012; Tzeng et al., 2003). This constant temporal relationship between heartbeat and inspiration is now known as cardioventilatory coupling and is thought to be mainly independent from RSA (Friedman et al., 2012; Krause et al., 2017). It is however true that a large amplitude of RSA is linked to a high degree of cardioventilatory coupling (Tzeng et al., 2003). Although cardioventilatory coupling is a weak phenomenon in alert and active human subjects, it is more defined during sedation (Galletly & Larsen, 1997), sleep and in conditions of low cognitive and behavioural activity (Raschke, 1991).

Little is known about what generates cardioventilatory coupling. Tzeng et al. (Tzeng et al., 2003) have proposed that the afferent pathway activated by the stretching of lung receptors could play a role in setting cardioventilatory coupling. This seems to be consistent with results found in mathematical models (McGuinness et al., 2004) and with the speculation that the arterial baroreceptors may be involved in this phenomenon.

The physiological role of cardioventilatory coupling is still under investigation, but studies suggest it may play a part in an efficient oxygen delivery by matching ventilation and perfusion (Friedman et al., 2012) and have a similar role to RSA. It is therefore an aspect of cardiorespiratory interactions that warrants further investigation. The principal methodology that has been proposed to evaluate cardioventilatory coupling assesses the determinism of the temporal latency between heartbeat and fiducial points of the respiratory signal (Galletly & Larsen, 1997; Tzeng et al., 2003), which can be extended to include the two directions of the causal relationship and both inspiratory and expiratory onset (Friedman et al., 2012), although inspiratory onset is usually preferred in literature for its easier delineation on the respiratory

signal. A practical example of this approach is depicted in Figure 1.3, in which the time interval between two consecutive R-wave peaks (RR) is plotted against the RI interval and a certain repeatability can be observed when only taking into consideration the heartbeats following inspiration onset (RI_{+1}).

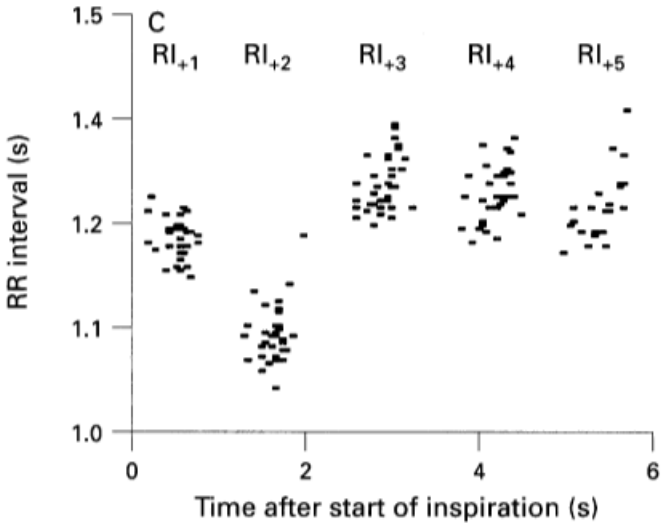

Figure 1.3 Examples of ECG RR interval plotted against time after start of inspiration. Note the relative constancy of the RR interval and time after start of the inspiration, as shown by the limited scattering of points along x- and y-axis, as a function of the heartbeat taken as a reference (i.e., 1, 2, 3, 4 and 5 cardiac beats after the inspiratory onset, namely RI_{+1}, RI_{+2}, RI_{+3}, RI_{+4} and RI_{+5}). Taken from (Galletly & Larsen, 1997).

1.3.3 Cardiorespiratory Phase Synchronization

Biological self-sustained oscillators exhibit the property of adjusting their phases when weakly interacting with each other (Glass & Mackey, 1988). More specifically, cardiorespiratory phase interactions take the form of the occurrence of *n* heartbeats at a relatively constant phase in *m* respiratory cycles. This phenomenon is referred to as *n:m* phase synchronization (Pikovsky et al., 2001). An example of this pattern is reported in Figure 1.4 for a healthy subject during deep sleep, where the occurrence of heartbeats shows clear preferential values within respiratory period.

Cardiorespiratory phase synchronization differs from RSA because the amount of RR changes is not considered. Only the relative position of the heartbeats with the respiratory cycle were monitored. Cardiorespiratory phase synchronization differs from cardioventilatory coupling as it pertains to the evaluation of the phase domain, instead of the time domain. Moreover, in cardiorespiratory phase synchronization the sequence of relative positions of the heartbeat must be repetitive in time, while in the cardioventilatory coupling the repetition is pertaining only to the heartbeats close to the onset or the offset of respiratory cycle. The difference between the two types of interaction is indicated for example by their different dependency on sleep stages: cardiorespiratory phase synchronization increases in deep sleep (Bartsch et al., 2012), while cardioventilatory coupling is maximised in light sleep (Raschke, 1991). Both phenomena, however, are thought to be reduced under stressful conditions (Niizeki & Saitoh, 2012).

Furthermore, phase synchronization can occur independently of RSA: in particular, RSA is linked to respiratory frequency, unlike phase synchronization (Bartsch et al., 2012).

Graphical tools have been devised to represent cardiorespiratory phase synchronization. Among these tools one of the most frequently exploited is the synchrogram, which allows for an efficient visual representation of phase interactions between two oscillatory behaviours (Kenner et al., 1976; Schäfer et al., 1998). This graph is a simple scattergram, plotting the relative phase of *n* heartbeats within an assigned number *m* of respiratory cycles as a function of time or progressive cardiac beat counter. In this format, periods of phase synchronization are highlighted by the formation of horizontal strips. The final effect on the synchrogram is that phase synchronization epochs with visible horizontal strips, visibly differ from periods of uncoupling where the variability of relative phase points about their mean position widens. An example of synchrogram can be found in Figure 1.5 for a healthy subject, where phase synchronization is highlighted in the centre of the plot as five strips of constant phase, in contrast with the more disorganized behaviour before and after.

Previous studies have highlighted a significant cardiorespiratory phase synchronization in healthy subjects in resting condition (Lotrič & Stefanovska, 2000; Schäfer et al., 1998; Toledo et al., 2002). In particular, this phenomenon is more evident during deep sleep (Bartsch et al., 2007, 2012; Jerath et al., 2014; Penzel et al., 2016) and is enhanced by relaxation (Cysarz & Büssing, 2005; Wu & Lo, 2010). Furthermore, phase locking was found to be more frequent during general anaesthesia (Kenwright et al., 2015) and to vary with the mode of mechanical ventilation (Mazzucco et al., 2017).

Phase synchronization, especially in healthy subjects in physiological conditions, has been shown to only occur intermittently and for short periods of times (Ahn & Rubchinsky, 2013; Bartsch et al., 2007, 2012; Penzel et al., 2016; Toledo et al., 2002, 1999). Consequently, the usual procedure is to perform the synchronization analysis over a window with limited length, and then iterating the analysis over the time horizon spanned by the synchrogram. The migration towards weaker phase synchronization regimes, featuring a more infrequent presence, or absence, of phase locked periods, seems to contain some physiological information, given that it occurs systematically in situations characterized by a dominant sympathetic control like the rapid eye movement sleep phase (Bartsch et al., 2007, 2012; Jerath et al., 2014; Penzel et al., 2016) or the execution of mental tasks (J. Zhang et al., 2010). The relevance of the information highlighted by the synchrogram led to the flourishing of automated quantification approaches (Bartsch et al., 2007; Mazzucco et al., 2017; Mrowka et al., 2000; Prokhorov et al., 2003; Rosenblum et al., 2001; Tass et al., 1998; Toledo et al., 2002, 1999; Vejmelka et al., 2009). All these techniques are based on the computation of the generalized phase difference or on the computation of the dispersion of relative phases computed over each identified phase group and then combined together to derive a final synchronization marker (Bettermann et al., 2002; Cysarz et al., 2004; Hamann et al., 2009; Mazzucco et al., 2017; Rosenblum et al., 2001) or calculated after aggregating the *n* groups of phases onto one class via centering (Tass et al., 1998; Toledo et al., 2002, Toledo et al., 1999). All the methods assessing phase variability (Bartsch et al., 2007; Mazzucco et al., 2017; Toledo et al., 2002), regardless of phase dispersion computation approach used (i.e., standard deviation, min-max difference, Shannon entropy, first Fourier mode), compare the final marker with a threshold to

either accept or reject the phase uncoupling hypothesis. The setting of the threshold is critical because the conclusions of a study dramatically depend on thresholding. The most common choice of threshold to assess phase dispersion via standard deviation or min-max difference is $2\pi \cdot m/n \cdot \delta$ with δ=5 (Bartsch et al., 2007; Hamann et al., 2009). This value was optimized in the context of sleep studies in healthy subjects and allowed for the detection of phase synchronization when the phase variability is 5 times more limited than the largest meaningful phase interval assigned a *n:m* phase locking ratio. However, there is no evidence that this value is reliable in all subjects, experimental conditions and pathologies. A more flexible, individualized, strategy for setting the threshold for the detection of phase synchronization assessment might increase the statistical power of the analysis and favour differentiation among groups and/or experimental conditions.

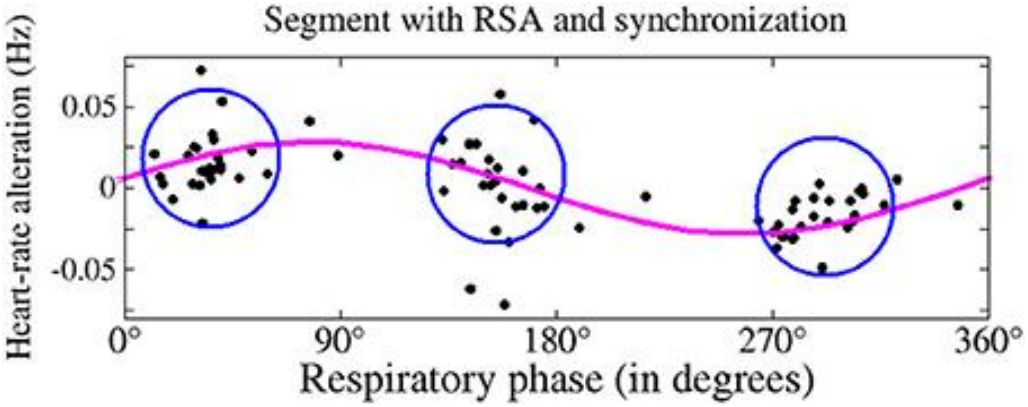

Figure 1.4 The graph, taken from a subject during deep sleep, shows the variation of the instantaneous HR with respect to its mean, as a function of the respiratory phase (0° = inspiration onset; 180° = expiration onset). The plot shows the simultaneous occurrence of respiratory sinus arrhythmia (magenta plot) and cardiorespiratory phase synchronization (blue circles) denoted as the more likely occurrence of heartbeat in specific phases of the respiratory cycle. Taken from (Penzel et al., 2016).

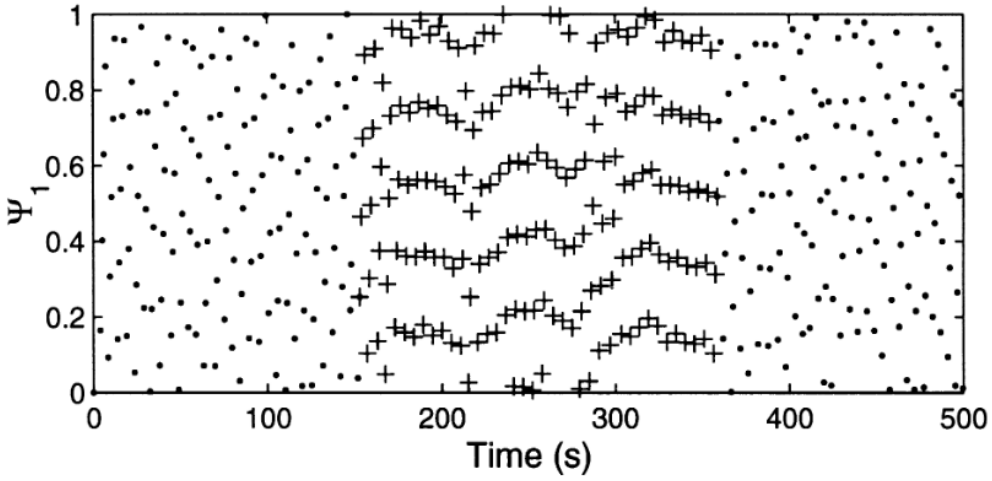

Figure 1.5 Example of cardiorespiratory phase synchronization represented by the synchrogram in a healthy subject. Periods of phase synchronization are detectable due to the formation of horizontal segments, as evident in the central part of the graph. Taken from (Lotrič & Stefanovska, 2000).

1.3.4 Cardiorespiratory Frequency Synchronization

Frequency synchronization occurs when an integer, stable number of heartbeats is present in each respiratory cycle, often with a ratio between 3 and 4 (i.e., a 3:1 or 4:1 synchronization ratio) and is considered to be linked to cardioventilatory coupling (Tzeng et al., 2003). These observations are confirmed in relatively simple mathematical models in which the heart and lungs are seen as two coupled oscillators (Ben-Tal, 2012), which also predict that certain ratios have a greater chance of being found experimentally (McGuinness et al., 2004).

This phenomenon has been observed in anesthetized patients (Galletly & Larsen, 1997) and healthy athletes (Schäfer et al., 1998) and can be observed as either a constant entrainment ratio over time or vary from breath to breath (Galletly & Larsen, 2001). It is worth noting that phase and frequency synchronization do not necessarily occur together (Lotrič & Stefanovska, 2000). An example of the frequency ratio variability between respiratory cycles is reported for a healthy subject in Figure 1.6: a stable relationship between cardiac frequency and respiratory frequency can be observed for the central portion of the recording, where cardiac frequency is fivefold the respiratory frequency.

A simple yet effective index of frequency synchronization termed pulse-respiration quotient (PRQ) has been defined as the ratio between HR expressed as beats per minute and respiratory frequency expressed as breaths per minute. PRQ is usually averaged over a defined time interval (Moser et al., 1995; Scholkmann & Wolf, 2019). This index captures several aspects of cardiorespiratory interactions: indeed, as shown in Figure 1.7, it is susceptible to age, gender and body position, specifically increasing under orthostatic stress.

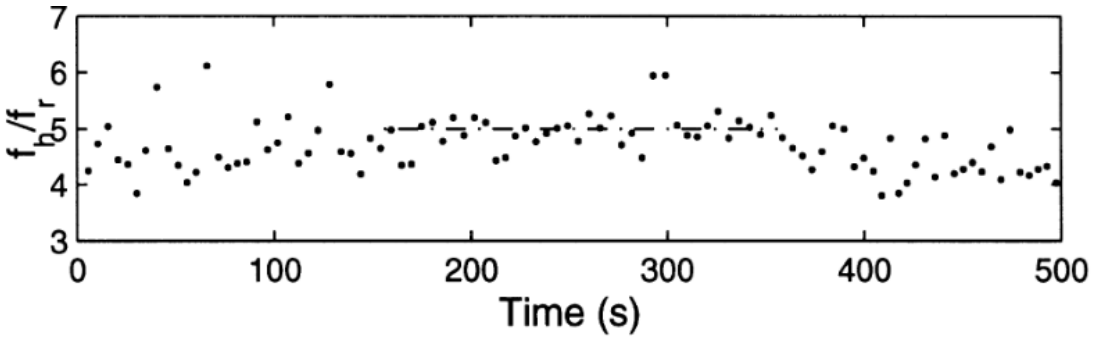

Figure 1.6 Example of frequency synchronization for a healthy subject. The ratio of cardiac frequency f_h to the respiratory rate fr is plotted versus time. Frequency synchronization takes the form of a stable fh/fr ratio over time in the central part of the graph. Taken from (Lotrič & Stefanovska, 2000).

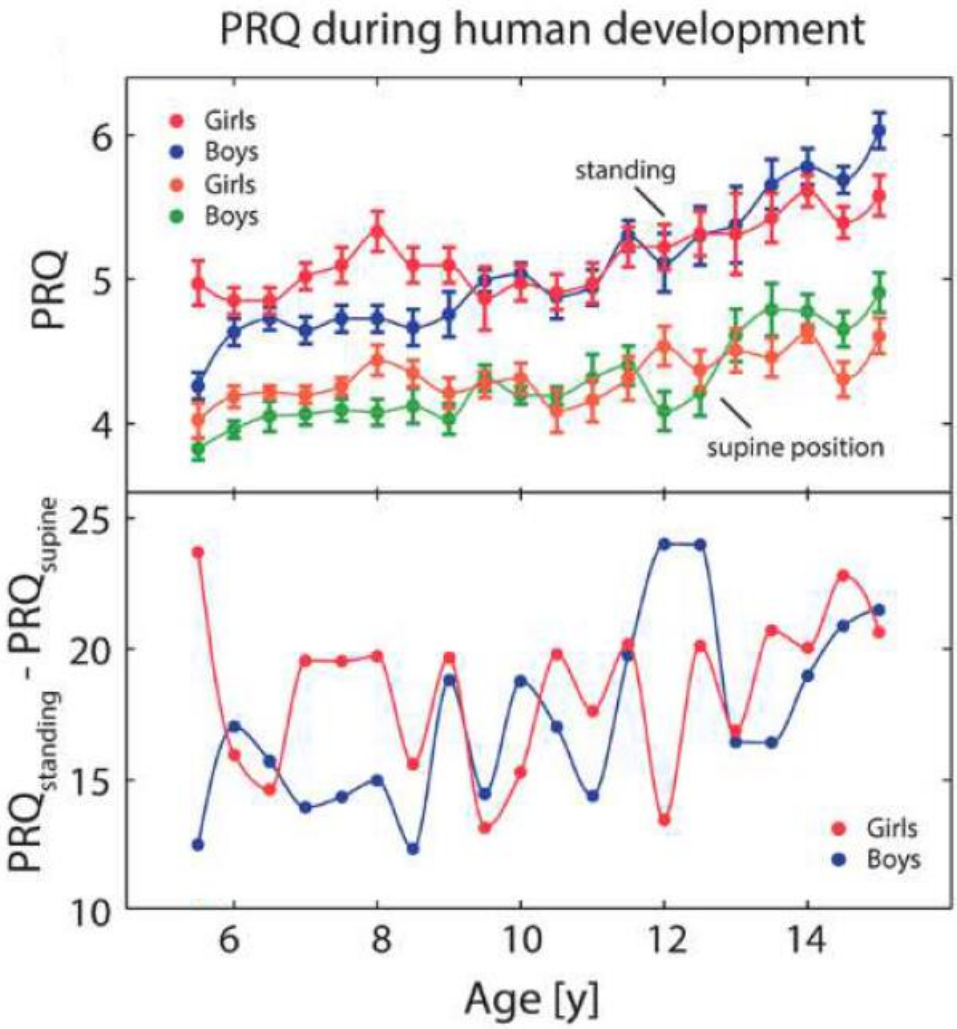

Figure 1.7 Pulse-respiration quotient (PRQ) during human development as a function of age. Trends are given according to gender and posture. Adapted from (Scholkmann & Wolf, 2019).

1.4 Effects of Sympathetic Modulation on Cardiorespiratory Interactions

Previous studies (Cogliati et al., 2004; Porta et al., 2012) have demonstrated that cardiorespiratory interaction gradually decreases during situations of sympathetic activation, while it increases in conditions of low cognitive and behavioural activity, such as quiet sleep (Penzel et al., 2016). From a physiological point of view, this has been attributed to the fact that the sympathetic arm of the autonomic nervous system (ANS) might contribute to the link from respiration to HRV, given that respiratory rhythms are present in sympathetic outflow (Cogliati et al., 2004; Seals et al., 1990) and sympathetic mechanisms may also modulate RSA (Taylor et al., 2001). It is therefore important to assess the changes in cardiorespiratory interactions in health and pathology, under different conditions of sympathetic modulation.

1.5 Head-up Tilt Test and Active Standing

The head-up tilt test (TILT) is used in clinical practice for the diagnosis of autonomic disorders such as vasovagal syncope, orthostatic hypotension, POTS, pure autonomic failure and multiple system atrophy (Bari et al., 2017; Dalla Vecchia et al., 2015; Jones & Gibbons, 2015; Teodorovich & Swissa, 2016; Watano et al., 2018). This is due to the fact that the gravitational stress of the tilting manoeuvre, i.e. the passive transition from a supine position to an upright one, stimulates the ANS (Kenny et al., 1986; Porta et al., 2012). Indeed, TILT is known to induce a sympathetic activation and a vagal withdrawal, needed to prevent the decrease of venous return and cardiac output resulting from the displacement of blood towards the lower part of the body.

Historically, TILT has also been used in research studies on healthy subjects and in pathological populations to study the pathophysiology of the ANS (Furlan et al., 2000; Pagani et al., 1986). In particular, the ANS response from the supine position to a 60-75° inclination of the tilt table is usually assessed, as shown in Figure 1.8, where the RR and respiratory (R) series are reported for a spontaneously breathing subject in supine rest (REST), 45° tilt and 90° tilt. Previous studies have established that cardiorespiratory interaction due to the presence of a direct causal link from R to RR progressively decreases with the increase of the tilt table angle (Porta et al., 2015, 2012; Q. Zhang et al., 2015).

On the other hand, the active standing (STAND) manoeuvre consists in an active transition from a recumbent to an orthostatic position and has also been demonstrated to induce a sympathetic activation and vagal withdrawal as well, even though it is believed to be a postural stimulus less intense than TILT (Lambrecht et al., 2007).

TILT and STAND cannot be considered physiologically equivalent manoeuvres (Kirbiš et al., 2013). This difference seems to be more evident in pathological populations (Plash et al., 2013), while it has been demonstrated that dissimilarities in ANS responses between STAND and TILT after one minute of upright position are negligible in healthy individuals (Tanaka et al., 1996). This is linked to the more powerful involvement of muscle engagement during STAND, favouring peripheral vasoconstriction and limiting the decrease of venous return during postural stimulus.

Since information regarding the effects of TILT and STAND on the various aspects of cardiorespiratory interactions remains lacking, the application of diverse tools developed for cardiorespiratory interaction assessment is warranted.

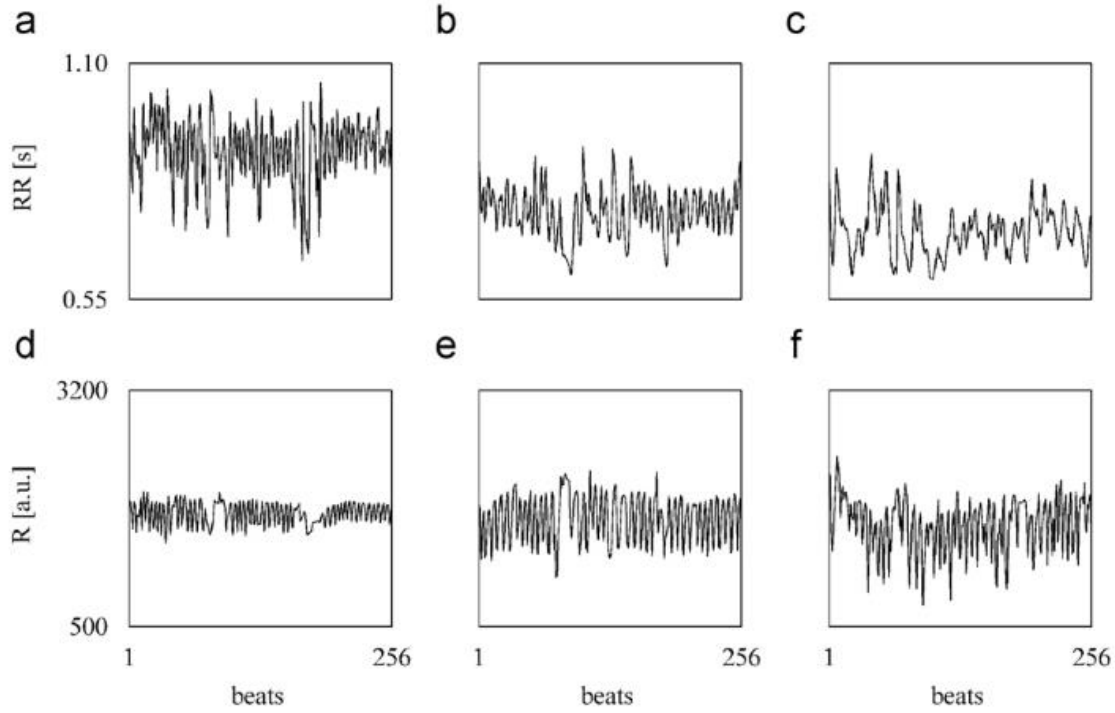

Figure 1.8 Examples of RR variability series and respiration (R) extracted from the ECG and the respiratory signal, under effect of graded TILT. Representative data are reported for a subject breathing spontaneously in the supine position (a,d), in TILT at 45° angle (b,e) and at 90° angle (c,f). Adapted from (Porta et al., 2012).

1.6 Inspiratory Muscle Training

IMT is currently considered a supplementary tool to enhance athletic performance, as it reduces perceived breathlessness and peripheral muscle fatigue, two of the main limitations in physical exercise (de Abreu et al., 2017; Hajghanbari et al., 2013). Furthermore, IMT has been investigated as a method to improve vagal control directed to the sinus node and to lower arterial blood pressure (Ferreira et al., 2013; Mello et al., 2012). Subjects undergoing IMT, in fact, have shown changes in their respiratory patterns, which in turns could potentially affect autonomic regulation: in particular, patients affected by cardiovascular disease have shown an increase in RSA, as indicated by the increase of high frequency (HF) power (0.15-0.5 Hz) component of HRV after low-intensity IMT, i.e. at 30% of maximal inspiratory pressure (MIP) (de Abreu et al., 2017).

However, the effects of low intensity IMT on athletes might be limited compared to sedentary or pathological individuals by a higher basal vagal tone. Higher-intensity IMT protocols have been taken into consideration for this purpose. For example, a novel critical inspiratory pressure (CIP) training protocol was proposed in (Rehder-Santos et al., 2019), consisting in an optimized

training load between 80% and 90% of MIP. Studies (Abreu et al., 2020; de Abreu et al., 2019) suggest that an intermediate IMT intensity, namely at 60% of the MIP (MIP60), might induce bradycardia and an increase in RSA at REST (as shown in Figure 1.9 by the power of the HF component of HRV), while low IMT intensity might only be able to induce a bradycardia at REST. Furthermore, CIP training was found to have no effect on HR at REST, and, conversely, tachycardia appeared during STAND, while the HF power remained unchanged before and after training, as pictured in Figure 1.9.

Since it is expected that IMT could affect directly cardiorespiratory interactions in its various forms, not limited to RSA but also including phase and frequency synchronization, the analysis of the effect of IMT of various intensities on cardiorespiratory interactions might clarify the power of this training in modifying the link between heart and respiratory system.

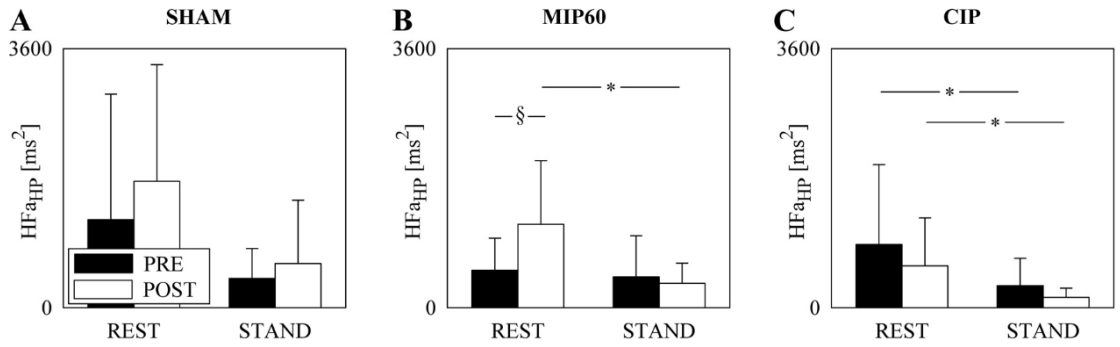

*Figure 1.9 Grouped error bar graphs of high frequency band (HF) power of heart period (HP) series expressed in absolute units (HFa_{HP}) taken as an indicator of vagal modulation, before (PRE, black bars) and after (POST, white bars) IMT, as a function of the experimental condition (i.e., REST and STAND) in the three considered groups, namely SHAM (A), MIP60 (B), and CIP (C). The values are reported as mean+standard deviation. The symbol * indicates statistically significant difference vs. REST within the same training condition (i.e., PRE or POST) with $p<0.05$. § indicates statistically significant difference vs. PRE within the experimental condition (i.e., REST or STAND) with $p<0.05$. Taken from (de Abreu et al., 2019).*

1.7 Prolonged Bed Rest and Head-Down Bed Rest

Bed rest has been used historically as a treatment for managing acute and chronic injury and illness and was particularly emphasized in the 19th century as the primary treatment for many disorders. However, in the 20th century, physicians became increasingly aware of the harmful effects of prolonged bed rest (Dock, 1944). Numerous physiological investigations and clinical observations have since confirmed its deconditioning effect: prolonged bed rest is associated with reductions in effective circulating blood volume and cardiac output (Perhonen et al., 2001), muscular atrophy (particularly of lower limbs), thromboembolism and infections (Allen et al., 1999; McIntyre, 2013). Furthermore, it predisposes patients to hospitalization-associated disability syndrome. Bed rest in the form of HDBR has been frequently implemented in experimental settings to simulate the consequence of microgravity condition experienced by the astronauts in space flights.

In terms of cardiovascular control, orthostatic intolerance and syncope have been observed in various clinical settings as a consequence of deconditioning (Feldstein & Weder, 2012; Guérin et al., 2016), affecting the quality of life and increasing the risk of falls for patients (Juraschek et al., 2017; Shibao et al., 2007). Similar forms of orthostatic intolerance have also been observed in astronauts returning to Earth (Diedrich et al., 2015, 2007; Ertl et al., 2002; Levine et al., 2002), concluding that exposure to microgravity impairs physiological responses to postural challenge, which under normal gravitational conditions can maintain venous return following orthostatic stress.

In a study by Barbic et al. (Barbic et al., 2019), vagal tone was found to be depressed in response to orthostatic stress after a 21-day HDBR, with a concomitant increase in HR. Furthermore, sympathetic efferent activity at the peripheral level was heightened during supine rest due to the deconditioning induced by the prolonged HDBR and orthostatic tolerance was decreased. This effect is depicted in Figure 1.10 as individual and mean values of duration of tilt before appearance of pre-syncope signs and symptoms, where a significant decrease in tolerance can be observed for all subjects. Furthermore, in subsequent studies on the same population (Cairo et al., 2019), sympathetic baroreflex regulation was found to be altered after prolonged HDBR.

It is yet unknown how the modifications in sympathetic tone elicited by prolonged HDBR could potentially impact the different forms of cardiorespiratory interaction.

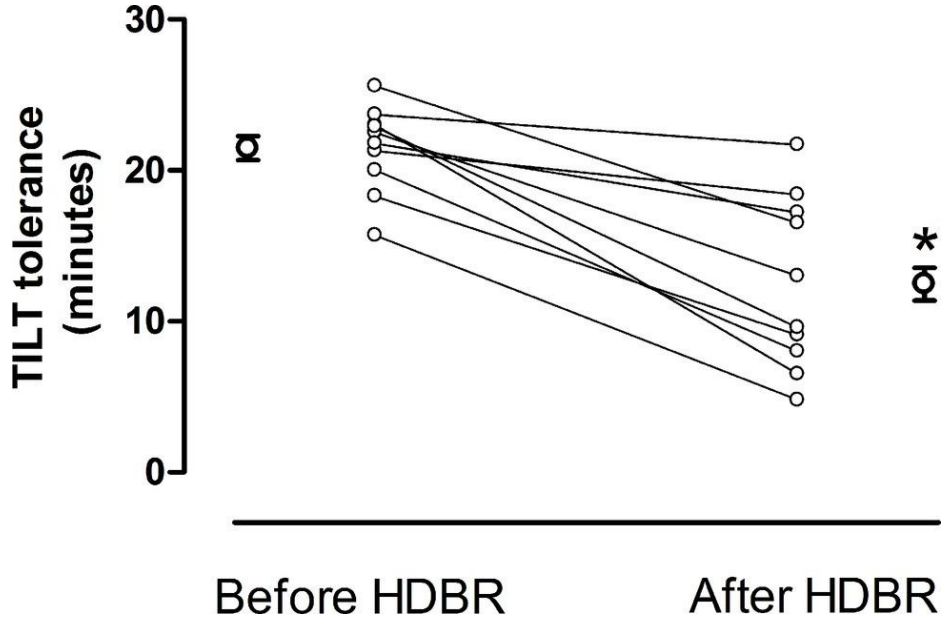

*Figure 1.10 Orthostatic tolerance to 80° head-up tilt before and after 21-day head-down bed rest (HDBR), computed as individual and mean values ± standard error of the time interval before appearance of signs and symptoms of presyncope, expressed in minutes. The symbol * indicates statistically significant difference before and after HDBR with $p<0.05$. Taken from (Barbic et al., 2019).*

1.8 Postural Orthostatic Tachycardia Syndrome

POTS is a cardiovascular autonomic disorder characterized by the following symptomatology presenting itself with a frequent occurrence and a chronic duration (more than 6 months)

(Dipaola et al., 2020; Sheldon et al., 2015): i) an increase in HR of ≥30 beats per minute (bpm) or ≥40 bpm for patients under age 19 and sustained tachycardia (>30 seconds), within 10 minutes of moving from a recumbent to a standing position; ii) absence of orthostatic hypotension (a fall in blood pressure of ≥20/10 mmHg).

Symptoms of cerebral hypoperfusion (i.e., light-headedness, blurred vision, cognitive difficulties, generalized weakness) and sympathetic hyperactivity (i.e., palpitations, chest pain, tremors) are often reported, as well as exercise intolerance and fatigue after standing. These symptoms are relieved by assuming the supine position (Benarroch, 2012). It is common for patients suffering from POTS to faint occasionally, however presyncope is a much more common condition. In addition, many patients experience other symptoms that are not associated with specific postures (Benarroch, 2012), including visceral pain and dysmotility of the bladder and other organs (Thieben et al., 2007), chronic fatigue (Ocon et al., 2012; Okamoto et al., 2012), fibromyalgia (Staud, 2008), sleep disturbances (Bagai et al., 2011; Orjatsalo et al., 2020), joint hypermobility and Ehlers–Danlos syndrome type III (Gazit et al., 2003), migraine and orthostatic headaches (Mokri & Low, 2003). Particularly frequent among POTS patients are gastrointestinal disturbances (abdominal pain, heartburn, irregular bowel movements, diarrhoea, constipation) (Thieben et al., 2007; Wang et al., 2015). Breathlessness is reported in >65% of POTS patients and is usually accompanied by a diagnosis of disordered breathing/ hyperventilation syndrome (Reilly et al., 2020).

No clear cause has been established for this form of dysautonomia, but patients often report symptom onset after an acute stressor like pregnancy, major surgery, or a presumed viral illness (Ruzieh et al., 2017). Likewise, its pathophysiology is still poorly understood and may reflect several distinct mechanisms (Benarroch, 2012), such as autonomic denervation (Kimpinski et al., 2012), autonomic autoimmunity (Ruzieh et al., 2017), hypovolemia (Benarroch, 2012; Kimpinski et al., 2012), hyperadrenergic stimulation (Kimpinski et al., 2012) and deconditioning (Benarroch, 2012).

The prevalence of POTS is estimated to be between 0.2% and 1.0%, affecting up to 3 million people in the United States (Lei et al., 2019), while prevalence in Europe is unknown (Freeman et al., 2011). Most cases arise at a young age (13-50 years old), with a female-to-male ratio of around 5:1 (Lei et al., 2019). Patients are often misdiagnosed, with a median diagnostic delay of 24 months and peaks up to 10 years (Shaw et al., 2019). Both the chronic and usually systemic symptoms and the psychological burden from this pathology can significantly lower quality of life. Furthermore, patients can progressively become physically deconditioned due to orthostatic intolerance, thus reducing their work ability (Barbic et al., 2020), up to, in some cases, becoming wheelchair- or bed-bound (Goldstein et al., 2002). Life expectancy is thought to be unaffected, but disability is considerable and equivalent to that in congestive heart failure and chronic obstructive pulmonary disease (Kavi et al., 2012).

It is known that POTS patients compared to healthy controls of similar age present unique alterations in their cardiovascular control system. These changes are already measurable at a clinical level (Furlan et al., 1998) in the recumbent position, even when patients report a complete absence of symptoms at rest. At baseline, the patients present in fact an increased sympathetic drive to blood vessels and to the sinoatrial node compared to controls, with a concomitant increase in HR. These observations are compatible with the presence of a

hyperadrenergic condition. Under passive orthostatic stress, a blunted vascular sympathetic discharge, with a concomitant exaggerated cardiac sympathetic modulation and excessive increase in HR, is evident (Furlan et al., 1998).

In a study comparing adolescent POTS patients and patients of similar age who presented symptoms indicating dysautonomia but for whom a POTS diagnosis had been excluded (Orjatsalo et al., 2020), vagal tone was found to be attenuated in both groups during TILT, with a significantly higher attenuation in POTS. Furthermore, study subjects suffering from POTS had a significantly lower quality of life.

The abnormalities in autonomic tone in supine resting condition and in response to orthostatism make POTS patients a particularly interesting population to study the effects of sympathetic modulation on cardiorespiratory interactions with different methods capable of capturing the different aspects of the link between heart and respiratory system.

1.9 Thesis Aims

The aim of this thesis is to describe and quantify cardiorespiratory interactions employing different methods from literature, adapted and optimized for the usual experimental settings in which HRV and respiratory signal are commonly acquired. Six analytical methods will be exploited for this purpose assessing transfer entropy (Barnett et al., 2009; Schreiber, 2000), cross-conditional entropy (Porta et al., 1999, 2000), squared coherence (Saul et al., 1991), cardioventilatory coupling (Galletly & Larsen, 1997), phase synchronization (Schäfer et al., 1998) and pulse-respiration quotient (Moser et al., 1995; Scholkmann & Wolf, 2019). These approaches will be employed with the goal of testing the effects of sympathetic activation on cardiorespiratory interactions in three protocols: i) amateur athletes undergoing an IMT during supine REST and active STAND ii) healthy volunteers undergoing a prolonged bed rest deconditioning, during supine REST and TILT iii) patients suffering from dysautonomia (POTS patients), during supine REST and TILT, at baseline and at one-year follow-up.

CHAPTER 2 - Methods

2.1 Introduction

The following chapter describes the methods employed in this thesis. All methods described have been adapted and optimized from literature in order to improve the evaluation of cardiorespiratory interactions in different experimental conditions. The methods will be applied to R and HP (approximated as RR) beat-to-beat series or to inspiratory onset (INSP), expiratory onset (EXP) and R-wave peak event series.

Sect.2.2 describes a method used to evaluate information transfer between R signals and HRV extracted from the electrocardiogram (ECG). The approach computes the transfer entropy (TE), namely the amount of information carried by HRV that can be derived from R above and beyond the amount of information that can be derived from past HP values. The method utilised to compute TE is model-based and fully linear. Sect.2.3 describes an additional information theory method used to quantify the amount of information carried by HRV that cannot be derived from the R series, i.e. cross-conditional entropy (CCE). According to its definition, CCE is completely different from TE. Moreover, the approach followed to calculate CCE is model-free and nonlinear, thus possibly capturing nonlinear dynamics arising from cardiorespiratory interactions. Sect.2.4 describes the squared coherence (K^2) method used to assess the interactions between HRV and the R signal in the frequency domain. The method utilised to compute K^2 is model-based and fully linear. Sect.2.5 lists the cardioventilatory coupling indexes employed to analyse the temporal coordination between heartbeat and the R signal. Sect.2.6 describes the method exploited to quantify cardiorespiratory phase synchronization via the synchrogram and the optimization strategy, proposed in this thesis, allowing the application of the method in an automatic way in real experimental settings. Sect.2.7 illustrates the method exploited to assess frequency synchronization and the PRQ index. The chapter ends with Sect.2.8 providing a summary of all the methods exploited to study cardiorespiratory interactions and the main characteristics of the tools.

2.2 Transfer Entropy

TE assesses the degree of association from a cause signal to an effect one in terms of the amount of information genuinely transferred from the cause to the effect (Schreiber, 2000), namely the amount of information carried by the effect that can be derived from the cause above and beyond the amount of information carried by the effect that can derived exclusively by the past of the effect.

The approach is based on the definition of the restricted universe of knowledge as the set formed by the effect series y and all the possible confounding factors and the full universe of knowledge as the same set, completed by including the presumed cause series x. The TE computes the reduction of information carried by the target signal y when the full universe of knowledge is considered (i.e., including x). Higher values of TE represent a greater causal strength from cause to effect.

In bivariate applications the approach defines the full universe of knowledge as Ω = $\{x,y\}$ and the restricted one after excluding the presumed cause as Ω\x = $\{y\}$. In order to fit the series in Ω, the class of autoregressive (AR) models with exogenous (X) input (ARX) was used (Baselli et al., 1997):

$$y(n) = A(z^{-1}) \cdot y(n) + B(z^{-1}) \cdot x(n) + w(n) \quad (1)$$

where n is the progressive counter $n = 1,2 \dots N$ of the discrete time of the series, $w(n)$ is a zero mean white Gaussian noise, $A(z^{-1})$ and $B(z^{-1})$ are polynomials with constant coefficients and z^{-1} is the unit backward shift operator (i.e., $z^{-1} \cdot y(n) = y(n-1)$) in the Z-domain. The number *p* of the coefficients is the model order.

For Ω\x, an AR model was employed:

$$y(n) = A(z^{-1}) \cdot y(n) + w(n) \quad (2)$$

In the case of cardiorespiratory interactions *x*=R and *y*=RR and the arm from R to RR is investigated.

After normalizing the RR and R series by subtracting their means and dividing by their standard deviations, the model coefficients were identified via traditional least squares approach and Cholesky decomposition method (Baselli et al., 1997). The ARX model order *p* was then optimized for Ω in the range from 8 to 16 according to the Akaike's figure of merit (Akaike, 1974), while the order of the model used for Ω\R was set as equal to the one estimated for Ω (Porta et al., 2015).

Defined the model prediction error as the difference between the current value of the RR series and the prediction provided by the model, the inability of the ARX and AR model to describe the dynamics of the RR series is quantified by the variances of their prediction errors, σ^2_{ARX} and σ^2_{AR} respectively.

The TE from R to RR in Ω, termed $TE_{R \to RR}$, was computed as:

$$TE_{R \to RR} = \frac{1}{2} \log \frac{\sigma^2_{AR}}{\sigma^2_{ARX}} \quad (3)$$

where log is the natural logarithm of the ratio between prediction error variance of RR in Ω\R and that of RR in Ω (Barnett et al., 2009; Porta et al., 2018). $TE_{R \to RR}$ is dimensionless. A graphical representation of the information quantities involved in its calculation are reported in Figure 2.1.

TE is a directional index, i.e. the TE from R to RR is different from the TE from RR to R. The asymmetry property of this function allows a quantification of cardiorespiratory interaction strength in the temporal direction from R to RR, disassociated from the reverse temporal direction.

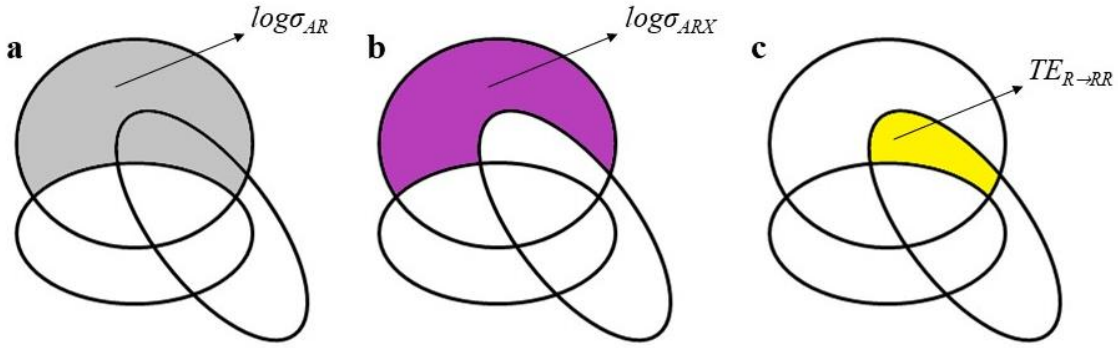

Figure 2.1 Venn diagrams of the information-theoretic quantities involved. The ellipses represent the amount of information carried by y, x and past of y. The filled-in portions represent, respectively, the logarithm of the standard deviation of the prediction error of the autoregressive (AR) model (a), the standard deviation of the prediction error of the AR model with exogenous input (ARX) (b) and the transfer entropy (TE) (c) from respiration (R) to RR interval. x = input, R; y = output, RR.

2.3 Cross-Conditional Entropy

A method that enables the measurement of the strength of the interactions between two signals is the CCE (Porta et al., 1999, 2000). CCE measures the amount of information carried by the effect signal y that cannot be derived from past values (and eventually present) of the cause x. CCE represents the generalization of the conditional entropy (CE) defined over a single signal as the amount of information carried by the signal that cannot be derived from its past (Porta et al., 1998).

After normalizing the two series x and y by subtracting their means and dividing by their standard deviations, the CCE can be computed from the Shannon entropy (SE). The SE of the pattern of length L formed by $y(n)$ and $x_{L-1}(n) = (x(n), \dots, x(n-L+2))$ is defined as

$$SE((y(n), x_{L-1}(n))) = -\sum p\big(y(n), x_{L-1}(n)\big) \cdot \log p\big(y(n), x_{L-1}(n)\big) \qquad 4$$

and the SE of the pattern $x_{L-1}(n)$ as

$$SE\big(x_{L-1}(n)\big) = -\sum p\big(x_{L-1}(n)\big) \cdot \log p\big(x_{L-1}(n)\big) \qquad 5$$

where the summation is performed over all possible combinations of the patterns under consideration, log represents the natural logarithm operator and p is the probability of finding a pattern in a cell obtained after coarse-graining the embedding space via a uniform partition over 6 quantization levels (Porta et al., 1999). CCE can be therefore computed as

$$CCE = SE(y(n), x_{L-1}(n)) - SE(x_{L-1}(n)) \qquad 6$$

as represented in Figure 2.2. At increasing values of L, the CCE tends to zero until a sufficient number of samples of the cause x allows for the complete prediction of the effect y. On the other hand, if the two series x and y are truly independent, the CCE remains high and constant provided that an infinite number of samples are considered. A decrease in CCE indicates that the knowledge of x is partially useful in predicting y.

Unfortunately, CCE always decreases towards zero while increasing L, if it is estimated from a limited number of samples, due to the progressively rougher approximation of the conditional probability by means of the conditional sample frequency while decreasing the number of samples. This bias is particularly limitative when standard partitions are applied to coarse-grain the embedding space (e.g., uniform and nonuniform partitions) (Porta et al., 1999). To limit the impact of this bias a corrective term is therefore introduced, thus leading to the definition of corrected CCE (CCCE). The CCCE is calculated as

$$CCCE\ (L) = CCE(L) + perc_{y/x} \cdot SE(y) \qquad 7$$

where the CCE is calculated with (6) and the corrective term is given by the product of $perc_{y/x}$, i.e. the fraction of $(y(n), x_{L-1}(n))$ patterns found only once in a given cell of the coarse-grained embedding space, and $SE(y)$, i.e. the SE of y regardless of x (Porta et al., 1999). At increasing values of L, CCCE decreases until a minimum is reached, according to the ability of the cause to predict the effect. For higher values of L (i.e., excessively long patterns), CCCE increases to the maximum uncertainty possible. In presence of independent processes CCCE remains high and constant. Finally, CCCE can be normalized, dividing by the estimated $SE(y)$, so that the resulting index is normalized. Thus, the normalized CCCE (NCCCE) is bound between 0 (strong interaction) and 1 (complete uncoupling). The minimum of the NCCCE over the pattern length L is taken as an index of the strength of the interactions between *x* and *y* in the causal direction from *x* to *y* (Porta et al., 2000).

However, studies (Porta et al., 2016) have shown that modifications of the complexity of the target variable might influence causality-based indexes such as NCCCE. It is therefore necessary to normalize such indexes in order to account for the complexity of the target y. The complexity of *y* is computed by applying the (4) to the pattern $(y(n), y_{L-1}(n))$, thus estimating the CE of *y*, given past values of *y*, representing the amount of information carried by the most recent sample of *y* that cannot be derived from previous samples of *y* (Porta et al., 1998). The bias of CE can be corrected as described in (6) when the pattern $(y(n), y_{L-1}(n))$ is considered. The resulting function is termed corrected CE and can be normalized by $SE(y)$ to obtain a function bound between 0, indicating complete regularity of *y*, and 1, denoting maximum complexity of *y* (Porta et al., 1998). The minimum of the normalized corrected CE was taken as normalized complexity index (NCI) (Porta et al., 2000). The ratio of NCCCE to NCI is employed to limit the influence of complexity of the target signal *y* on the residual complexity of *y* given *x* (Porta et al., 2016).

In the case of cardiorespiratory interactions *x*=R and *y*=RR, thus computing the CCCE from R to RR.

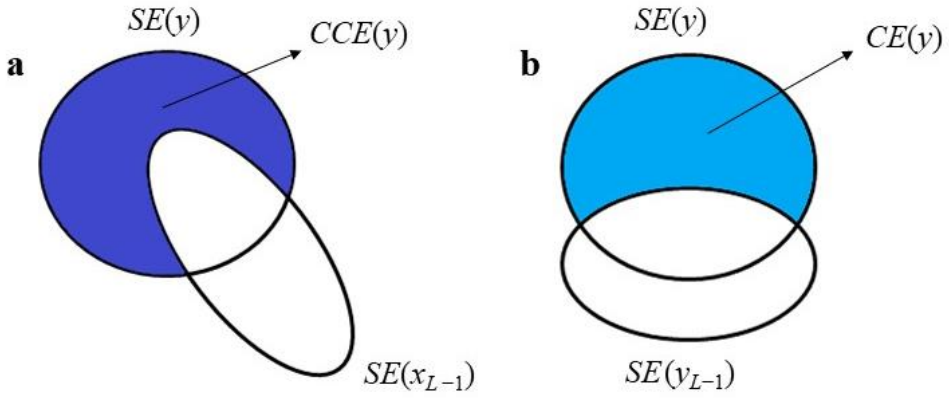

Figure 2.2 Venn diagrams of the information-theoretic quantities involved. The ellipses represent the Shannon entropy (SE) of the x_{L-1}, y_{L-1} and y series. The filled-in portion of the diagrams represents the two calculated quantities, namely cross-conditional entropy (CCE) (a) and conditional entropy (CE) (b). x = input, R; y = output, RR.

2.4 Squared Coherence

The degree of linear coupling between two series can be computed via the traditional definition of squared coherence function K^2. K^2 is a function of the frequency f and is dependent on the squared cross-spectrum modulus between the two series and their respective power spectra. The cross-spectrum and power spectra are estimated according to a parametric approach based on a bivariate AR model:

$$\boldsymbol{y}(n) = \boldsymbol{A}(z) \cdot \boldsymbol{y}(n) + \boldsymbol{w}(n) \qquad 8$$

where $\boldsymbol{y}(n) = (y_1, y_2)^T$ is the column vector of the two series y_1 and y_2 being modelled, $\boldsymbol{w}(t)$ is the column vector of the two white uncorrelated noises and $\boldsymbol{A}(z)$ is the 2x2 matrix that models the causal influence of the past of the processes on themselves (main diagonal) and on each other (antidiagonal) via polynomials with constant coefficients, i.e. $A_{i,j}(z^{-1})$ with i,j=1,2, where z^{-1} is the unit backward shift operator in the Z-domain. The number p of coefficients of the polynomials is the model order. Once the power spectral densities of y_1 and y_2 (defined as $S_{11}(f)$ and $S_{22}(f)$) and their cross-spectral density ($S_{12}(f)$) are estimated from the model, K^2 can be calculated as

$$K^2_{1,2}(f) = \frac{|S_{12}(f)|^2}{S_{11}(f) \cdot S_{22}(f)} \qquad 9$$

where $|\cdot|^2$ indicates the squared modulus operator.

When evaluated at a specific f K^2 can assume values ranging from 0 to 1, where 0 indicates perfect uncorrelation, while 1 indicates full correlation between the two processes y_1 and y_2.

In the context of cardiorespiratory interactions, the two processes are represented by the RR and R series. The coefficients of the model were identified via a traditional least squares method

and the model order *p* was fixed at 10 (Porta et al., 2000). The function $K^2_{RR,R}(f)$ was sampled in correspondence with the respiratory frequency f_R, estimated as the weighted average of the central frequency of the R spectral components in the HF band.

Squared coherence, unlike CCE, cannot account for potential nonlinear forms of interaction. For example, when *n:m* cardiorespiratory dynamics are found (i.e., *n* heartbeats in *m* respiratory cycles), coherence is low because the dominant rhythms of the two oscillators do not have the same frequency. Furthermore, unlike the two previously discussed approaches, $K^2_{RR,R}(f)$ is a symmetric function, independent of the definition of cause and effect. Therefore, high coherence could be due to mechanisms that operate along the R→RR direction or along the RR→R direction or along both directions. Conversely, it is null when RR-R interactions do not occur along either directions.

2.5 Cardioventilatory Coupling

The intervals between the R-wave detected on the ECG and the INSP (or EXP) event were computed, indicated respectively as RI and RE in the following. RI and RE were calculated with respect to the closest R-wave preceding and following INSP and EXP, denoted respectively as RI_{-1}, RE_{-1}, RI_{+1}, and RE_{+1} (Friedman et al., 2012).

The SE of the interval distribution was assessed for each of the four identified interval types over 40 consecutive beats and was calculated as

$$SE = -\sum p_{10}(n) \cdot \log p_{10}(n) \qquad 10$$

where $\log(\cdot)$ represents the natural logarithm operator and p_{10} represents the probability of finding an interval in each of the 10 bins used to coarse-grain the distribution, spanning from 0 to the mean value of RR interval in the recording (Galletly & Larsen, 1999). An example of the resulting histogram p_{10} for the RE_{-1} time interval is given in Figure 2.3.

The SE reaches its maximum when the distribution of the interval is uniform, i.e.

$$SE_{max} = -\log\frac{1}{N} \qquad 11$$

where N is the total number of bins of the distribution (i.e., 10 in the present application). The SE index was normalized by this boundary value, thus obtaining a normalized SE (NSE) (Galletly & Larsen, 1999), ranging from 0 to 1. NSE was averaged over the entire recording. A departure of the resulting NSE from 1 indicates that the RI and RE distributions are not uniform and the heartbeat occurs at some repetitive phase with respect to INSP (or EXP).

The NSE was computed over RI_{-1}, RE_{-1}, RI_{+1}, and RE_{+1}, indicated as NSE_{RI-1}, NSE_{RE-1}, NSE_{RI+1}, and NSE_{RE+1} respectively.

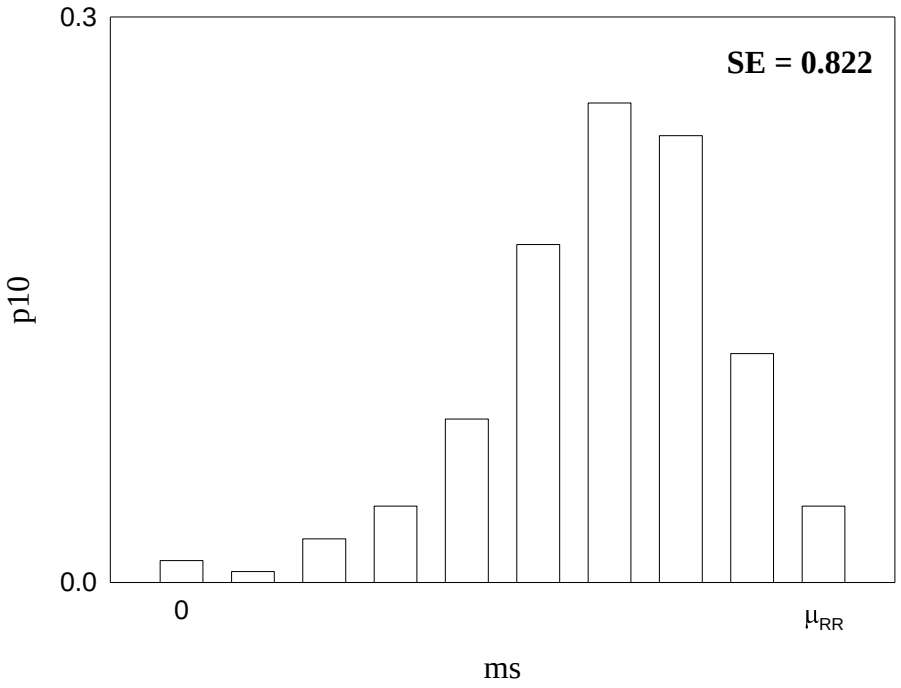

Figure 2.3 Example of probability distribution (p_{10}) of RE_{-1} latencies computed over a healthy subject. μ_{RR} = mean RR value; SE = Shannon Entropy of the distribution.

2.6 Synchrogram

The synchrogram is a graphical tool that allows an efficient visual representation of phase interactions between two oscillatory behaviours (Kenner et al., 1976; Schäfer et al., 1998). This graph is a simple scattergram, plotting the relative phase of *n* heartbeats within an assigned number *m* of respiratory cycles as a function of time or progressive cardiac beat counter. In this graph, periods of phase synchronization are highlighted by the formation of horizontal strips.

2.6.1 Building the synchrogram

The synchrogram was built as described in (Schäfer et al., 1998). The unwrapped instantaneous respiratory phase $\phi_R(t_k)$ was first estimated by adding 2π every new INSP and linearly interpolating the phase values overtime between two consecutive INSP events, thus obtaining a piecewise-linear curve, monotonically increasing with time until the end of the recording session. The unwrapped phase of the *k*-th heartbeat was computed by sampling the unwrapped instantaneous phase $\phi_R(t_k)$ at the time t_k of the *k*-th heartbeat. After assigning the *n:m* ratio, the unwrapped phase of the *k*-th heartbeat was wrapped modulo $2\pi \cdot m$ (i.e., $\psi_H(t_k) = \phi_R(t_k) mod(2\pi \cdot m)$). The synchrogram is built by plotting $\psi_H(t_k)$ as a function of the cardiac beat count *k*, as pictured in Figure 2.4 for an assigned 3:1 ratio, which highlights a segment of phase synchronization in the middle of the scattergram.

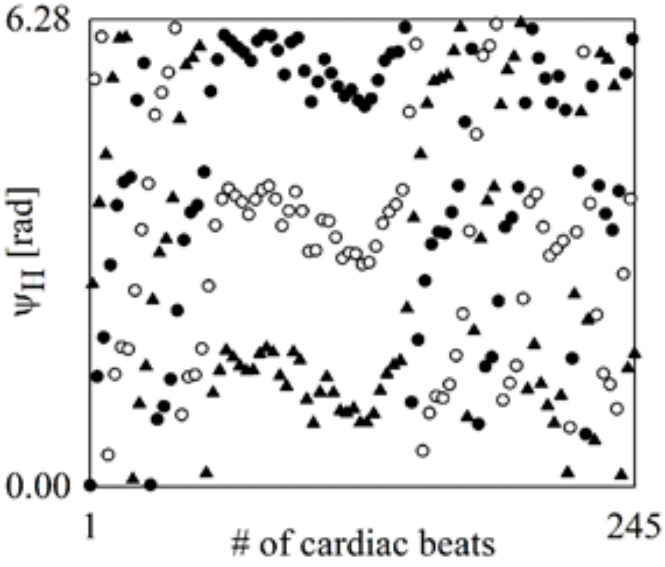

Figure 2.4 The scattergram shows an example of synchrogram. Synchrograms are built according to the n:m ratio assuring the highest value of synchronization (SYNC%), namely 3:1 ratio in the pictured example. The relative phase ψ_H was plotted against the cardiac beat counter using different symbols according to the group of phases it belongs to. Horizontal segments are visible in the central part of the synchrogram. From (Mazzucco et al., 2017).

2.6.2 Assigning the phase locking ratio

The synchrogram is built after assuming a phase locking ratio *n*:*m*. This assumption is necessary to fix the number *m* of cycles of the respiratory activity spanned by the synchrogram and, consequently, the full range of phase values (i.e., from 0 to $2\pi \cdot m$). The assignment of *n* allows the assignment of the number of phase groups considered in the analysis. To limit the number of *n*:*m* ratios to be tested the procedure described in (Cysarz et al., 2004) was followed. Briefly, the starting point was the rounding of the ratio f_H/f_R, where f_H and f_R are the mean heart and respiratory frequencies respectively, i.e. the rounding of the PRQ, to the closest integer n_0. The initial guess of n_0 events per m=1 respiratory cycle allowed the setting of the slowest and fastest rates of driven events per m=1 respiratory cycle. These boundary values corresponded to the simple phase locking ratios (n_0–1):1 and (n_0+1):1. Given these two extremes, all possible *n*:*m* locking ratios were given by varying *n* between (n_0–1)·*m* and (n_0+1)·*m* for any value of *m* with *m*>0. For example, if the f_H/f_R=3.33, then n_0=3 and the limits are 2:1 and 4:1. Therefore, the following ratios were tested: 2:1, 3:1 and 4:1 with *m*=1; 4:2, 5:2, 6:2, 7:2 and 8:2 with *m*=2; 6:3, 7:3, 8:3, 9:3, 10:3, 11:3 and 12:3 with *m*=3, and so on.

2.6.3 Quantitative synchrogram analysis

According to the *n*:*m* phase locking ratio, one phase value every *n* was taken from the entire set of $\psi_H(t_k)$ values in order to attribute each wrapped phase to one of the *n* phase groups. For each defined cluster the difference between the maximum and the minimum $\psi_H(t_k)$ was computed within a window of length L and the maximum difference over the *n* groups was

stored. When computing the maximum phase difference within a group of phases the circularity of phases making 0 and $2\pi \cdot m$ equivalent values was taken into account. The procedure is visualised and detailed in Figure 2.5.

If the maximum difference over the n groups was below a defined phase variability threshold ε, then the null hypothesis of phase desynchronization was rejected over that window. The procedure was reiterated over the entire recording, while moving the window across time in steps of 1 cardiac beat. The percentage of windows where synchronization was detected was computed. This index, labelled as SYNC%, is taken as a marker of the cardiorespiratory phase synchronization strength under the hypothesis that the more frequent the synchronization, the stronger the n:m phase locking regime, as desynchronization periods are less likely. According to (Bartsch et al., 2007; Hamann et al., 2009; Schäfer et al., 1998), the length of the window was set at $L = 2n$.

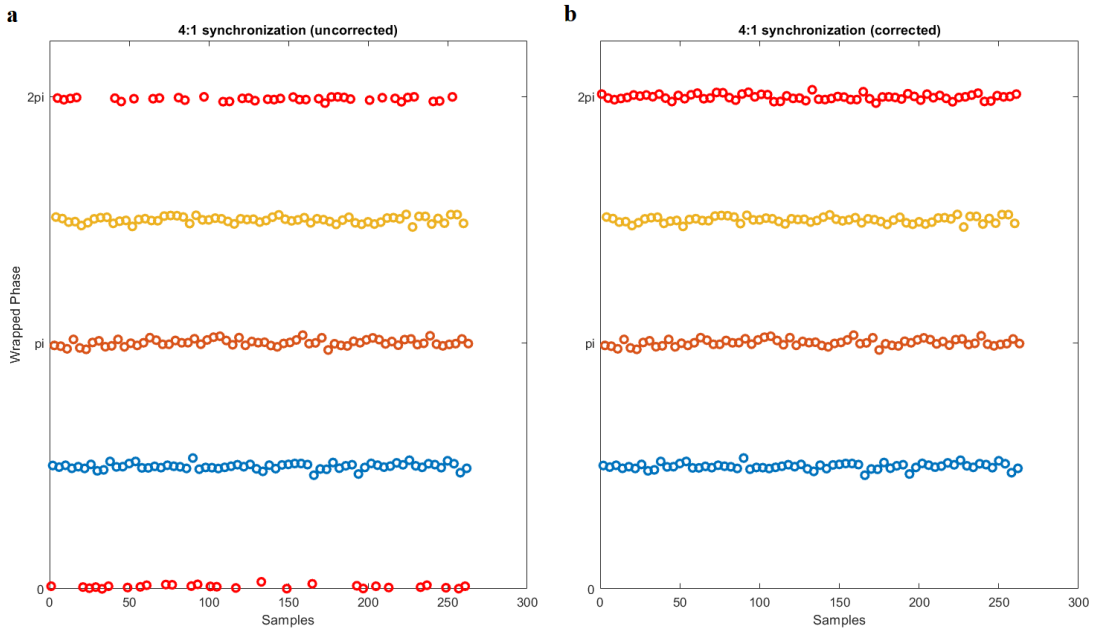

Figure 2.5 Example of synchrograms from a simulation of 4:1 phase synchronization with 3% of white gaussian noise added to illustrate the approach used to correct circularity of phase. Without the correction (a) the first phase group (red) oscillates around the inspiratory onset fiducial point, with a relative phase that assumes values close to 2π or 0, thus creating an artificial desynchronization. After correction (b) all values from the same phase group are correctly clustered together.

2.6.4 Optimizing phase variability threshold

The thresholding procedure is a critical step for the detection of the phase synchronization. Instead of setting the threshold to accept/reject the null hypothesis of phase uncoupling to its most frequently adopted value $\varepsilon = 2\pi \cdot m/\delta \cdot n$ with δ =5, the present thesis proposes an optimization strategy for the setting of the parameter δ, an example of which can be observed in Figure 2.6. Assigned the n:m phase locking ratio, the SYNC% calculation was repeated for δ values varied between 1 and 5 in steps of 0.2, thus starting from the largest value of phase resolution $\varepsilon = 2\pi \cdot m/n$ up to the most commonly adopted value in the cardiorespiratory phase

synchronization studies, namely $\varepsilon = 2\pi \cdot m/\delta \cdot n$ with δ=5. Under the null hypothesis of phase desynchronization, unmatched pairs, formed by associating inspiratory onsets derived from a subject with heartbeat occurrences derived from another subject, were generated (Porta et al., 2018; Schreiber, 2000). All possible unmatched pairs within the same group of subjects and same experimental condition were considered. SYNC% over the unmatched pairs as a function of δ was computed using the same *n*:*m* ratio as in the matched event series. The 95th percentile of SYNC% over the unmatched pairs was calculated at each δ. If the value of SYNC% computed over the matched couple was above the 95th percentile of SYNC% calculated over the unmatched pairs, a significant phase synchronization was detected at that specific value of δ. The optimal value of δ was defined as the one maximizing the distance between the SYNC% curve computed over matched event series and the 95th percentile of SYNC% calculated over the unmatched pairs. The corresponding value of SYNC% over the matched couple was used for all further evaluations. This procedure was repeated for any *n*:*m* phase locking ratio tested in the analysis. If the course of SYNC% computed over matched event series did not exceed the 95th percentile of SYNC% computed over unmatched couples for any value of δ, then the null hypothesis of phase uncoupling was accepted.

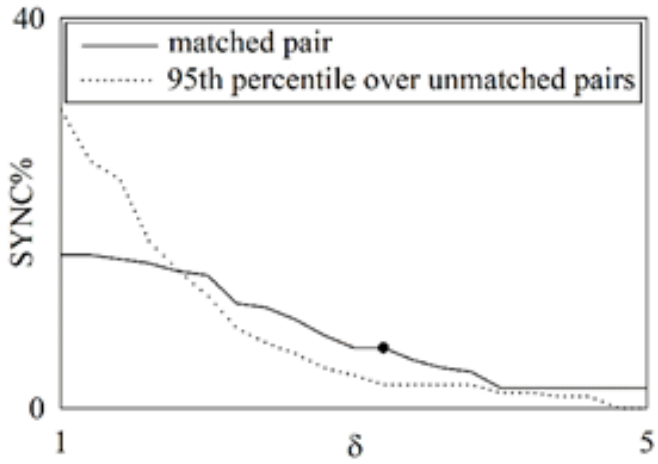

Figure 2.6 Line diagram showing the SYNC% index as a function of phase variability threshold δ. The solid and the dotted lines represent, respectively, SYNC% assessed over the matched pair and to the 95th percentile of SYNC% computed over all the unmatched pairs. SYNC% is computed according to the n:m ratio assuring the highest value of SYNC%, namely 3:1 ratio in the pictured example. The solid black circle indicates the value of SYNC% computed over the matched pair that maximizes over δ the distance between the solid and dotted lines with solid line above the dotted one.

2.7 Frequency synchronization and PRQ

Cardiorespiratory frequency synchronization can be gauged using the PRQ, which is calculated as the ratio between f_H and f_R, measured instantaneously and averaged over a defined time interval (Scholkmann & Wolf, 2019). The estimations of f_H and f_R are obtained, respectively, from the RR interval between two consecutive R-waves detected on the ECG and the mean length of each respiratory cycle, calculated from one inspiratory onset and the next. The resulting index represents the *n:m* synchronization ratio (discussed in the previous sections) when *m* is fixed at 1, i.e. the number of heartbeats occurring in a single respiratory cycle.

2.8 Summary of the tools exploited for cardiorespiratory interaction assessment

In order to characterize an analytical method, four features are taken into consideration.

The first feature considered is whether an approach is model-based or model-free, i.e. whether a model was employed for the calculation of the index or not. Computation of K^2 and TE requires manually choosing *a priori* models and optimizing their parameters based on the time series under analysis, while the other indexes are calculated directly from the data.

The second feature pertains the aspects of interactions investigated by the approaches. Specifically, TE, CCE and K^2 examine bivariate interactions in their totality and are influenced from frequency, amplitude and phase interactions. Cardioventilatory coupling indexes, on the other hand, mainly take into consideration a possible temporal coordination between the two event series under analysis (i.e. the latency between INSP or EXP and preceding or following heartbeat) and, as such, are more related to some specific aspects of phase among event series. Finally, the synchrogram approach and the PRQ represent, respectively, phase and frequency synchronization between the two series.

The third feature account for nonlinear characteristics or only for the linear part of the dynamic, i.e. whether linear relations are at the basis of the computed index. TE, K^2 and PRQ are linear methods because the models underlying their computation account for the statistical moment of order 2, unlike CCE, cardioventilatory coupling or synchrogram analysis that are model-free methods capable of accounting for statistical moments of higher order.

Finally, the fourth feature under investigation is causality. Noncausal methods (i.e. K^2, synchrogram, PRQ) are unable to distinguish the contribution in a given temporal direction to that in the reverse one or to bivariate closed loop interactions. Conversely, causal methods assign a time direction to the interactions, without being influenced by its opposite direction. In the context of the cardiorespiratory system, TE and CCE evaluate the mechanisms along the R→RR pathway, while cardioventilatory coupling can, depending on the index, assess temporal relationships from INSP (or EXP) to the heartbeat or vice versa.

To summarize the methodologies described in this chapter, Table 2.1 reports the main features of each approach, thus highlighting their differences and complementarity.

Table 2.1 Summary of methodologies for cardiorespiratory interaction evaluation applied on all available datasets

Method	Description
Transfer Entropy (Barnett et al., 2009; Schreiber, 2000)	model-based accounts for frequency, amplitude and phase information linear causal (R→RR)
Cross-conditional Entropy (Porta et al., 1999, 2000)	model-free accounts for frequency, amplitude and phase information nonlinear causal (R→RR)
Squared Coherence (Saul et al., 1991)	model-based accounts for frequency, amplitude and phase information linear noncausal (R↔RR)
Cardioventilatory Coupling indexes (Galletly & Larsen, 1997)	model-free assesses temporal coordination and partially accounts for phase and frequency synchronization nonlinear causal (INSP→heartbeat, heartbeat→INSP) causal (EXP→heartbeat, heartbeat→EXP)
Synchrogram (Schäfer et al., 1998)	model-free assesses phase synchronization nonlinear noncausal (INSP↔heartbeat)
Pulse-Respiration Quotient (Scholkmann & Wolf, 2019)	model-free assesses frequency synchronization linear noncausal (R↔RR)

CHAPTER 3 - Experimental Protocols and Data Analysis

3.1 Introduction

At the beginning of this chapter, Sect.3.2 is dedicated to the processing procedure for the extraction of the occurrence of the QRS complexes, respiratory fiducial points (i.e., INSP and EXP events) and resampling respiratory signal on a beat-to-beat basis. In the following sections (i.e., Sects.3.3, 3.4 and 3.5), three different experimental protocols used in the present thesis are detailed: i) 11-week IMT performed on amateur athletes, with assessments before and after training completion in REST and STAND conditions (protocol 1); ii) a 21-day HDBR deconditioning protocol performed on healthy adults, preceded and followed by TILT sessions (protocol 2); iii) patients affected by a form of dysautonomia, namely POTS, undergoing TILT sessions at recruitment and after one year (protocol 3). The chapter ends with Sect.3.6 describing the statistical analysis performed for each experimental protocol.

3.2 Series Extraction

The ECG and R signals recorded across all the experimental protocols were processed to extract, respectively, the occurrence of QRS complexes and timing of INSP and EXP. R-wave peaks were identified on the ECG by a threshold-based algorithm working on the ECG first derivative. The R-wave apex was fixed by means of parabolic interpolation. The time interval between two consecutive R-wave peaks (RR) were taken as an estimate of the heart period (HP). RR was measured over time, thus obtaining the beat-to-beat variability series of RR. Maxima and minima of the R signal were detected by setting a confidence interval about the mean value of the R signal. The amplitude of the confidence interval was defined as a fraction of the difference between a maximum and a minimum chosen graphically over the R signal by the user. Peaks and valleys outside this confidence interval were identified. Their temporal occurrences were taken as EXP and INSP. All the identified fiduciary points (R-wave peaks and INSP and EXP event markers) were visually checked and manually corrected in case of erroneous detections. In the presence of ectopic beats, the series were linearly interpolated using values obtained from normal sinus beats. No more than 5% of corrections were allowed. Furthermore, each acquired R signal was sampled in correspondence of the identified QRS complexes in order to obtain a R series on a beat-to-beat basis synchronous with the RR series.

The inverse of RR (i.e., 1/RR) expressed in bpm was used to estimate the instantaneous HR over time (f_H). f_R was calculated as the inverse of the temporal distance between two consecutive INSP and expressed in breaths per minute.

RR and R series of 256 consecutive values that satisfied the criteria of stationarity (Magagnin et al., 2011) were chosen within each experimental session. Specifically, data were not extracted for analysis within a window of 3 minutes after postural change, in order to account for the non-

stationarities present during this transient period. These series were used to compute TE, CCE, and K^2. The synchrogram was computed directly from the series of the events denoting the position of QRS complexes and INSP events, while cardioventilatory coupling was assessed from both INSP and EXP events in conjunction with the QRS complex events. The PRQ was derived from the RR series and the sequence of the INSP events.

3.3 PROTOCOL 1: Inspiratory Muscle Training in Amateur Athletes

Thirty male recreational cyclists (age: from 20 to 40 years) were followed before (PRE) and after (POST) performing IMT. All the experimental procedures were performed at the Cardiovascular Physical Therapy Laboratory, Department of Physical Therapy, UFSCar, São Carlos, Brazil. Subjects in this longitudinal, randomized, controlled, blind study were allocated in three groups, performing different levels of IMT (de Abreu et al., 2019; Rehder-Santos et al., 2019): i) a SHAM group (n=9) undergoing an IMT of very limited intensity; ii) a group undergoing an IMT at MIP60, namely an intermediate fraction (i.e., 60%) of the MIP (n=10); iii) a group undergoing an IMT of high intensity at CIP (n=11) corresponding to an optimized IMT intensity between 80% and 90% of the maximal inspiratory pressure. The subjects in the three training groups were similar in terms of age, body mass index, MIP and maximal expiratory pressure (MEP) (Rehder-Santos et al., 2019). Mean peak oxygen uptake (peak VO_2) was 41.4 ± 8.8, 47.97 ± 9.0, 49.8 ± 11.8 $mL \cdot (kg \cdot min)^{-1}$, respectively for SHAM, MIP60 and CIP groups.

The subjects performed IMT for 1 hour, 3 days per week, for 11 weeks, using a linear inspiratory loading device (PowerBreathe, Ironman K5, HaB Ltd, UK). The training protocol, randomization, masking procedures and level of blinding are described in more details in (34-36). The training protocol was registered in the ClinicalTrials.gov (NCT02984189). In the PRE and POST sessions, each subject was recorded at REST and during STAND. Specifically, ECG from lead MC5 was acquired via a bioamplifier (BioAmp FE132, ADInstruments, Australia) and R signal was recorded through a piezoelectric thoracic belt (Marazza, Monza, Italy) at a sampling frequency of 1000 Hz (Power Lab 8/35, ADInstruments, Australia) for 15 minutes at REST. Then, the subject was asked to actively assume the upright position and signals were acquired for additional 15 minutes during STAND. The STAND session always followed the REST one. During the acquisition, subjects were instructed to breathe spontaneously and were not allowed to talk.

The study was approved by the Human Research Ethics Committee of UFSCar (Protocol:1.558.731, São Carlos, Brazil). All the included participants provided a written informed consent and the study adhered to the principles of the Declaration of Helsinki for research studies involving humans.

3.4 PROTOCOL 2: Prolonged Head-down Bed Rest in Healthy Adults

Ten healthy male volunteers (age: 33±1 years) were monitored while participating in the European Space Agency Medium-Term Bedrest Study (identified in ClinicalTrials.gov as NCT01655979) (Buehlmeier et al., 2014) taking place at the Institute of Aerospace Medicine, German Aerospace Center, Cologne, Germany. Data acquired during two different

experimental campaigns carried out over the same group of subjects were pooled (Buehlmeier et al., 2014). Lead II ECG (Dual Bio Amp, AD Instruments PtY Ltd, Australia) and R signal using a piezoelectric thoracic belt (Marazza, Monza, Italy) were acquired at 500 Hz for 15 minutes at REST and during 80° TILT.
During TILT, subjects were monitored for symptoms of orthostatic intolerance, such as pallor, light-headedness, blurred vision, sweating and nausea. An increase of HP of more than 80% compared to REST and/or a decrease of systolic arterial pressure of more than 40% were also considered signs of presyncope. When the presyncope condition was achieved, TILT was terminated. If the subject did not exhibit apparent presyncope signs and symptoms, TILT was carried out for 15 minutes.

The protocol was repeated after a physical deconditioning period in which the subject remained in HDBR position at -6° for 21 days (Buehlmeier et al., 2014). After 21-day HDBR, the tilt table inclination was changed directly from -6° to 80° during TILT.

The study was approved by the ethics committee of the Aerztekammer Nordrhein (Approval #2008294, Dusseldorf, Germany), All the included participants provided a written informed consent and the study adhered to the principles of the Declaration of Helsinki for research studies involving humans.

3.5 PROTOCOL 3: Postural Orthostatic Tachycardia Syndrome Patients

Twelve female POTS patients (age: 36±10 years) were instrumented at recruitment (BASELINE) and after one year (FOLLOW-UP), during which they were monitored, and their symptoms managed pharmacologically and/or by inducing lifestyle changes. The subjects underwent recording sessions at REST and during 75° TILT. All the experimental procedures were performed at the Syncope Unit of IRCCS Humanitas Research Hospital, Rozzano, Italy and the study was funded by the Italian Ministry of Health (Grant RF-2013-02355242). Lead II ECG (Dual Bio Amp, AD Instruments PtY Ltd, Australia) and R signal using a piezoelectric thoracic belt (Marazza, Monza, Italy) were continuously recorded for 20 minutes in the REST position and during 15 minutes of TILT. Biological signals were digitized at 400 Hz by an analog-to-digital converter and recorded by a data acquisition system (PowerLab 16/35 and LabChart-pro 8.0 software; ADInstruments Pty Ltd, Australia) for offline analysis. Plasma Norepinephrine (NE) and Epinephrine (E) were assessed after 5 minutes of REST and after 5 minutes of TILT (mean values are reported in Table 3.1 and Table 3.2). All patients were studied during pharmacological wash-out from any drug potentially affecting cardiovascular autonomic control, i.e. betablockers, ivabradine and midodrine, and were asked to refrain from caffeine on the day of the study.

The study was approved by the Ethical Review Board of IRCCS Humanitas Research Hospital (Approval #1611/2016, Rozzano, Italy). All the included participants provided a written informed consent and the study adhered to the principles of the Declaration of Helsinki for research studies involving humans.

Table 3.1 Values of plasma Norepinephrine (NE) and Epinephrine (E), assessed after 5 minutes of REST in BASELINE and FOLLOW-UP

Method	NE (mg/dl)	E (mg/dl)
BASELINE	404.10±124.59	40.40±22.15
FOLLOW-UP	313.80±172.77	44.67±47.92

Values are reported as mean±standard deviation.

Table 3.2 Values of plasma Norepinephrine (NE) and Epinephrine (E), assessed after 5 minutes of TILT in BASELINE and FOLLOW-UP

Method	NE (mg/dl)	E (mg/dl)
BASELINE	668.30±248.08	56.80±38.68
FOLLOW-UP	636.36±518.91	56.00±42.85

Values are reported as mean±standard deviation.

3.6 Statistical Analysis

Statistical analysis was carried out using a commercial statistical program (Sigmaplot, v.14.0, Systat Software, Inc., Chicago, IL, USA). Regardless of the type of statistical test the level of significance was set to 0.05.

3.6.1 Statistical Analysis of Data Relevant to Inspiratory Muscle Training in Amateur Athletes

Data normality was tested using the Shapiro-Wilk test. Two-way repeated measures analysis of variance (two factor repetition, Holm-Sidak test for multiple comparisons) was used to assess the impact of IMT (i.e., PRE versus POST) within the same experimental condition (i.e., REST or STAND) and to assess the effect of the postural challenge given the same training condition.

3.6.2 Statistical Analysis of Data Relevant to Prolonged Head-down Bed Rest in Healthy Adults

Data normality was tested using the Shapiro-Wilk test. Two-way analysis of variance (Holm-Sidak test for multiple comparisons) was used to assess the effects of long term HDBR (i.e., PRE versus POST) within the same experimental condition (i.e., REST or TILT) and to assess the effect of the postural challenge given the same HDBR condition.

3.6.3 Statistical Analysis of Data Relevant to Postural Orthostatic Tachycardia Syndrome Patients

Data normality was tested using the Shapiro-Wilk test. Two-way repeated measures analysis of variance (two factor repetition, Holm-Sidak test for multiple comparisons) was used to assess the temporal evolution of the pathology (i.e., BASELINE versus FOLLOW-UP) within the same experimental condition (i.e., REST or STAND) and to assess the effect of the postural challenge at the same timepoint.

CHAPTER 4 - Results

4.1 Introduction

The following chapter introduces the results of TE, NCCCE, K^2, cardioventilatory coupling, phase synchronization and PRQ for each of the three experimental datasets described in the Chapter 3. Sect.4.2 deals with the results obtained in protocol 1 (i.e., the IMT protocol in amateur athletes) by comparing PRE and POST sessions and REST and STAND conditions for subjects in each training group separately. Sect.4.3 describes results obtained in protocol 2 (i.e., HDBR in healthy volunteers) by comparing PRE and POST sessions and REST and TILT conditions for all study subjects. Finally, Sect.4.4 reports the results obtained in protocol 3 (i.e., POTS patients) by comparing REST and TILT conditions at BASELINE and at FOLLOW-UP after one year.

4.2 PROTOCOL 1: Inspiratory Muscle Training in Amateur Athletes

A reliable extraction of INSP was carried out only in 8 subjects during SHAM, in 10 subjects during MIP60 and in 7 subjects during CIP corresponding to the 89%, 100% and 64% of the entire groups. When the INSP and EXP events could be reliably detected at REST, they could be reliably derived during STAND as well. When the INSP and EXP events could be reliably detected in PRE, they could be reliably derived in POST as well. Therefore, a two-way repeated measures statistical analysis scheme with the repetition of two factors could be applied. This limited rate of success was due to the absence of a clearly identifiable and univocal minimum in the R signal due to the presence of a prolonged apnoea after EXP just before INSP began again.

4.2.1 Transfer Entropy

The grouped error bar graphs of Figure 4.1 summarize the results of TE from R to RR in SHAM (Figure 4.1a), MIP60 (Figure 4.1b) and CIP (Figure 4.1c). Data are reported in PRE and POST condition at REST (solid black bars) and during STAND (solid white bars). No significant change was found between PRE and POST regardless of the IMT type. Similar trends can be observed between REST and STAND in all groups. The only significant difference was found in the SHAM group and took the form of a TE decrease during STAND compared to REST in the PRE condition. In general, a certain decrease of the TE during STAND compared to REST was evident in PRE in all groups and tended to remain evident in POST with the exception of the MIP60 group.

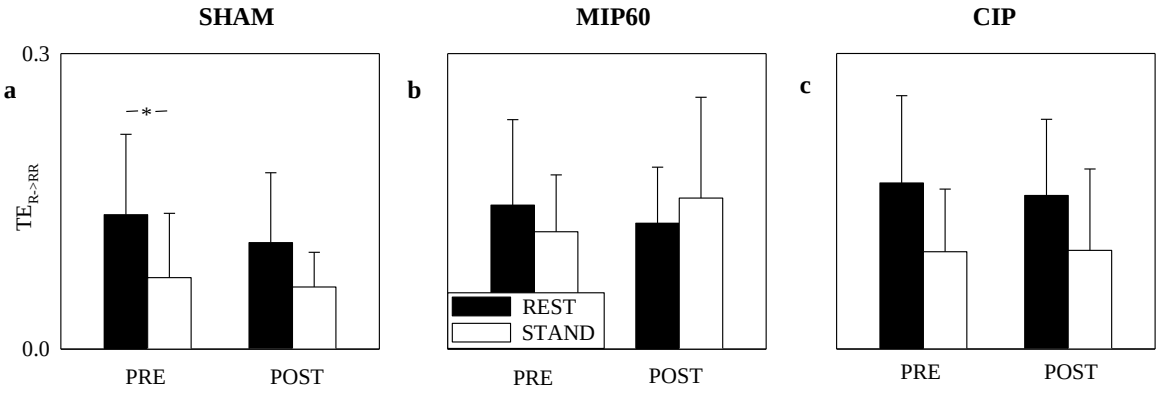

*Figure 4.1 The grouped error bar graphs show the TE from R to R ($TE_{R\rightarrow RR}$) computed in protocol 1 (amateur athletes). The grouped error bar graphs refer to SHAM (a), MIP60 (b) and CIP (c) as a function of the training status (i.e., PRE and POST). Indexes were calculated at REST (solid black bars) and during STAND (solid white bars). The symbol * indicates p<0.05 between experimental conditions either PRE or POST training.*

4.2.2 Normalized Cross Conditional Entropy

Figure 4.2 has the same structure as Figure 4.1 but shows the NCCCE in SHAM (Figure 4.2a), MIP60 (Figure 4.2b) and CIP (Figure 4.2c). A statistically significant increase of NCCCE during STAND compared to REST was detected in POST condition in SHAM, MIP60 and CIP. The same trend of NCCCE during STAND was observed in PRE condition only in the CIP group, although this tendency was present in the SHAM and MIP60 groups as well. No significant modifications between PRE and POST were found and this finding held in all groups.

Figure 4.3 has the same structure as Figure 4.1 but summarizes the results on NCCCE divided by NCI in SHAM (Figure 4.3a), MIP60 (Figure 4.3b) and CIP (Figure 4.3c). The REST-STAND differences observed in Figure 4.2 became significant regardless of group, and the only significant PRE-POST change occurred in TILT for the CIP group.

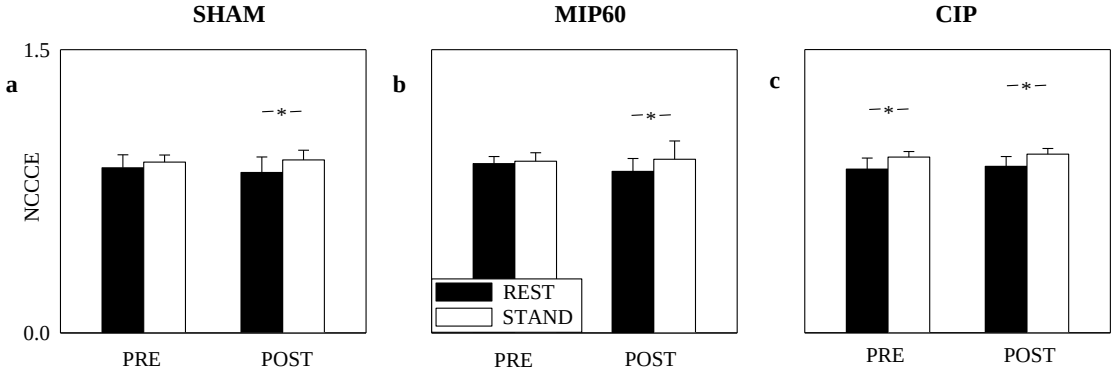

*Figure 4.2 The grouped error bar graphs show the NCCCE from R to RR computed in protocol 1 (amateur athletes). The grouped error bar graphs refer to SHAM (a), MIP60 (b) and CIP (c) as a function of the training status (i.e., PRE and POST). Indexes were calculated at REST (solid black bars) and during STAND (solid white bars). The symbol * indicates p<0.05 between experimental conditions either PRE or POST training.*

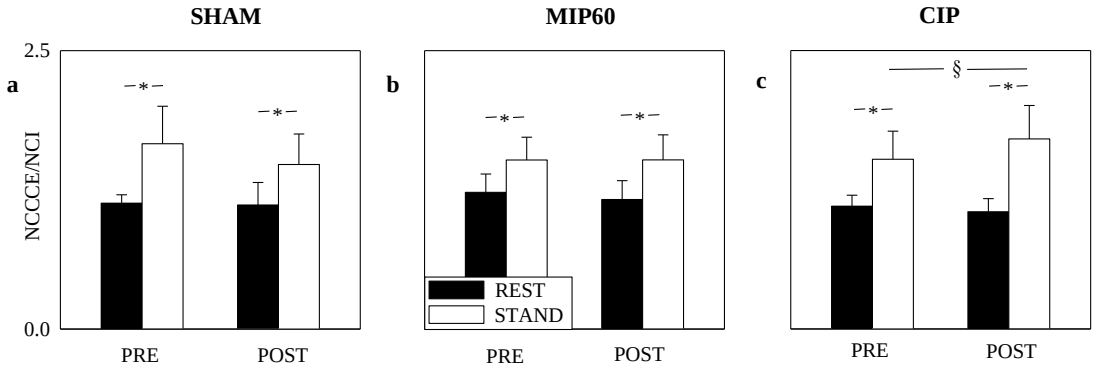

*Figure 4.3 The grouped error bar graphs show the NCCCE from R to RR divided by NCI of RR, computed in protocol 1 (amateur athletes). The grouped error bar graphs refer SHAM (a), MIP60 (b) and CIP (c) as a function of the training status (i.e., PRE and POST). Indexes were calculated at REST (solid black bars) and during STAND (solid white bars). The symbol * indicates p<0.05 between experimental conditions either PRE or POST training.*

4.2.3 Squared Coherence

Figure 4.4 shows the result of K^2 in SHAM (Figure 4.4a), MIP60 (Figure 4.4b) and CIP (Figure 4.4c). Figure 4.4 uses the same graphical conventions as Figure 4.1. The effect of STAND was visible in PRE and POST conditions when the SHAM and CIP groups were considered. This effect took the form of a decrease of K^2 during STAND compared to REST. A trend toward a decrease of K^2 during STAND was visible in MIP60 as well. Regardless of group, the influence of IMT was not detected.

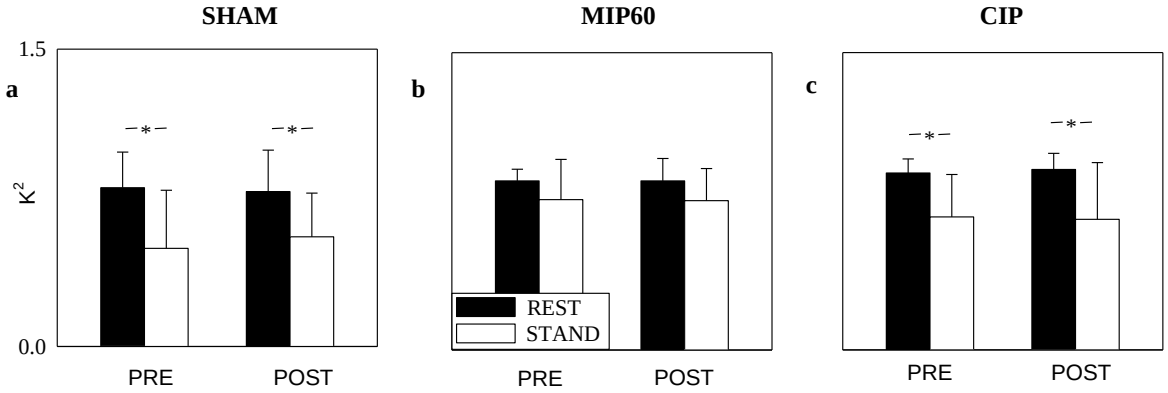

*Figure 4.4 The grouped error bar graphs show the K2 between R and RR computed in protocol 1 (amateur athletes). The grouped error bar graphs refer to SHAM (a), MIP60 (b) and CIP (c) as a function of the training status (i.e., PRE and POST). Indexes were calculated at REST (solid black bars) and during STAND (solid white bars). The symbol * indicates p<0.05 between experimental conditions either PRE or POST training.*

4.2.4 Cardioventilatory Coupling Indexes

The grouped error bar graphs in Figure 4.5 represent the NSE computed on RE_{-1} (Figure 4.5a), RE_{+1} (Figure 4.5b), RI_{-1} (Figure 4.5c), RI_{+1} (Figure 4.5d), intervals in the SHAM group. Data are reported as a function of the timeline of the protocol (i.e., PRE and POST) and experimental condition (i.e., REST and STAND) like in Figure 4.1. No trend can be discerned in Figure 4.5

either due to the postural change or the training. Figure 4.6 and 4.7 have the same structure of Figure 4.5, but show data relevant to the MIP60 and CIP groups respectively. In Figures 4.6 and 4.7 a significant increase of NSE of RE_{-1} and RE_{+1} was observed during STAND compared to REST in POST. Like in SHAM group, no effect of IMT was visible in the MIP60 (Figure 4.6) and CIP (Figure 4.7).

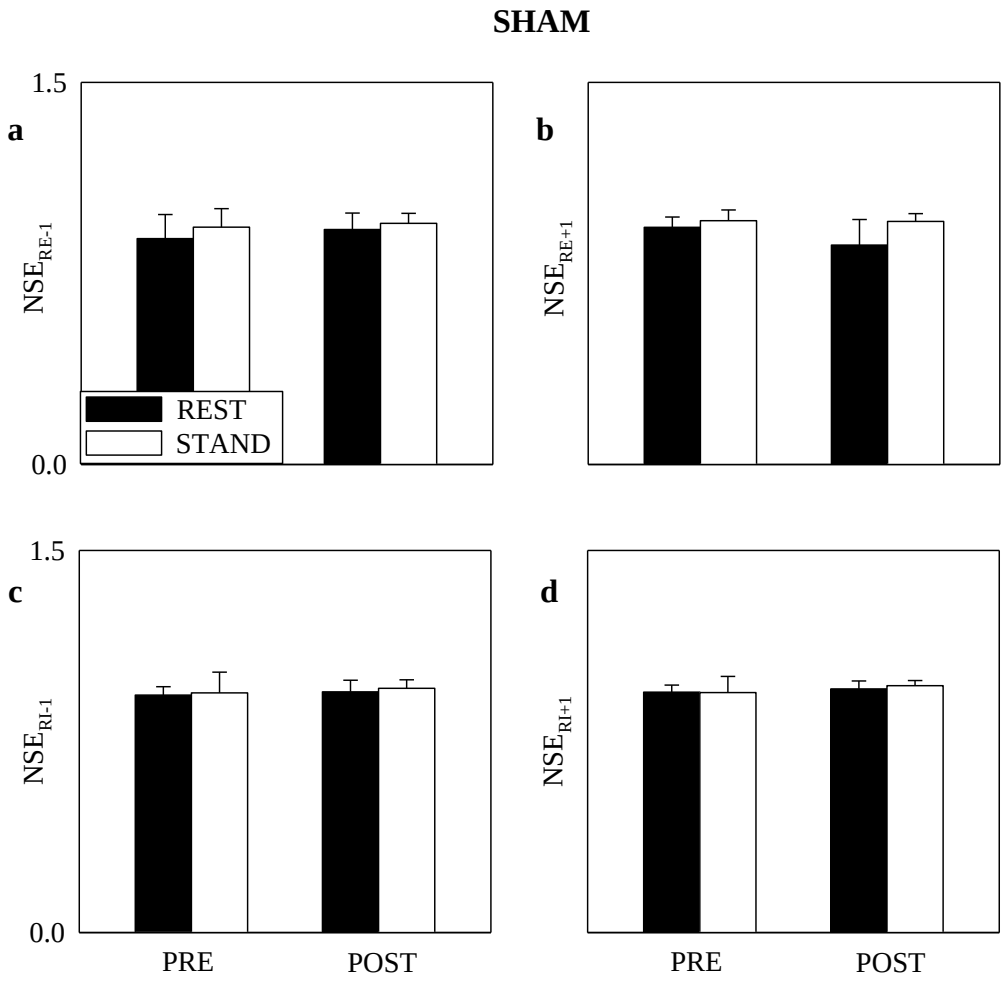

Figure 4.5 The grouped error bar graphs show the NSE of the latency distribution calculated between the ECG R-wave and the respiratory phase onset in protocol 1 (amateur athletes). The grouped error bar graphs refer to the SHAM group. Indexes were calculated at REST (solid black bars) and during STAND (solid white bars). RI: time interval between R-wave and INSP; RE: time interval between R-wave and EXP; NSE_{RE-1}: NSE of RE computed with respect to the last ECG R-wave before EXP (a); NSE_{RE+1}: NSE of RE computed with respect to the first ECG R-wave after EXP (b); NSE_{RI-1}: NSE of RI computed with respect to the last ECG R-wave before INSP (c); NSE_{RI+1}: NSE of RI computed with respect to the first ECG R-wave after INSP (d).

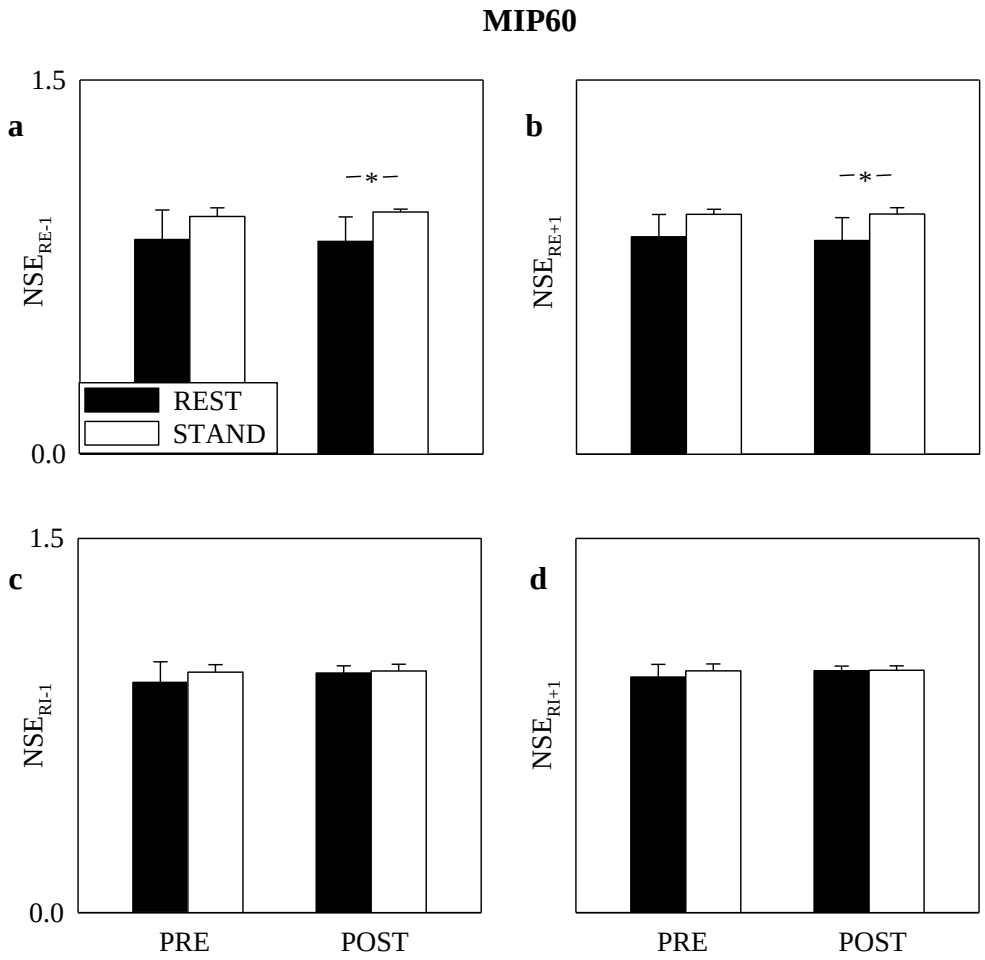

*Figure 4.6 The grouped error bar graphs show the NSE of the latency distribution calculated between the ECG R-wave and the respiratory phase onset in protocol 1 (amateur athletes). The grouped error bar graphs refer to the MIP60 group. Indexes were calculated at REST (solid black bars) and during STAND (solid white bars). RI: time interval between R-wave and INSP; RE: time interval between R-wave and EXP; NSE_{RE-1}: NSE of RE computed with respect to the last ECG R-wave before EXP (a); NSE_{RE+1}: NSE of RE computed with respect to the first ECG R-wave after EXP (b); NSE_{RI-1}: NSE of RI computed with respect to the last ECG R-wave before INSP (c); NSE_{RI+1}: NSE of RI computed with respect to the first ECG R-wave after INSP (d). The symbol * indicates $p<0.05$ between experimental conditions either PRE or POST training.*

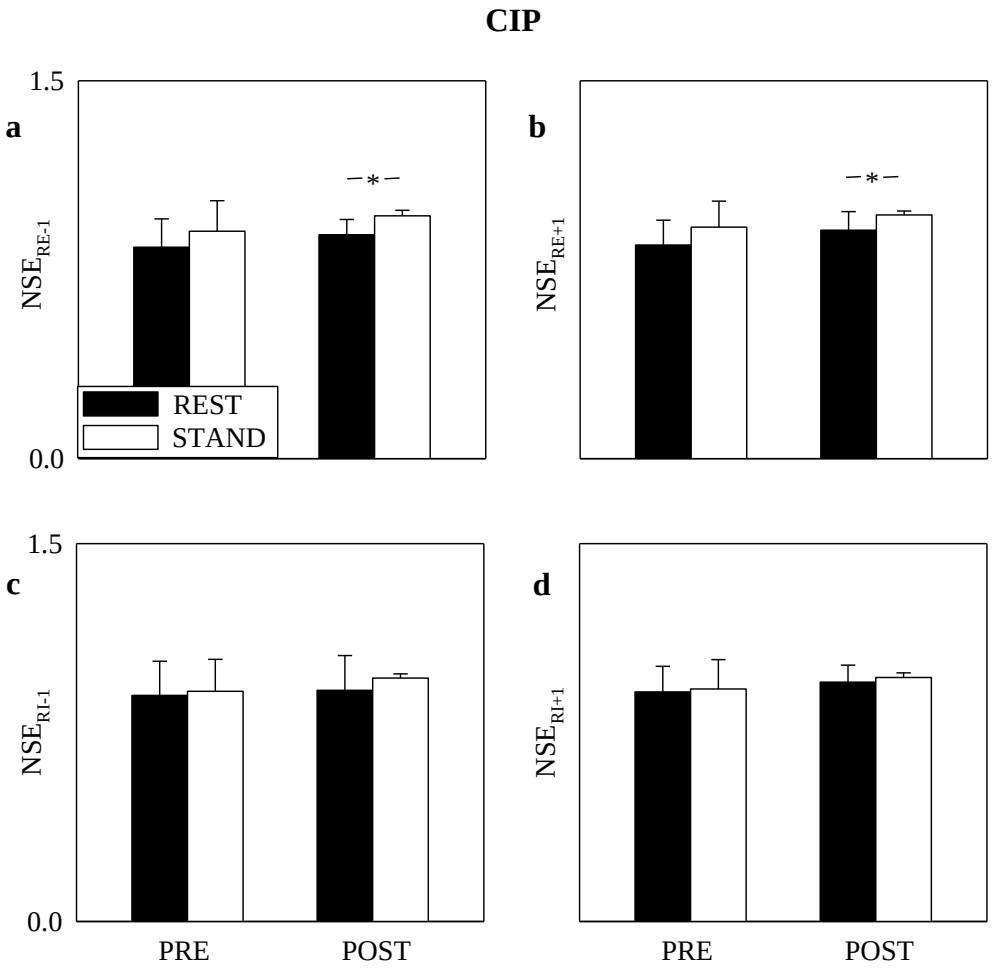

*Figure 4.7 The grouped error bar graphs show the NSE of the latency distribution calculated between the ECG R-wave and the respiratory phase onset in protocol 1 (amateur athletes). The grouped error bar graphs refer to the CIP group. Indexes were calculated at REST (solid black bars) and during STAND (solid white bars). RI: time interval between R-wave and INSP; RE: time interval between R-wave and EXP; NSE_{RE-1}: NSE of RE computed with respect to the last ECG R-wave before EXP (a); NSE_{RE+1}: NSE of RE computed with respect to the first ECG R-wave after EXP (b); NSE_{RI-1}: NSE of RI computed with respect to the last ECG R-wave before INSP (c); NSE_{RI+1}: NSE of RI computed with respect to the first ECG R-wave after INSP (d). The symbol * indicates $p<0.05$ between experimental conditions either PRE or POST training.*

4.2.5 Synchronization index

The grouped error bar graphs of Figure 4.8 depicts the SYNC% in the SHAM (Figure 4.8a), MIP60 (Figure 4.8b) and CIP (Figure 4.8c) groups. Graphical conventions are similar to Figure 4.1. It can be observed that a decrease of SYNC% is present during STAND compared to REST in most cases. This decrease is particularly evident in POST condition in SHAM and MIP60 group. The effect of IMT on SYNC% was not significant.

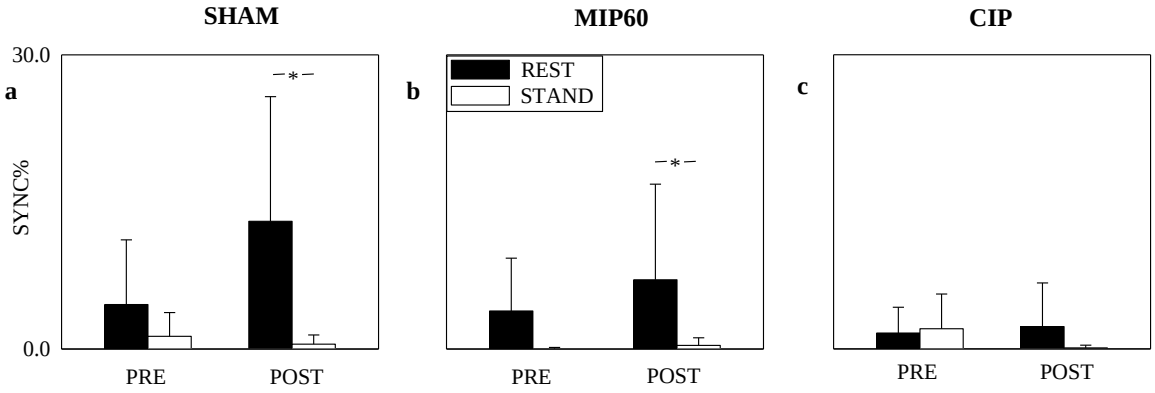

*Figure 4.8 The grouped error bar graphs show SYNC% computed in protocol 1 (amateur athletes). The grouped error bar graphs refer to SHAM (a), MIP60 (b) and CIP (c) as a function of the training status (i.e., PRE and POST). Indexes were calculated at REST (solid black bars) and during STAND (solid white bars). The symbol * indicates $p<0.05$ between experimental conditions either PRE or POST training.*

4.2.6 Pulse-Respiration Quotient

Figure 4.9 depicts the PRQ calculated in SHAM (Figure 4.9a), MIP60 (Figure 4.9b) and CIP (Figure 4.9c). Graphical conventions are similar to Figure 4.1. As expected, during STAND PRQ always increased with relation to REST and this result held regardless of training status and group. A significant effect of training was visible solely in the CIP group: indeed, PRQ raised in POST compared to PRE as a result of the post-training increase of HR in presence of an unchanged f_R.

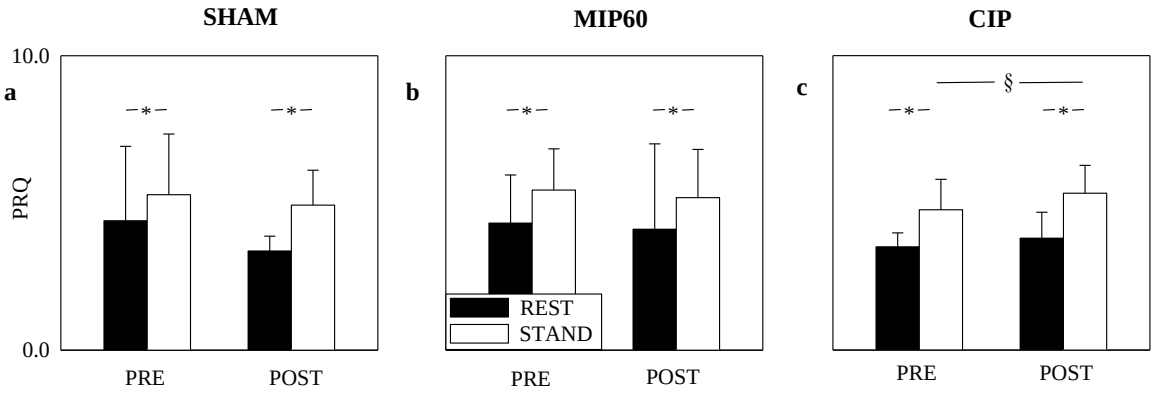

*Figure 4.9 The grouped error bar graphs show the PRQ computed in protocol 1 (amateur athletes). The grouped error bar graphs refer to SHAM (a), MIP60 (b) and CIP (c) as a function of the training status (i.e., PRE and POST). Indexes were calculated at REST (solid black bars) and during STAND (solid white bars). The symbol § indicates $p<0.05$ between PRE and POST training within the same experimental condition. The symbol * indicates $p<0.05$ between experimental conditions either PRE or POST training.*

4.3 PROTOCOL 2: Prolonged Head-down Bed Rest in Healthy Adults

One recording at REST before prolonged HDBR was discarded for poor quality of the respiratory signal. Therefore, the total number of analyses was different across experimental conditions and timepoints. As a consequence, we applied a standard two-way statistical analysis scheme without any repetition of factors.

4.3.1 Transfer Entropy

The grouped error bar graph of Figure 4.10 summarizes results of TE from R to RR in PRE and POST condition. TE was computed at REST (solid black bars) and during TILT (solid white bars). Although TE tends to decrease during TILT, there is no significant change across experimental conditions and the effect of HDBR was not visible as well.

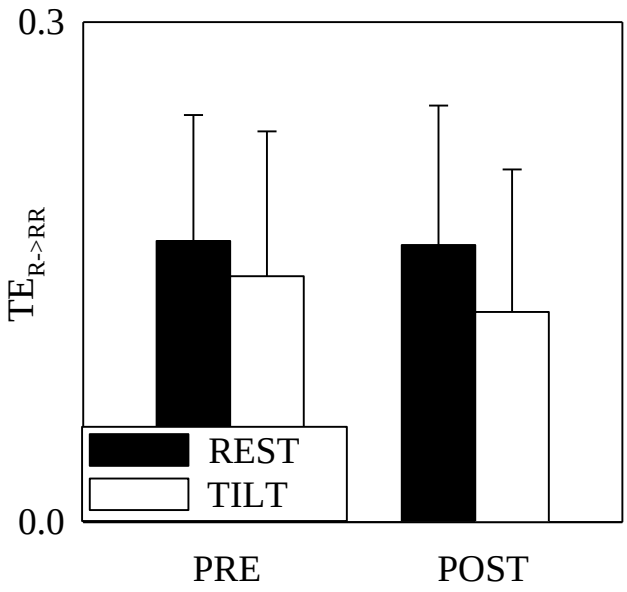

Figure 4.10 The grouped error bar graph shows the TE from R to RR, $TE_{R\rightarrow RR}$, computed in protocol 2 (healthy adults) as a function of the time line of the protocol (i.e., PRE and POST). Indexes were calculated at REST (solid black bars) and during STAND (solid white bars).

4.3.2 Normalized Cross Conditional Entropy

Figure 4.11 has the same structure of Figure 4.10 but it represents NCCCE (Figure 4.11a) and NCCCE/NCI (Figure 4.11b). NCCCE was found to be altered in POST compared to PRE at REST. This effect, however, disappears in NCCCE/NCI. TILT did not affect NCCCE regardless of the timepoint of the protocol (i.e., PRE or POST). Conversely, NCCCE/NCI increased during TILT compared to REST in both PRE and POST.

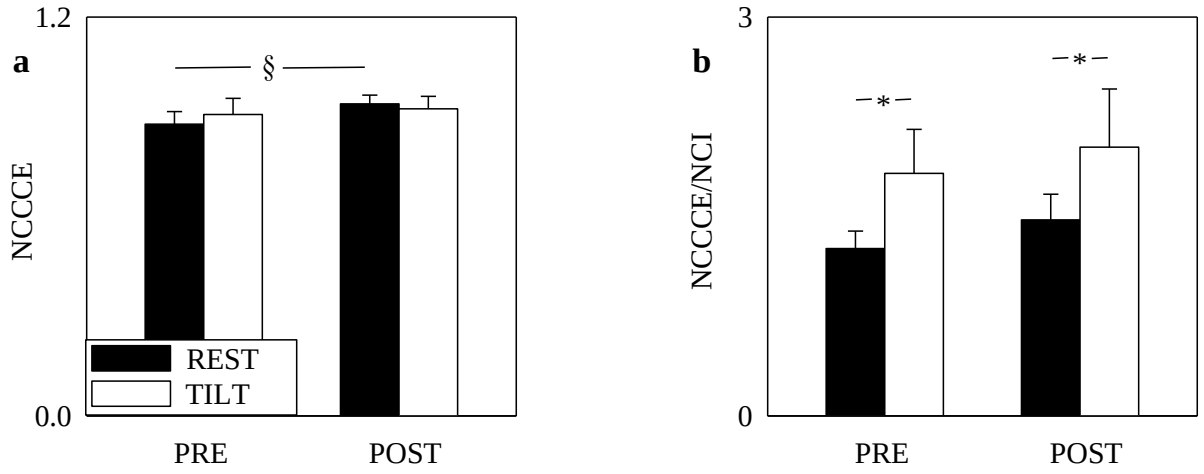

*Figure 4.11 The grouped error bar graphs show the NCCCE (a) from R to RR and the NCCCE from R to RR divided by NCI of RR (b) computed in protocol 2 (healthy adults) as a function of the time line of the protocol (i.e., PRE and POST). Indexes were calculated at REST (solid black bars) and during STAND (solid white bars). The symbol § indicates $p<0.05$ between PRE and POST HDBR within the same experimental condition. The symbol * indicates $p<0.05$ between experimental conditions either PRE or POST HDBR.*

4.3.3 Squared Coherence

The grouped error bar graph of Figure 4.12 reports K^2. The graphical conventions of Figure 4.12 are similar to Figure 4.10. While no significant change of K^2 is detected across experimental conditions and timepoints of the protocol, data suggest a trend toward a decrease in K^2 during TILT compared to REST both in PRE and POST.

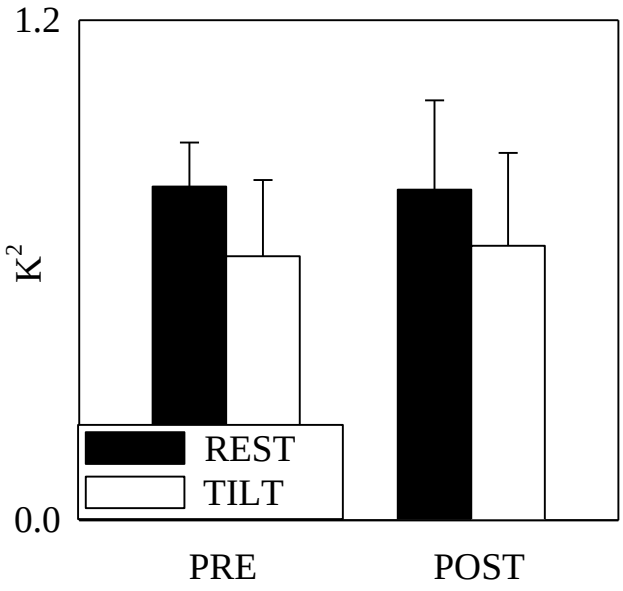

Figure 4.12 The grouped error bar graph shows the K^2 between R and RR computed in protocol 2 (healthy adults) as a function of the time line of the protocol (i.e., PRE and POST). Indexes were calculated at REST (solid black bars) and during STAND (solid white bars).

4.3.4 Cardioventilatory Coupling Indexes

The grouped error bar graphs in Figure 4.13 show the results on the NSE computed over RE_{-1}, (Figure 4.13a), RE_{+1} (Figure 4.13b), RI_{-1} (Figure 4.13c), and RI_{+1} (Figure 4.13d). Figure 4.13 has the same structure as Figure 4.10. No significant difference can be observed, and this result held regardless of experimental condition and timepoint of the protocol. However, a trend pointing toward an increase of NSE of all time intervals during TILT compared to REST can be observed and this tendency is present in PRE and POST. Furthermore, it can be observed that NSE computed over the RI tended to assume lower values compared to those calculated over RE.

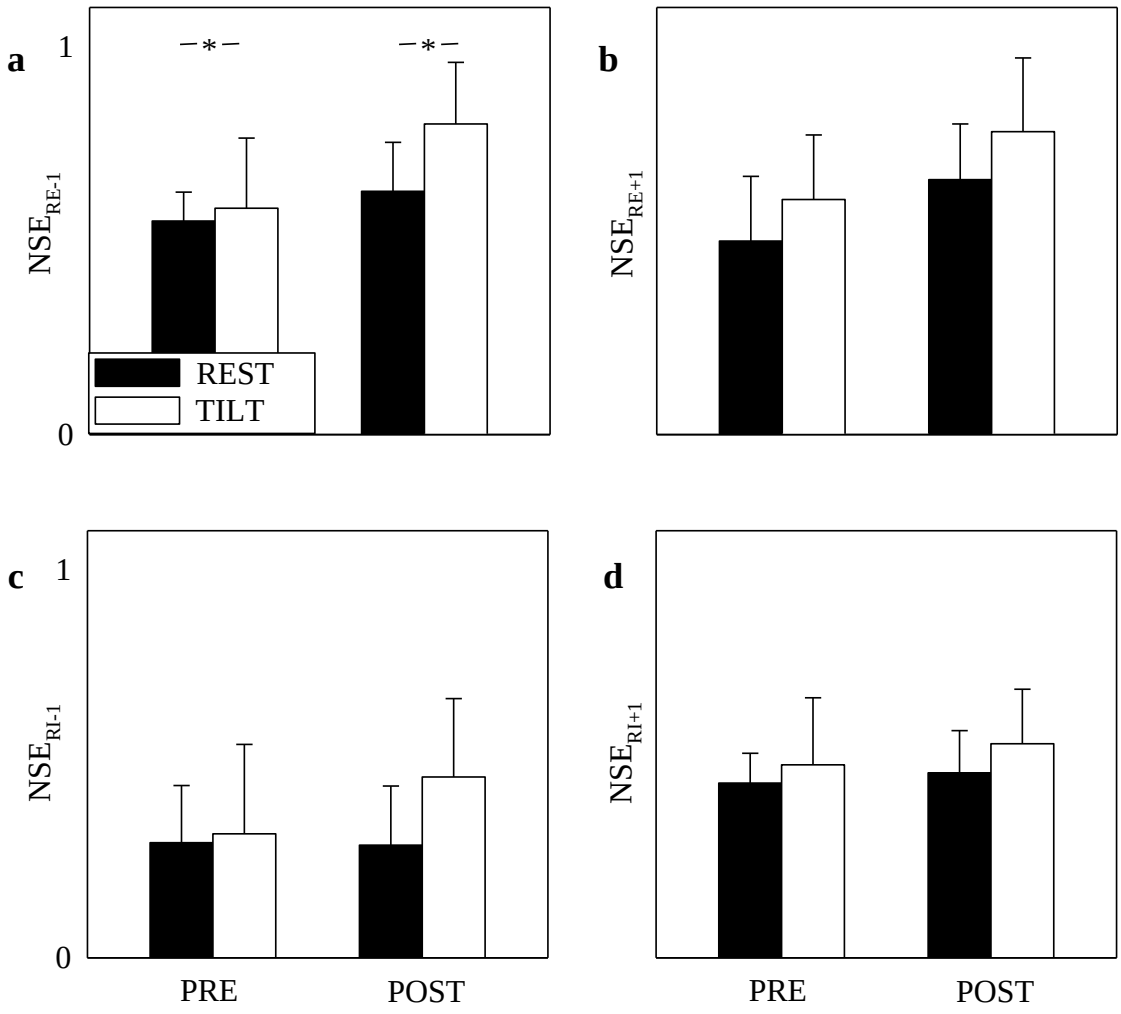

*Figure 4.13 The grouped error bar graphs show the NSE of the latency distribution calculated between the ECG R-wave and the respiratory phase onset computed in protocol 2 (healthy adults) as a function of the time line of the protocol (i.e., PRE and POST). Indexes were calculated at REST (solid black bars) and during STAND (solid white bars). RI: time interval between R-wave and INSP; RE: time interval between R-wave and EXP; NSE_{RE-1}: NSE of RE computed with respect to the last ECG R-wave before EXP (a); NSE_{RE+1}: NSE of RE computed with respect to the first ECG R-wave after EXP (b); NSE_{RI-1}: NSE of RI computed with respect to the last ECG R-wave before INSP (c); NSE_{RI+1}: NSE of RI computed with respect to the first ECG R-wave after INSP (d). The symbol * indicates $p<0.05$ between experimental conditions either PRE or POST HDBR.*

4.3.5 Synchronization index

The grouped error bar graph of Figure 4.14 reports SYNC%. The graphical conventions of Figure 4.14 are similar to Figure 4.10. Both the effects of TILT and HDBR were not significant. Remarkably, SYNC% was negligible at REST and null at TILT. This observation held in both PRE and POST conditions.

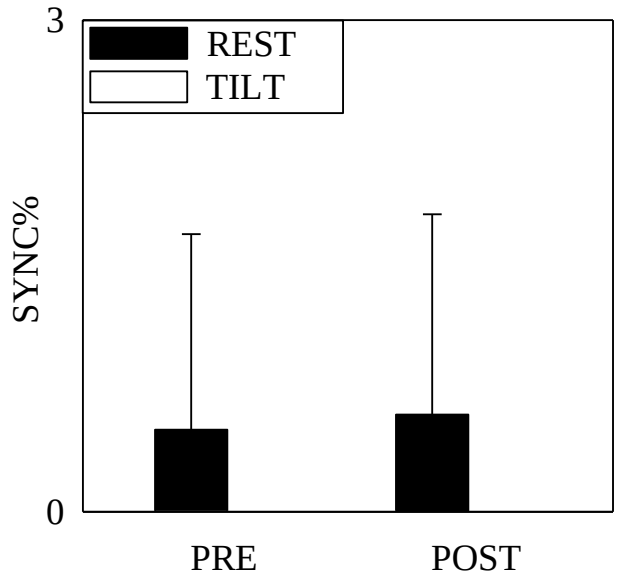

Figure 4.14 The grouped error bar graph shows SYNC% computed in protocol 2 (healthy adults) as a function of the time line of the protocol (i.e., PRE and POST). Indexes were calculated at REST (solid black bars) and during STAND (solid white bars).

4.3.6 Pulse-Respiration Quotient

The grouped error bar graph of Figure 4.15 reports PRQ. Graphical conventions of Figure 4.15 are similar to Figure 4.10. The PRQ increased during TILT with respect to REST but the increase was significant only in POST. The effect of HDBR was not detectable both at REST and during TILT.

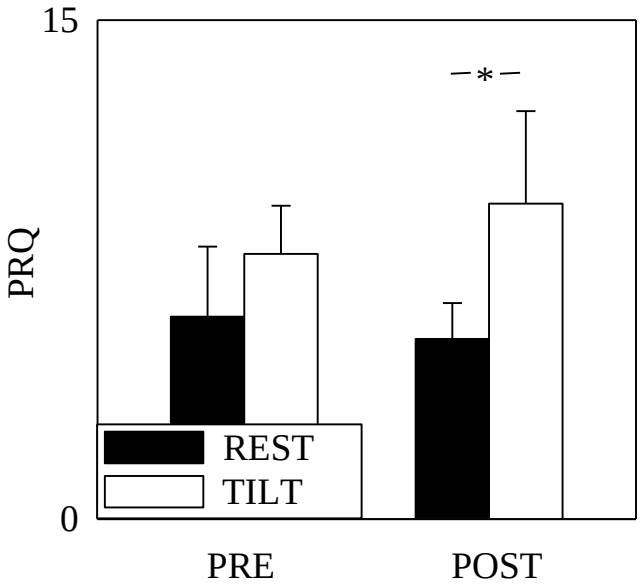

*Figure 4.15 The grouped error bar graph shows the PRQ computed in protocol 2 (healthy adults) as a function of the time line of the protocol (i.e., PRE and POST). Indexes were calculated at REST (solid black bars) and during STAND (solid white bars). The symbol * indicates p<0.05 between experimental conditions either PRE or POST HDBR.*

4.4 PROTOCOL 3: Postural Orthostatic Tachycardia Syndrome Patients

One subject could not maintain the TILT position without showing signs of orthostatic intolerance for more than a few minutes, both at BASELINE and FOLLOW-UP. Therefore, the beat-to-beat event and variability series relevant to this subject at REST in BASELINE and FOLLOW-UP were discarded in order to allow for the application of a two-way repeated measures statistical analysis scheme with the repetition of two factors.

4.4.1 Transfer Entropy

The grouped error bar graph in Figure 4.16 describes TE from R to RR at BASELINE and one year FOLLOW-UP. TE was computed during REST (solid black bars) and during STAND (solid white bars). While TE tended to decrease during TILT compared to REST, there was no significant change across timepoints of the protocol.

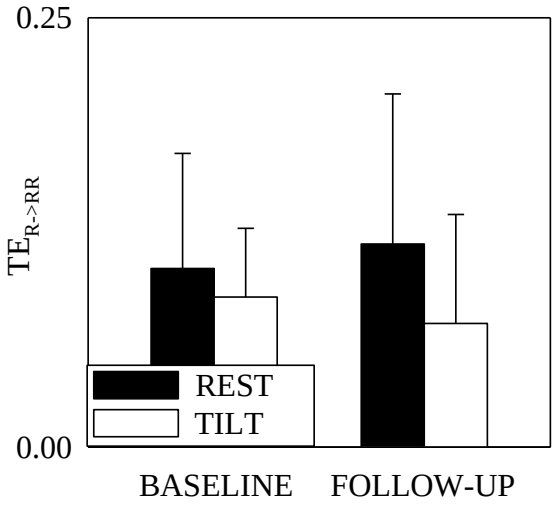

Figure 4.16 The grouped error bar graph shows the TE from R to RR, TER→RR, computed in protocol 3 (POTS patients) as a function of the time line of the protocol (i.e., BASELINE and FOLLOW-UP). Indexes were calculated at REST (solid black bars) and during STAND (solid white bars).

4.4.2 Normalized Cross Conditional Entropy

The grouped error bar graph in Figure 4.17 has the same structure as Figure 4.16 but shows NCCCE (Figure 4.17a) and NCCCE/NCI (Figure 4.17b). NCCCE did not exhibit differences either across experimental conditions or across timepoints. The NCCCE/NCI index increased during TILT compared to REST in both PRE and POST. NCCCE/NCI did not vary overtime.

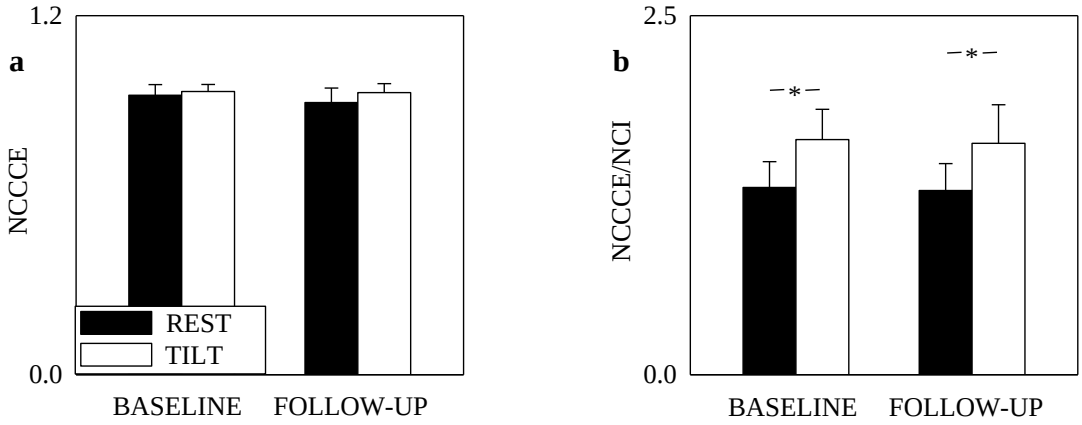

*Figure 4.17 The grouped error bar graphs show the NCCCE (a) from R to RR and the NCCCE from R to RR divided by NCI of RR (b) computed in protocol 3 (POTS patients) as a function of the time line of the protocol (i.e., BASELINE and FOLLOW-UP). Indexes were calculated at REST (solid black bars) and during STAND (solid white bars). The symbol * indicates $p<0.05$ between experimental conditions at a specific timepoint.*

4.4.3 Squared Coherence

The grouped error bar graph of Figure 4.18 depicts K^2. Graphical conventions are similar to Figure 4.16. A trend to decrease during TILT with respect to REST could be observed both at BASELINE and FOLLOW-UP. No significant change was present across timepoints of the protocol, although there was a tendency toward a decrease of K^2 in FOLLOW-UP.

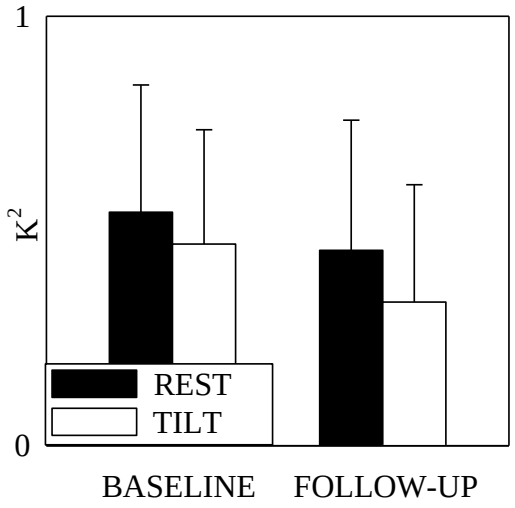

Figure 4.18 The grouped error bar graph shows the K^2 between R and RR computed in protocol 3 (POTS patients) as a function of the time line of the protocol (i.e., BASELINE and FOLLOW-UP). Indexes were calculated at REST (solid black bars) and during STAND (solid white bars).

4.4.4 Cardioventilatory Coupling Indexes

The groups error bar graphs in Figure 4.19 represent the NSE computed over RE_{-1} (Figure 4.19a), RE_{+1} (Figure 4.19b), RI_{-1} (Figure 4.19c), and RI_{+1} (Figure 4.19d) intervals. Graphical conventions are similar to Figure 4.16. No trend could be discerned due to the temporal evolution of the pathology in the NSE of the RE intervals and this result held both at REST and during TILT. Conversely, the NSE of the RI intervals increased during the FOLLOW-UP compared to BASELINE only at REST. In general, an increase of NSE of RI and RE was detectable during TILT compared to REST and this finding held at BASELINE and FOLLOW-UP. This increase was significant in the case of the NSE of RI_{-1} and RI_{+1} at BASELINE and in the case of the NSE of RE_{-1} in FOLLOW-UP.

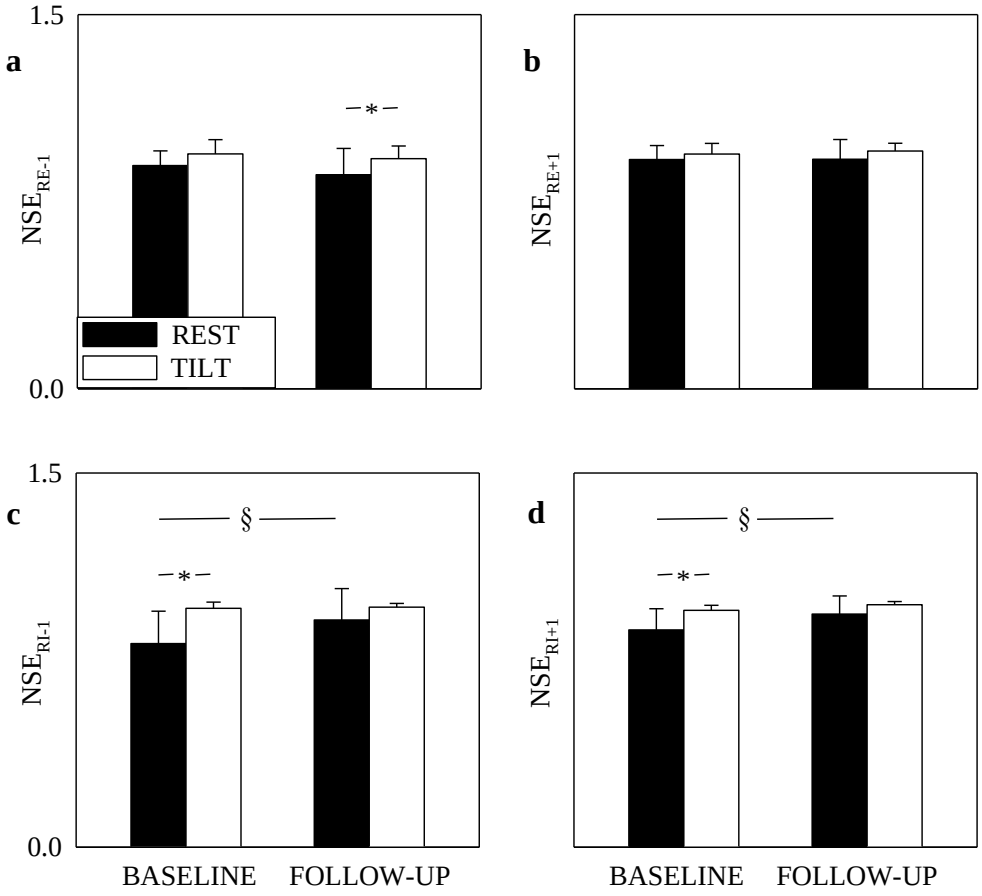

*Figure 4.19 The grouped error bar graphs show the NSE of the latency distribution calculated between the ECG R-wave and the respiratory phase onset computed in protocol 3 (POTS patients) as a function of the time line of the protocol (i.e., BASELINE and FOLLOW-UP). Indexes were calculated at REST (solid black bars) and during STAND (solid white bars). RI: time interval between R-wave and INSP; RE: time interval between R-wave and EXP; NSE_{RE-1}: NSE of RE computed with respect to the last ECG R-wave before EXP (a); NSE_{RE+1}: NSE of RE computed with respect to the first ECG R-wave after EXP (b); NSE_{RI-1}: NSE of RI computed with respect to the last ECG R-wave before INSP (c); NSE_{RI+1}: NSE of RI computed with respect to the first ECG R-wave after INSP (d). The symbol § indicates $p<0.05$ between the two timepoints within the same experimental condition. The symbol * indicates $p<0.05$ between experimental conditions at a specific timepoint.*

4.4.5 Synchronization index

The grouped error bar graph in Figure 4.20 summarizes SYNC%. Figure 4.20 has the same structure as Figure 4.16. SYNC% did not vary with either experimental condition or timepoint of the protocol.

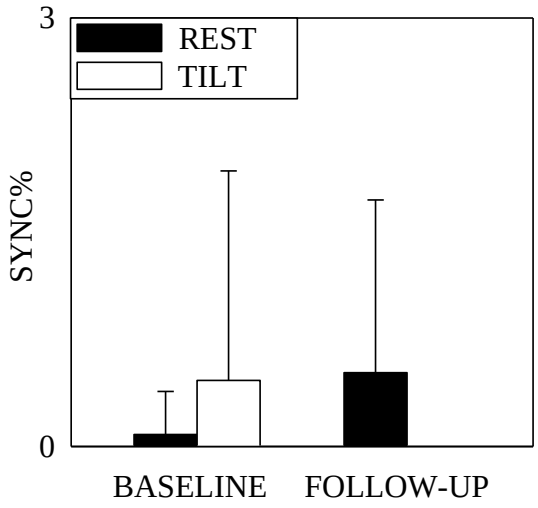

Figure 4.20 The grouped error bar graph shows SYNC% computed in protocol 3 (POTS patients) as a function of the time line of the protocol (i.e., BASELINE and FOLLOW-UP). Indexes were calculated at REST (solid black bars) and during STAND (solid white bars).

4.4.6 Pulse-Respiration Quotient

The results on PRQ are presented in the grouped error bar graph in Figure 4.21. Graphical conventions are similar to Figure 4.16. TILT significantly raised PRQ both at BASELINE and FOLLOW-UP. Conversely, the time factor did not affect PRQ.

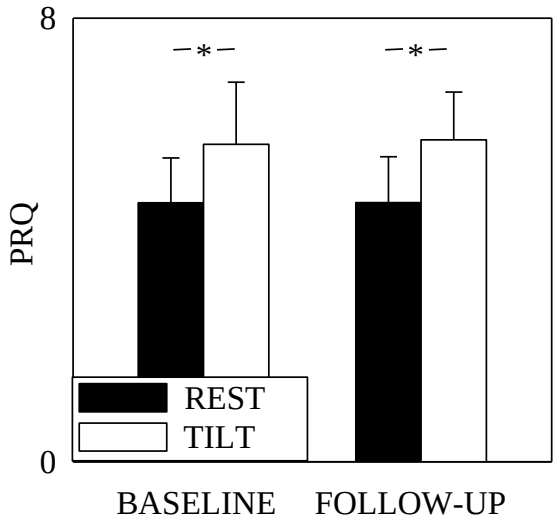

*Figure 4.21 The grouped error bar graph shows the PRQ computed in protocol 3 (POTS patients) as a function of the time line (i.e., BASELINE and FOLLOW-UP). Indexes were calculated at REST (solid black bars) and during STAND (solid white bars). The symbol * indicates $p<0.05$ between experimental conditions at a specific timepoint.*

CHAPTER 5 - Discussion

5.1 Introduction

The following chapter discusses the results obtained and their significance in the study of cardiorespiratory interactions, for each of the three experimental protocols used in the present thesis. Sect.5.2 details methodological findings, discussing the necessity of integrating multiple approaches of cardiorespiratory interaction assessment in different experimental conditions for a more complete outlook on this phenomenon. In Sect.5.3 the most significant results obtained in protocol 1 are considered by taking into account both the effects of postural change and training. Sect.5.4 discusses the effects of orthostatic challenge and physical deconditioning in healthy volunteers according to the findings of protocol 2. In the Sect.5.5 the most relevant results of the protocol 3 obtained on POTS patients are discussed in terms of the effects of orthostatic stress and the temporal evolution of the pathology under clinical management of the symptoms.

5.2 Discussion of methodological findings

The six methodologies employed in the present dissertation, based on the computation of TE, NCCCE, K^2, NSE of RE and RI intervals, SYNC% and PRQ, investigate different aspects of cardiorespiratory interactions. Indeed, TE from R to RR assesses the amount of information carried by RR that can be derived from R above and beyond the amount of information derived from past values of RR, NCCCE from R to RR quantifies the amount of information carried by RR that cannot be derived from R, K^2 between R and RR measures the degree of linear association between RR and R series at f_R, NSE of RE and RI intervals estimates the degree of complexity of the distribution of time intervals between the closest R-wave and INSP or EXP events, SYNC% measures the percentage of windows in which a significant phase synchronization between heartbeat and the R signal is detected and, finally, PRQ provides an estimate of the type and strength of frequency coupling between heart and R rhythms through its absolute value and variability respectively. As summarised in Table 2.1, the methods exploited in this thesis not only measure different quantities but also require different approaches for their computation. As a matter of fact, TE employs a linear model-based approach grounded on the bivariate AR model, NCCCE utilised a model-free approach based on uniform quantization capable of describing nonlinear features that might be present in RR-R dynamical interactions, K^2 is, like TE, a linear model-based approach based on bivariate AR model, NSE of RE and RI intervals is computed via a model-free method directly grounded on event marker series of the heartbeats and respiratory phase onsets, SYNC% is estimated via a nonlinear model-free method based on the graphical representation of relative phase of heartbeats within an assigned number of respiratory cycles (i.e., the synchrogram) and on the automatic assessment of the degree of phase pattern repetition overtime, and, finally, PRQ is a time domain model-free index calculated as the ratio of the cardiac to respiratory rate. The methods account for different features of the two interacting signals. Indeed, while TE, NCCCE, and K^2 can account for amplitude and phase interactions between the RR series and

the R signal, NSE of RE and RI intervals and SYNC% exclusively describe phase interactions, given that they operate over event series. SYNC% is specifically more powerful when the phase interactions occur according to complex phase patterns, while NSE of RE and RI intervals looks at the phase interactions between heartbeat and R exclusively at the onset of respiratory phases. Frequency interactions are described by all the approaches but with different ability. Indeed, TE and K^2 can account for frequency interactions occurring mainly at the respiratory rate due to their inherent linearity, while NCCCE has the possibility of describing frequency interactions at different rates given its inherent nonlinearity. Furthermore, NSE of RE and RI, SYNC% and PRQ are sensitive to frequency interactions at different rates given that they work over series of events.

This variety of approaches allows for a more comprehensive perspective on the cardiorespiratory interactions. The simultaneous application of all these methods proves that the derived indexes have different power of detection of changes in cardiorespiratory interaction strength, due to postural change or intervention across three experimental protocols. In particular, TE and K^2 indexes were not found to be particularly susceptible to orthostatic stress (de Abreu et al., 2019). Indeed, TE and K^2 tended to decrease during postural challenge in protocol 1, 2 and 3 even though significance was reached only in few occasions (e.g., in protocol 1 in the SHAM group). NCCCE was affected to some extent by postural stimulus. Indeed, a tendency to increase of NCCCE during orthostatic challenge was observed in all protocols and this tendency was stronger in protocol 1. When NCCCE was normalized by NCI, this tendency became more robust in all protocols and often significant, thus stressing the importance of this normalization to better appreciate the decrease on cardiorespiratory interactions with the postural stimulus (Porta et al., 2016). Furthermore, the NSE of RE and RI tended to increase with postural stimulus, thus indicating a sort of desynchronization between heartbeat and respiratory phase onset. This tendency was stronger over RE and after MIP60 and CIP trainings in protocol 1 and over RI in protocol 3. The different statistical power of NSE markers computed over RE and RI intervals in relation to the protocol suggested the possibility that RE and RI intervals cold be under control of different coupling mechanisms and the importance of their concurrent assessment. The SYNC% index exhibited a tendency to decrease during orthostatic stimulus and this tendency was particularly strong in protocol 1 in POST in SHAM and MIP60 groups (Cairo et al., 2020). As expected from literature (Scholkmann & Wolf, 2019), the PRQ was able to detect changes in frequency coupling in relation to the orthostatic stress and this finding was observed regardless of the protocol. Indeed, the increase of PRQ was found to be significant mainly because the higher heart rate induced by the challenge was not accompanied by a modification of the breathing rate. This observation suggested a certain degree of redundancy of this index compared to cardiac frequency when respiratory rate did not vary. All considered indexes were particularly weak in detecting the effects of the intervention exploited in each of the three protocols, namely IMT in protocol 1, HDBR in protocol 2 and clinical management in protocol 3. Indeed, very few significant differences between the two different timepoints of the protocols (i.e., PRE and POST or BASELINE and FOLLOW-UP) were detected, thus indicating the limited power of the intervention in modifying cardiorespiratory interaction strength.

Considerations about the methodological dissimilarities and differences in effectiveness across all indexes suggest that the simultaneous exploitation of all methodologies in cardiorespiratory

studies is advantageous, as it is not possible either to know beforehand which ones are going to be more powerful in the specific experimental protocol under analysis or to foresee which is the aspect of cardiorespiratory coupling more affected by the pathophysiological condition of the subject. Furthermore, thanks to this multi-method approach, different aspects of cardiorespiratory interactions can be evaluated concurrently. This simultaneous evaluation can be carried out with a relatively negligible computational cost, as none of the approaches requires intensive resources.

It is necessary to point out that the disappointing performance of some indexes (e.g., TE) in discerning the effects of postural challenge is partially explained by the inability of a bivariate RR-R approach in interpreting the role of baroreflex. A trivariate approach including beat-to-beat systolic arterial pressure into the analysis could potentially increase the efficacy of some indexes (Abreu et al., 2020), by removing baroreflex mediated effects. However, it is essential in cardiorespiratory studies to evaluate the performance of bivariate methodologies, as they are considered the preferred approach in applicative contexts due to their convenience. For example, bivariate methods could be potentially advantageous when only an ECG signal is available in practical applications. Indeed, in this framework, both the RR and R signals necessary for computation of cardiorespiratory interaction indexes can be extracted from the ECG given that the R signal could be derived from the modifications of the R-wave amplitude reflecting cardiac axis movements synchronous with R.

5.3 Inspiratory Muscle Training in Amateur Athletes: Discussion of experimental results

5.3.1 Effects of STAND on cardiorespiratory dynamical interactions in amateur athletes

Regardless of the approach used, cardiorespiratory interaction strength generally decreased during STAND when compared to REST in amateur athletes. This result is in line with previous studies observing that cardiorespiratory interactions are reduced in situations of sympathetic activation (Cogliati et al., 2004; Porta et al., 2012), while they generally increase in conditions of low cognitive and behavioural activity (Penzel et al., 2016).

This effect can be observed across all approaches used and takes the form of a trend, albeit not significant, toward a decrease of TE from R to RR in most training groups and conditions (Figure 4.1) and of a significant loss of coherence K^2 between HR and R during STAND both before and after SHAM and CIP training (Figure 4.4) (Abreu et al., 2020). These results indicate a loss of linear interactions, when taking into account, respectively, solely the time direction from R to RR (i.e., R→RR) and when evaluating both directions of interactions at the same time (i.e., R↔RR). Similar considerations can be made for the other indexes: in particular, NCCCE exhibited a significant increase under orthostatic stress in POST in the SHAM and MIP60 groups (Figure 4.2), thus indicating a loss of interaction between RR and R. This finding could potentially be an effect of training, but statistical significance can be observed after the normalization of NCCCE by NCI in all the three training groups and regardless of the training status (Figure 4.3), thus making the loss of cardiorespiratory interaction strength a likely effect of STAND instead. The more robust assessment of the decrease of cardiorespiratory interactions during STAND obtained via the NCCCE normalized by NCI compared to the sole evaluation of NCCCE is the likely effect of taking into account the well-known decrease of

NCI of RR during postural challenge that might bias toward lower values the NCCCE. In agreement with these considerations, all cardioventilatory coupling indexes (i.e., the NSE of RE and RI intervals reported in Figures 4.5, 4.6 and 4.7) and the synchronization marker (i.e., SYNC% reported in Figure 4.8) also indicate a generally weaker cardiorespiratory coupling and a loss of interaction between heartbeat and R in response to STAND. Remarkably, the REST-STAND difference is more likely to be significant in POST, thus indicating a possible after-training strengthening of the sympathetic response to the orthostatic stress. It is important to point out a different ability of cardioventilatory coupling indexes in detecting REST-STAND changes, possibly evidencing different mechanisms of cardioventilatory coupling. Indeed, the statistical power of NSE of RE interval is higher than that of NSE of RI interval in suggesting the increased dispersion of latency value between heartbeat and respiratory phase onset during STAND compared to REST. As represented in Figure 4.9, the PRQ index increased under orthostatic stress. The change from REST to STAND is generally associated in literature (Scholkmann & Wolf, 2019) with an increase in this ratio, with the magnitude of increase depending on the individual subject and their health status. Values of PRQ in the three training groups were compatible with the range (3–6 beats/breath) usually observed in humans.

Taking together all the above mentioned observations, this thesis concludes that sympathetic activation and vagal withdrawal linked to STAND profoundly limit cardiorespiratory interactions.

5.3.2 Effects of inspiratory muscle training on cardiorespiratory dynamical interactions in amateur athletes

Peak VO_2 estimated at recruitment was found to be similar across all groups and in accordance with values typical of active male subjects. Therefore, it can be hypothesized that the three groups started at similar levels of cardiorespiratory fitness before IMT, and that eventual changes in cardiorespiratory interaction strength after IMT could be attributed to the training protocol itself. Potentially, sufficiently intense IMT could promote central respiratory network modifications through the activation of the afferent pulmonary, atrial and barosensory stretch-activated receptor circuits at the breathing rate during training (Eckberg, 2003). Based on the hypothesis that afferent pathways activated by the stretching of the lung receptors could play a role in setting cardiorespiratory interaction level (Tzeng et al., 2003), it might be expected that IMT of significant intensity (i.e., moderate or high) could produce a PRE-POST difference as a consequence of the strong solicitation of this pathway during training. However, it is worth recalling that athletes are known to have a higher vagal tone than non-trained individuals (Al-Ani et al., 1996), which could reflect in stronger basal cardiorespiratory interactions and this baseline condition could make the detection of post-training improvement of cardiorespiratory interaction strength more difficult.

Analyses of data relevant to protocol 1 indicated no strong effect of IMT and this conclusion held regardless of IMT intensity. Indeed, no significant PRE-POST change was found by TE (Figure 4.1) and K^2 (Figure 4.4) (de Abreu et al., 2019), as well as by NCCCE (Figure 4.2) and NCCCE normalized by NCI (Figure 4.3). Results shown in Figure 4.5, Figure 4.6 and Figure 4.7 suggest that moderate and high intensity IMT might be not fully ineffective in modifying cardioventilatory coupling (Cairo et al., 2020). As a matter of fact, an increase in variability of latencies between R-wave and EXP was observed during STAND compared to REST solely

after MIP60 and CIP training. This effect might be beneficial given that the increased variability between heartbeat and respiration can be taken as an indicator of a greater flexibility of the cardiorespiratory system (Mazzucco et al., 2017). However, the effect of IMT on cardioventilatory coupling seems to be quite weak given that no direct PRE-POST difference was detected. Concerning cardiorespiratory phase synchronization, IMT influences on SYNC% (Figure 4.8) seem to be very weak as well. Indeed, regardless of the intensity of the IMT no direct difference between SYNC% measured in PRE and POST conditions was detected (Cairo et al., 2020). However, some features might indicate that the effect of IMT on SYNC% was not null. Indeed, if the decrease of SYNC% during STAND was due to vagal withdrawal driven by the reduced venous return and baroreflex unloading, this effect should be expected in all the groups in PRE. Conversely, this decrease was significant exclusively in POST in SHAM and MIP60 groups. This observation might indicate a weak effect of training at medium, and even at negligible, intensity of the IMT and this result seems to be the consequence of the SYNC% increase at REST. The decrease of SYNC% during STAND, observed in SHAM and MIP60 in POST, was not visible in the CIP group. Given the limited SYNC% at REST in the CIP group, the lack of STAND-REST difference in POST could be a drawback of the high intensity IMT or a sort of overtraining experienced by this group. The PRQ is the unique marker of the cardiorespiratory interactions directly evidencing a significant PRE-POST change. Indeed, PRQ significantly increase during POST compared to PRE during STAND. This finding was detected only in the CIP group and it should be considered a negative effect of high intensity IMT. Indeed, it might indicate the need of a greater sympathetic tone resulting in a higher HR to cope with postural challenge and a more reactive response of sympathetic control to stressors after CIP training.

Taking into account all the above mentioned observations, this thesis concludes that the impact of IMT on cardiorespiratory interactions is quite limited and this conclusion held regardless of the training intensity. This limited impact is observable also at the level of vagal control, given that only MIP60 induced a significant increase of the respiratory sinus arrhythmia and this effect was visible exclusively at REST (de Abreu et al., 2019). Thus, we hypothesise that training modalities with a more evident impact on cardiac vagal control might be more helpful than IMT in modifying cardiorespiratory phase synchronization. This hypothesis should be tested in future studies by comparing SYNC% after IMT with SYNC% derived after different types of trainings (e.g., aerobic or resistance training).

5.4 Prolonged Head-Down Bed Rest in Healthy Adults: Discussion of experimental results

5.4.1 Effects of passive tilt test on cardiorespiratory dynamical interactions in healthy volunteers

Considerations relevant to the response to TILT in protocol 2 are similar to those reported in Sect.5.3.1 regarding to the effect of STAND in protocol 1 on the strength of cardiorespiratory interactions in healthy subjects. More specifically, a trend toward a decrease in TE and K^2 during TILT (Figures 4.10 and 4.12) indicates weaker linear cardiorespiratory interactions, using both causal and non-causal approaches respectively, in response to an orthostatic stressor. This conclusion was confirmed by the increase of the normalization of NCCCE by NCI during TILT, while NCCCE was weaker in detecting REST-TILT changes (Figure 4.11). Regarding cardioventilatory coupling indexes, the NSE of RE and RI intervals indicated a tendency toward

an increased dispersion of the latency between heartbeat and respiratory phase onsets during TILT with respect to REST and this conclusion was consistently achieved across all four indexes (Figure 4.13). Taking together the results of protocol 1 and 2, this thesis supports the hypothesis that cardioventilatory coupling indexes are generally susceptible to sympathetic activation and vagal withdrawal caused by postural change. As to phase synchronization, SYNC% decreased to 0 in all subjects during TILT (Figure 4.14) even though this decrease was not sufficiently relevant to become significant, mainly due to the limited value of SYNC% found at REST. Finally, the PRQ index (Figure 4.15) exhibited the expected increase induced by orthostatic stress and this difference was more evident after HDBR.

Taking together all the above mentioned observations, this thesis concludes sympathetic activation and vagal withdrawal linked to TILT have a sizable impact on cardiorespiratory interactions. Results are in agreement with those collected in the protocol 1 during STAND but in this specific protocol the influence of the orthostatic stimulus appears to be less strong as denoted by more limited statistical power of the REST-TILT changes, thus suggesting that the effects of postural stimulus on the cardiorespiratory interactions of amateur athletes might be stronger than those in normal healthy subjects of similar age.

5.4.2 Effects of deconditioning induced by prolonged head-down bed rest on cardiorespiratory dynamical interactions in healthy volunteers

It has been demonstrated in the same cohort (Barbic et al., 2019) that prolonged HDBR has significant effects on sympathetic outflow, measured by muscle sympathetic nerve activity. Interestingly, the increase in sympathetic activity after HDBR was not sufficient to produce important tonic and phasic vasomotor responses. Furthermore, a significant decrease of orthostatic tolerance and impairment of the sympathetic baroreflex control were reported due to deconditioning (Barbic et al., 2019; Cairo et al., 2019).

The deconditioning caused by prolonged HDBR does not seem to affect the strength of cardiorespiratory interactions in a significant way. Indeed, a robust tendency of TE, NCCCE, NCCCE/NCI, K^2, cardioventilatory coupling indexes and SYNC% in directly differentiating PRE and POST sessions was not evident (Figures 4.10, 4.11, 4.12, 4.13 and 4.14). The unique index that might suggest some effect of HDBR was the PRQ marker. Indeed, only in POST sessions a significant REST-STAND difference was detected (Figure 4.15). However, this effect seems to be more related to the rise of HR associated to deconditioning (Eckberg et al., 2010; Ertl et al., 2002; Levine et al., 2002) than to a real alteration of the cardiorespiratory interaction mechanisms.

5.5 Postural Orthostatic Tachycardia Syndrome Patients: Discussion of experimental results

5.5.1 Effects of passive tilt test on cardiorespiratory dynamical interactions in POTS patients

The POTS population is characterized by an increased sympathetic drive that is manifest even at REST. In spite of this situation, trends of all indexes confirm that TILT was capable of reducing cardiorespiratory interaction strength. Indeed, TE (Figure 4.16) and K^2 (Figure 4.18) tended to decrease during TILT compared to REST. More important REST-TILT changes were detected by NCCCE divided by NCI (Figure 4.17), NSE of RE and RI intervals (Figure 4.19)

and PRQ (Figure 4.21). Consistently with protocols 1 and 2, postural stressor increased NCCCE divided by NCI, NSE of RE and RI intervals and PRQ. These findings stress that these markers can be used not only in healthy individuals but also in pathological subjects to characterize cardiorespiratory interaction strength. Indeed, the considered indexes can preserve their ability in distinguishing experimental conditions even in groups that might exhibit lower magnitude of the cardiorespiratory link due to a higher sympathetic drive. Unfortunately, the lack of a healthy age- and gender-matched group did not allow the check of the conjecture that the exploited markers in POTS groups could be consistently lower that those measured in a control population. SYNC% (Figure 4.20) denoted the weakest ability in separating REST from STAND mainly due to its limited values at REST (less than 1%). The negligible values of SYNC% at REST are consistent with the notion that POTS leads to an increased sympathetic tone. The significant increase of PRQ observed during TILT is compatible with the aberrant response to postural stressor of the POTS group, which leads to an abnormal HR rise accompanied by a non-significant change in respiratory frequency (Thieben et al., 2007).

Taking together all the above mentioned observations, this thesis concludes that, in a pathological population featuring an augmented sympathetic drive, cardiorespiratory interaction magnitude can be reduced by a challenge evoking an additional sympathetic response and the considered markers can be fruitfully exploited to typify these changes.

5.5.2 Effects of clinical management of POTS patients on cardiorespiratory dynamical interactions

As demonstrated by the values of catecholamines reported in Table 3.1 and Table 3.2, the cohort of patients under study shows an unmodified neurohormonal control after one year FOLLOW-UP both during REST and TILT. No differences between BASELINE and FOLLOW-UP values either at REST or during TILT were detected when TE, NCCCE, K^2, SYNC% or PRQ were considered (Figures 4.16, 4.17, 4.18, 4.20 and 4.21). As such, this thesis concludes that the clinical management of symptoms seems to be able to limit the progression of the pathology, which might otherwise lead to a worsening of cardiorespiratory interaction magnitude after one year. However, clinical management was also unable to improve cardiorespiratory functioning. This result is in agreement with (Dipaola et al., 2020), which suggests that symptoms in these patients remain substantially stable over two years of observation. The sole marker that presented a change one year later was the NSE of the RI interval: indeed, at REST it increased in the FOLLOW-UP session compared to BASELINE. This result indicated an increased uncoupling between heartbeat and R and, as such, seems to suggest a negative evolution of the disease in spite of the clinical management of patients. Since over the same group, the patients did report a perceived improvement over time in the overall symptomatic burden, as well as in the perception of quality of life, as evaluated through questionnaires (Dipaola et al., 2020), this negative situation might be revealed by some of the considered indexes such as the NSE of RI.

Taking together all the above mentioned observations, this thesis concludes that the proposed indexes can be usefully employed to monitor overtime certain aspects of cardiorespiratory interactions in a pathological population featuring an augmented sympathetic drive.

CHAPTER 6 - Conclusions

The aim of this doctoral dissertation is to describe and quantify cardiorespiratory interactions in different scenarios of health and disease by employing a variety of methods of bivariate analysis taken from literature and optimized for the present application. The evaluation of cardiorespiratory interactions is based on the computation of TE, NCCCE, K^2, NSE of RE and RI intervals, SYNC% and PRQ. The simultaneous computation of all these markers allows for the evaluation of different aspects of cardiorespiratory interactions. The methodologies were applied in different protocols carried out in healthy and pathological individuals. More specifically, the markers were computed in young healthy athletes undergoing IMT protocols expected to strengthen cardiorespiratory interactions, in healthy subjects undergoing a deconditioning protocol (i.e., prolonged HDBR) which was expected to increase the baseline values of sympathetic activity, and in dysautonomic patients exhibiting an exaggerated sympathetic drive and abnormal cardiac response to postural stimulus. The conclusions are divided into methodological and experimental and listed in Sects.6.1 and 6.2 respectively.

6.1 Methodological conclusions

Several methods were employed in the present thesis to quantify the magnitude of cardiorespiratory interactions. They were applied on the beat-to-beat variability series of HP and R signal and on the event series of heartbeat occurrence and respiratory phase onsets. The methods evaluate different aspects of cardiorespiratory interactions because they compute diverse metrics and have different characteristics. In particular, some indexes account for causality by evaluating the interactions along a specific temporal direction (e.g., TE assesses the R-RR interactions from R to RR), while others assess interactions regardless of temporal direction (e.g., K^2). Some markers are based on linear models (e.g., TE and K^2), while others are model-free and can describe nonlinear relations between RR and R (e.g., NCCCE). Some indexes account for interactions involving amplitude and phase of the RR variability and R signal (e.g., TE, K^2 and NCCCE), while others are more specific and describe only phase interactions among event series (i.e., SYNC% and NSE of RE and RI intervals). Some markers are defined in the time domain (e.g., PRQ), while others are defined in frequency (i.e., K^2) and information domain (i.e., TE and NCCCE). Some markers are specifically devoted to assessing the degree of phase synchronization occurring according to specific complex phase locking patterns (i.e., SYNC%), while others have more limited abilities and only describe the frequency coupling phenomenon (i.e., PRQ). The common characteristic of the indexes is that they are calculated over two signals, namely the beat-to-beat RR variability and the R signal or the event series of heartbeats derived from the ECG and the INSP and EXP series, derived from the R signal. This characteristic makes all these approaches applicable with limited hardware resources even outside the well-controlled conditions of the research laboratory and during daily activities. The minimal requirement is an ECG recorder given that the R signal can be easily derived from the variation of the amplitude of the main electrocardiographic waveforms (i.e., QRS complex and T-wave). This observation, together with the limited computational resources required by the algorithms exploited for the computation of indexes, favour the

practical application of the proposed framework and the simultaneous computation of all indexes.

This thesis stresses the relevance of the concurrent computation of all the indexes because they measure different aspects of the cardiorespiratory dynamical interactions. This conclusion is corroborated by the different statistical power of the indexes in detecting the effect of postural challenge and the consequence of an intervention such as training, deconditioning procedure or clinical management. Moreover, the thesis stresses the importance of applying specific procedures to make the computation of markers more robust. For example, the optimization of SYNC% allows its computation without the need of an arbitrary assignment of the threshold below which heartbeat and R are deemed to be synchronized, thus favouring automatic analyses. Additionally, the normalization of NCCCE from R to RR by the NCI of RR allows for a better identification of the cardiorespiratory uncoupling induced by an orthostatic challenge, by limiting the detrimental effect of the decreased complexity of the RR (Porta et al., 2016). Furthermore, this thesis highlights the relevance of using different fiducial points in assessing phase coupling between heartbeat and R. Indeed, results of NSE computed over RE and RI intervals are different, thus suggesting that mechanisms of cardioventilatory coupling governing the link of heartbeat to EXP and INSP could be distinct. Remarkably, in previous studies INSP events have been preferred due to their more robust delineation compared to the EXP ones. Based on these results, the reliability of R phase onsets is not the unique factor that should be considered in deciding which type of respiratory onset ought to be used in cardioventilatory coupling strength assessment (Cairo et al., 2020b).

6.2 Experimental conclusions

All methodologies were applied in protocols of respiratory training and deconditioning in healthy subjects and in a cohort of dysautonomic patients. Different experimental manoeuvres and physiological or clinical interventions were exploited to induce a modification of the cardiorespiratory interactions secondary to a variation of the sympathetic drive. Among the physiological manoeuvres known to strongly increase the sympathetic drive, STAND and TILT were employed. Among the physiological interventions, IMT could potentially reduce sympathetic activity and/or affect directly cardiorespiratory mechanisms, while the deconditioning induced by HDBR increases sympathetic drive. Clinical management of POTS patients could potentially reduce the sympathetic drive in this population exhibiting an abnormally high sympathetic control in baseline condition. This thesis stresses that all indexes gave a coherent view about the effect of postural stimuli on cardiorespiratory interactions in health and disease. Indeed, in all protocols cardiorespiratory interaction strength decreased in response to the orthostatic challenge. However, the statistical power of the indexes was different. TE and K^2 appeared to be particularly weak in detecting the effect of postural challenge on cardiorespiratory interactions. NCCCE divided by NCI, NSE of RE and RI interval and SYNC% exhibited much stronger ability in this regard, while PRQ seemed to be too closely related to HR in presence of no significant modification of the respiratory rate. Conversely, all indexes appeared to be weak in detecting the chronic effects of IMT and HDBR on a healthy population and the long-term consequences of the clinical management in POTS patients. The thesis concludes that the different aspects of cardiorespiratory interactions can be

modified acutely but the chronic effects of a long-term treatment or intervention on the magnitude of cardiorespiratory interactions are negligible and/or could be confused with the variability of markers.

6.3 Future Developments

The present doctoral dissertation highlighted a number of areas in which further research would be beneficial.

The methods employed in the present work do not take into account the dynamical properties of cardiorespiratory interactions during transients triggered by a specific stimulus. Therefore, the employed methodologies could be adapted to be time-variant in order to study their evolution during a specific experimental condition. Some of the employed methodologies have already been adapted for these applications, i.e. model-based methods such as squared coherence (Cerutti et al., 2001).

In addition, it is necessary to highlight that the use of HRV measures to study the sympathovagal influence on cardiorespiratory interactions could potentially overstate the effect of vagal contributions with respect to sympathetic ones, as HRV is more intrinsically linked to vagal control (Pomeranz et al., 1985). Therefore, for a more complete understanding of the phenomena described in the present thesis, in the future it will be necessary to accompany ECG and respiratory activity recordings to simultaneous direct recordings of sympathetic activity (e.g. muscle sympathetic nerve activity via microneurography) in order to verify our hypothesis of predominant sympathetic influence over cardiorespiratory interactions.

Furthermore, due to the complexity of the mechanisms responsible for cardiorespiratory interactions, the origin of the observed phenomena and their dependence on respiratory patterns remains partially unclear. In the future, the mutual association between different cardiorespiratory interaction indexes could be evaluated through correlation analysis, as well as the relationship between cardiorespiratory interaction measures and respiratory sinus arrhythmia amplitude or respiratory rate.

Finally, respiration analysis could be complemented by the acquisition of different respiratory signals, to clarify whether conclusions might vary depending on the types of monitored variable (e.g. flow, volume, diaphragmatic activity or respiratory movements).

Bibliography

Abreu, R. M. de, Catai, A. M., Cairo, B., Rehder-Santos, P., Silva, C. D. da, Signini, É. D. F., Sakaguchi, C. A., & Porta, A. (2020). A Transfer Entropy Approach for the Assessment of the Impact of Inspiratory Muscle Training on the Cardiorespiratory Coupling of Amateur Cyclists. *Frontiers in Physiology*, *11*. https://doi.org/10.3389/fphys.2020.00134

Ahn, S., & Rubchinsky, L. L. (2013). Fine temporal structure of neural synchronization. *BMC Neuroscience*, *14*(317), 1–2. https://doi.org/10.1186/1471-2202-14-s1-p336

Akaike, H. (1974). A New Look at the Statistical Model Identification. *IEEE Transactions on Automatic Control*, *19*(6), 716–723. https://doi.org/10.1109/TAC.1974.1100705

Al-Ani, M., Munir, S. M., White, M., Townend, J., & Coote, J. H. (1996). Changes in R-R variability before and after endurance training measured by power spectral analysis and by the effect of isometric muscle contraction. *European Journal of Applied Physiology and Occupational Physiology*, *74*(5), 397–403. https://doi.org/10.1007/BF02337719

Allen, C., Glasziou, P., & del Mar, C. (1999). Bed rest: A potentially harmful treatment needing more careful evaluation. *Lancet*, *354*(9186), 1229–1233. https://doi.org/10.1016/S0140-6736(98)10063-6

Baekey, D. M., Dick, T. E., & Paton, J. F. R. (2008). Pontomedullary transection attenuates central respiratory modulation of sympathetic discharge, heart rate and the baroreceptor reflex in the *in situ* rat preparation. *Experimental Physiology*, *93*(7), 803–816. https://doi.org/10.1113/expphysiol.2007.041400

Bagai, K., Song, Y., Ling, J. F., Malow, B., Black, B. K., Biaggioni, I., Robertson, D., & Raj, S. R. (2011). Sleep disturbances and diminished quality of life in postural tachycardia syndrome. *Journal of Clinical Sleep Medicine*, *7*(2), 204–210. https://doi.org/10.5664/jcsm.28110

Barbic, F., Minonzio, M., Cairo, B., Shiffer, D., Zamuner, A. R., Cavalieri, S., Dipaola, F., Magnavita, N., Porta, A., & Furlan, R. (2020). Work ability assessment and its relationship with cardiovascular autonomic profile in postural orthostatic tachycardia syndrome. *International Journal of Environmental Research and Public Health*, *17*(21). https://doi.org/10.3390/ijerph17217836

Barbic, F., Heusser, K., Minonzio, M., Shiffer, D., Cairo, B., Tank, J., Jordan, J., Diedrich, A., Gauger, P., Zamuner, R. A., Porta, A., & Furlan, R. (2019). Effects of Prolonged Head-Down Bed Rest on Cardiac and Vascular Baroreceptor Modulation and Orthostatic Tolerance in Healthy Individuals. *Frontiers in Physiology*, *10*, 1061. https://doi.org/10.3389/fphys.2019.01061

Bari, V., de Maria, B., Mazzucco, C. E., Rossato, G., Tonon, D., Nollo, G., Faes, L., & Porta, A. (2017). Cerebrovascular and cardiovascular variability interactions investigated through conditional joint transfer entropy in subjects prone to postural syncope. *Physiological Measurement*, *38*(5), 976–991. https://doi.org/10.1088/1361-6579/aa638c

Barnett, L., Barrett, A. B., & Seth, A. K. (2009). Granger causality and transfer entropy Are equivalent for gaussian variables. *Physical Review Letters*, *103*(23). https://doi.org/10.1103/PhysRevLett.103.238701

Bartsch, R. P., Kantelhardt, J. W., Penzel, T., & Havlin, S. (2007). Experimental evidence for phase synchronization transitions in the human cardiorespiratory system. *Physical Review Letters*, *98*(5), 054102. https://doi.org/10.1103/PhysRevLett.98.054102

Bartsch, R. P., Schumann, A. Y., Kantelhardt, J. W., Penzel, T., & Ivanov, P. C. (2012). Phase transitions in physiologic coupling. *Proceedings of the National Academy of Sciences of the United States of America*, *109*(26), 10181–10186. https://doi.org/10.1073/pnas.1204568109

Baselli, G., Porta, A., & Cerutti, S. (1997). Spectral decomposition in multichannel recordings based on multivariate parametric identification. *IEEE Transactions on Biomedical Engineering*, *44*(11), 1092–1101. https://doi.org/10.1109/10.641336

Benarroch, E. E. (2012). Postural tachycardia syndrome: A heterogeneous and multifactorial disorder. In *Mayo Clinic Proceedings* (Vol. 87, Issue 12, pp. 1214–1225). Elsevier Ltd. https://doi.org/10.1016/j.mayocp.2012.08.013

Ben-Tal, A. (2012). Computational models for the study of heart-lung interactions in mammals. In *Wiley Interdisciplinary Reviews: Systems Biology and Medicine* (Vol. 4, Issue 2, pp. 163–170). NIH Public Access. https://doi.org/10.1002/wsbm.167

Ben-Tal, A., Shamailov, S. S., & Paton, J. F. R. (2012). Evaluating the physiological significance of respiratory sinus arrhythmia: Looking beyond ventilation-perfusion efficiency. *Journal of Physiology*, *590*(8), 1989–2008. https://doi.org/10.1113/jphysiol.2011.222422

Bettermann, H., Cysarz, D., & van Leeuwen, P. (2002). Comparison of two different approaches in the detection of intermittent cardiorespiratory coordination during night sleep. *BMC Physiology*, *2*, 1–17. https://doi.org/10.1186/1472-6793-2-1

Buehlmeier, J., Mulder, E., Noppe, A., Frings-Meuthen, P., Angerer, O., Rudwill, F., Biolo, G., Smith, S. M., Blanc, S., & Heer, M. (2014). A combination of whey protein and potassium bicarbonate supplements

during head-down-tilt bed rest: Presentation of a multidisciplinary randomized controlled trial (MEP study). *Acta Astronautica*, *95*(1), 82–91. https://doi.org/10.1016/j.actaastro.2013.11.001

Cairo, B., de Maria, B., Bari, V., Vaini, E., Heusser, K., Tank, J., Jordan, J., Barbic, F., Furlan, R., Marinou, K., Dalla Vecchia, L., & Porta, A. (2019). Information-domain method for the quantification of the complexity of the sympathetic baroreflex regulation in healthy subjects and amyotrophic lateral sclerosis patients. *Physiological Measurement*, *40*(3). https://doi.org/10.1088/1361-6579/ab0d4b

Cairo, B., Abreu, R. M., Bari, V., de Maria, B., Vaini, E., Rehder-Santos, P., Sakaguchi, C. A., Silva, C. D., Signini, E. F., Catai, A. M., & Porta, A. (2020, July 1). Effects of Inspiratory Muscle Training and Postural Challenge on Cardiorespiratory Coupling in Amateur Athletes. *2020 11th Conference of the European Study Group on Cardiovascular Oscillations: Computation and Modelling in Physiology: New Challenges and Opportunities, ESGCO 2020*. https://doi.org/10.1109/ESGCO49734.2020.9158142

Cairo, B., Abreu, R. M., Bari, V., Gelpi, F., de Maria, B., Rehder-Santos, P., Sakaguchi, C. A., Silva, C. D., Favari Signini, É., Catai, A. M., & Porta, A. (2020). Optimizing phase variability threshold for automated synchrogram analysis of cardiorespiratory interactions in amateur cyclists. *Philosophical Transactions of the Royal Society A: Mathematical, Physical and Engineering Sciences*, *Accepted*.

Cerutti, S., Bianchi, A. M., & Mainardi, L. T. (2001). Advanced spectral methods for detecting dynamic behaviour. *Autonomic Neuroscience: Basic and Clinical*, *90*(1–2), 3–12. https://doi.org/10.1016/S1566-0702(01)00261-2

Cogliati, C., Colombo, S., Gnecchi Ruscone, T., Gruosso, D., Porta, A., Montano, N., Malliani, A., & Furlan, R. (2004). *Acute-Blockade Increases Muscle Sympathetic Activity and Modifies Its Frequency Distribution*. https://doi.org/10.1161/01.CIR.0000146335.69413.F9

Cysarz, D., Bettermann, H., Lange, S., Geue, D., & van Leeuwen, P. (2004). A quantitative comparison of different methods to detect cardiorespiratory coordination during night-time sleep. *BioMedical Engineering Online*, *3*, 1–13. https://doi.org/10.1186/1475-925X-3-44

Cysarz, D., & Büssing, A. (2005). Cardiorespiratory synchronization during Zen meditation. *European Journal of Applied Physiology*, *95*(1), 88–95. https://doi.org/10.1007/s00421-005-1379-3

Dalla Vecchia, L., de Maria, B., Marinou, K., Sideri, R., Lucini, A., Porta, A., & Mora, G. (2015). Cardiovascular neural regulation is impaired in amyotrophic lateral sclerosis patients. A study by spectral and complexity analysis of cardiovascular oscillations. *Physiological Measurement*, *36*(4), 659–670. https://doi.org/10.1088/0967-3334/36/4/659

de Abreu, R. M., Porta, A., Rehder-Santos, P., Cairo, B., da Silva, C. D., de Favari Signini, É., Sakaguchi, C. A., & Catai, A. M. (2019). Effects of inspiratory muscle-training intensity on cardiovascular control in amateur cyclists. *American Journal of Physiology - Regulatory Integrative and Comparative Physiology*, *317*(6), R891–R902. https://doi.org/10.1152/ajpregu.00167.2019

de Abreu, R. M., Rehder-Santos, P., Minatel, V., dos Santos, G. L., & Catai, A. M. (2017). Effects of inspiratory muscle training on cardiovascular autonomic control: A systematic review. In *Autonomic Neuroscience: Basic and Clinical* (Vol. 208, pp. 29–35). Elsevier B.V. https://doi.org/10.1016/j.autneu.2017.09.002

de Meersman, R. E. (1992). Respiratory sinus arrhythmia alteration following training in endurance athletes. *European Journal of Applied Physiology and Occupational Physiology*, *64*(5), 434–436. https://doi.org/10.1007/BF00625063

Diedrich, A., Mandsager, K. T., & Robertson, D. (2015). Orthostatic intolerance and vasovagal syncope after spaceflight. In *Vasovagal Syncope* (pp. 309–317). Springer International Publishing. https://doi.org/10.1007/978-3-319-09102-0_26

Diedrich, A., Paranjape, S. Y., & Robertson, D. (2007). Plasma and blood volume in space. *American Journal of the Medical Sciences*, *334*(1), 80–86. https://doi.org/10.1097/MAJ.0b013e318065b89b

Dipaola, F., Barberi, C., Castelnuovo, E., Minonzio, M., Fornerone, R., Shiffer, D., Cairo, B., Zamuner, A. R., Barbic, F., & Furlan, R. (2020). Time course of autonomic symptoms in postural orthostatic tachycardia syndrome (Pots) patients: Two-year follow-up results. *International Journal of Environmental Research and Public Health*, *17*(16), 1–13. https://doi.org/10.3390/ijerph17165872

Dock, W. (1944). The evil sequelae of complete bed rest. *Journal of the American Medical Association*, *125*(16), 1083–1085. https://doi.org/10.1001/jama.1944.02850340009004

Eckberg, D. L. (1983). Human sinus arrhythmia as an index of vagal cardiac outflow. *Journal of Applied Physiology Respiratory Environmental and Exercise Physiology*, *54*(4), 961–966. https://doi.org/10.1152/jappl.1983.54.4.961

Eckberg, D. L. (2003). The human respiratory gate. *Journal of Physiology*, *548*(2), 339–352. https://doi.org/10.1113/jphysiol.2002.037192

Eckberg, D. L., Halliwill, J. R., Beightol, L. A., Brown, T. E., Taylor, J. A., & Goble, R. (2010). Human vagal baroreflex mechanisms in space. *The Journal of Physiology*, *588*(7), 1129–1138. https://doi.org/10.1113/jphysiol.2009.186650

Elstad, M., O'Callaghan, E. L., Smith, A. J., Ben-Tal, A., & Ramchandra, R. (2018). Cardiorespiratory interactions in humans and animals: Rhythms for life. *American Journal of Physiology - Heart and Circulatory Physiology*, *315*(1), H6–H17. https://doi.org/10.1152/ajpheart.00701.2017

Elstad, M., Toska, K., Chon, K. H., Raeder, E. A., & Cohen, R. J. (2001). Respiratory sinus arrhythmia: Opposite effects on systolic and mean arterial pressure in supine humans. *Journal of Physiology*, *536*(1), 251–259. https://doi.org/10.1111/j.1469-7793.2001.t01-1-00251.x

Elstad, M., Walløe, L., Holme, N. L. A., Maes, E., & Thoresen, M. (2015). Respiratory sinus arrhythmia stabilizes mean arterial blood pressure at high-frequency interval in healthy humans. *European Journal of Applied Physiology*, *115*(3), 521–530. https://doi.org/10.1007/s00421-014-3042-3

Ertl, A. C., Diedrich, A., Biaggioni, I., Levine, B. D., Robertson, R. M., Cox, J. F., Zuckerman, J. H., Pawelczyk, J. A., Ray, C. A., Buckey, J. C., Lane, L. D., Shiavi, R., Gaffney, F. A., Costa, F., Holt, C., Blomqvist, C. G., Eckberg, D. L., Baisch, F. J., & Robertson, D. (2002). Human muscle sympathetic nerve activity and plasma noradrenaline kinetics in space. *The Journal of Physiology*, *538*(1), 321–329. https://doi.org/10.1113/jphysiol.2001.012576

Farmer, D. G. S., Dutschmann, M., Paton, J. F. R., Pickering, A. E., & McAllen, R. M. (2016). Brainstem sources of cardiac vagal tone and respiratory sinus arrhythmia. *Journal of Physiology*, *594*(24), 7249–7265. https://doi.org/10.1113/JP273164

Feldstein, C., & Weder, A. B. (2012). Orthostatic hypotension: A common, serious and underrecognized problem in hospitalized patients. In *Journal of the American Society of Hypertension* (Vol. 6, Issue 1, pp. 27–39). Elsevier. https://doi.org/10.1016/j.jash.2011.08.008

Ferreira, J. B., Plentz, R. D. M., Stein, C., Casali, K. R., Arena, R., & Lago, P. D. (2013). Inspiratory muscle training reduces blood pressure and sympathetic activity in hypertensive patients: A randomized controlled trial. *International Journal of Cardiology*, *166*(1), 61–67. https://doi.org/10.1016/j.ijcard.2011.09.069

Freeman, R., Wieling, W., Axelrod, F. B., Benditt, D. G., Benarroch, E., Biaggioni, I., Cheshire, W. P., Chelimsky, T., Cortelli, P., Gibbons, C. H., Goldstein, D. S., Hainsworth, R., Hilz, M. J., Jacob, G., Kaufmann, H., Jordan, J., Lipsitz, L. A., Levine, B. D., Low, P. A., … van Dijk, J. G. (2011). Consensus statement on the definition of orthostatic hypotension, neurally mediated syncope and the postural tachycardia syndrome. *Clinical Autonomic Research*, *21*(2), 69–72. https://doi.org/10.1007/s10286-011-0119-5

Friedman, L., Dick, T. E., Jacono, F. J., Loparo, K. A., Yeganeh, A., Fishman, M., Wilson, C. G., & Strohl, K. P. (2012). Cardio-ventilatory coupling in young healthy resting subjects. *Journal of Applied Physiology*, *112*(8), 1248–1257. https://doi.org/10.1152/japplphysiol.01424.2010

Furlan, R., Jacob, G., Snell, M., Robertson, D., Porta, A., Harris, P., & Mosqueda-Garcia, R. (1998). Chronic Orthostatic Intolerance. *Circulation*, *98*(20), 2154–2159. https://doi.org/10.1161/01.CIR.98.20.2154

Furlan, R., Porta, A., Costa, F., Tank, J., Baker, L., Schiavi, R., Robertson, D., Malliani, A., & Mosqueda-Garcia, R. (2000). Oscillatory patterns in sympathetic neural discharge and cardiovascular variables during orthostatic stimulus. *Circulation*, *101*(8), 886–892. https://doi.org/10.1161/01.CIR.101.8.886

Galletly, D. C., & Larsen, P. D. (1997). Cardioventilatory coupling during anaesthesia. *British Journal of Anaesthesia*, *79*(1), 35–40. https://doi.org/10.1093/bja/79.1.35

Galletly, D. C., & Larsen, P. D. (2001). Inspiratory timing during anaesthesia: A model of cardioventilatory coupling. *British Journal of Anaesthesia*, *86*(6), 777–788. https://doi.org/10.1093/bja/86.6.777

Galletly, D., & Larsen, P. (1999). Ventilatory frequency variability in spontaneously breathing anaesthetized subjects. *British Journal of Anaesthesia*, *83*(4), 552–563. https://doi.org/10.1093/bja/83.4.552

Gazit, Y., Nahir, A. M., Grahame, R., & Jacob, G. (2003). Dysautonomia in the joint hypermobility syndrome. *American Journal of Medicine*, *115*(1), 33–40. https://doi.org/10.1016/S0002-9343(03)00235-3

Glass, L., & Mackey, M. C. (1988). *From Clocks to Chaos. The Rhythms of Life.* Princeton University Press.

Goldstein, D. S., Robertson, D., Esler, M., Straus, S. E., & Eisenhofer, G. (2002). Dysautonomias: Clinical disorders of the autonomic nervous system. *Annals of Internal Medicine*, *137*(9), 753–763. https://doi.org/10.7326/0003-4819-137-9-200211050-00011

Guérin, A., Bureau, M. L., Ghazali, N., Gervais, R., Liuu, E., Seité, F., Bellarbre, F., Ingrand, P., & Paccalin, M. (2016). Factors associated with orthostatic hypotension in hospitalized elderly patients. *Aging Clinical and Experimental Research*, *28*(3), 513–517. https://doi.org/10.1007/s40520-015-0451-z

Hajghanbari, B., Yamabayashi, C., Buna, T. R., Coelho, J. D., Freedman, K. D., Morton, T. A., Palmer, S. A., Toy, M. A., Walsh, C., Sheel, A. W., & Reid, W. D. (2013). Effects of respiratory muscle training on performance in athletes: A systematic review with meta-analyses. In *Journal of Strength and Conditioning Research* (Vol. 27, Issue 6, pp. 1643–1663). J Strength Cond Res. https://doi.org/10.1519/JSC.0b013e318269f73f

Hamann, C., Bartsch, R. P., Schumann, A. Y., Penzel, T., Havlin, S., & Kantelhardt, J. W. (2009). Automated synchrogram analysis applied to heartbeat and reconstructed respiration. *Chaos*, *19*(1), 015106. https://doi.org/10.1063/1.3096415

Hayano, J., & Yasuma, F. (2003). Hypothesis: Respiratory sinus arrhythmia is an intrinsic resting function of cardiopulmonary system. In *Cardiovascular Research* (Vol. 58, Issue 1, pp. 1–9). Cardiovasc Res. https://doi.org/10.1016/S0008-6363(02)00851-9

Hayano, J., Yasuma, F., Okada, A., Mukai, S., & Fujinami, T. (1996). Respiratory Sinus Arrhythmia. *Circulation*, *94*(4), 842–847. https://doi.org/10.1161/01.CIR.94.4.842

Hellman, J. B., & Stacy, R. W. (1976). Variation of respiratory sinus arrhythmia with age. *Journal of Applied Physiology*, *41*(5 (I)), 734–738. https://doi.org/10.1152/jappl.1976.41.5.734

Hirsch, J. A., & Bishop, B. (1981). Respiratory sinus arrhythmia in humans: How breathing pattern modulates heart rate. *American Journal of Physiology - Heart and Circulatory Physiology*, *10*(4), 620–629. https://doi.org/10.1152/ajpheart.1981.241.4.h620

Jerath, R., Harden, K., Crawford, M., Barnes, V. A., & Jensen, M. (2014). Role of cardiorespiratory synchronization and sleep physiology: Effects on membrane potential in the restorative functions of sleep. *Sleep Medicine*, *15*(3), 279–288. https://doi.org/10.1016/j.sleep.2013.10.017

Jones, P. K., & Gibbons, C. H. (2015). Autonomic function testing: An important diagnostic test for patients with syncope. In *Practical Neurology* (Vol. 15, Issue 5, pp. 346–351). BMJ Publishing Group. https://doi.org/10.1136/practneurol-2015-001102

Juraschek, S. P., Daya, N., Appel, L. J., Miller, E. R., Windham, B. G., Pompeii, L., Griswold, M. E., Kucharska-Newton, A., & Selvin, E. (2017). Orthostatic Hypotension in Middle-Age and Risk of Falls. *American Journal of Hypertension*, *30*(2), 188–195. https://doi.org/10.1093/ajh/hpw108

Karemaker, J. M. (2009). Counterpoint: Respiratory sinus arrhythmia is due to the baroreflex mechanism. *Journal of Applied Physiology*, *106*(5), 1742–1743. https://doi.org/10.1152/japplphysiol.91107.2008a

Katona, P. G., & Jih, F. (1975). Respiratory sinus arrhythmia: noninvasive measure of parasympathetic cardiac control. *Journal of Applied Physiology*, *39*(5), 801–805. https://doi.org/10.1152/jappl.1975.39.5.801

Kavi, L., Gammage, M. D., Grubb, B. P., & Karabin, B. L. (2012). Postural tachycardia syndrome: Multiple symptoms, but easily missed. In *British Journal of General Practice* (Vol. 62, Issue 599, pp. 286–287). British Journal of General Practice. https://doi.org/10.3399/bjgp12X648963

Kenner, T., Pessenhofer, H., & Schwaberger, G. (1976). Method for the analysis of the entrainment between heart rate and ventilation rate. *Pflügers Archiv European Journal of Physiology*, *363*(3), 263–265. https://doi.org/10.1007/BF00594612

Kenny, R. A., Bayliss, J., Ingram, A., & Sutton, R. (1986). Head-Up Tilt: a Useful Test for Investigating Unexplained Syncope. *The Lancet*, *3271. Anne*(8494), 1352–1355. https://doi.org/10.1016/S0140-6736(86)91665-X

Kenwright, D. A., Bernjak, A., Draegni, T., Dzeroski, S., Entwistle, M., Horvat, M., Kvandal, P., Landsverk, S. A., McClintock, P. V. E., Musizza, B., Petrovčič, J., Raeder, J., Sheppard, L. W., Smith, A. F., Stankovski, T., & Stefanovska, A. (2015). The discriminatory value of cardiorespiratory interactions in distinguishing awake from anaesthetised states: A randomised observational study. *Anaesthesia*, *70*(12), 1356–1368. https://doi.org/10.1111/anae.13208

Kimpinski, K., Figueroa, J. J., Singer, W., Sletten, D. M., Iodice, V., Sandroni, P., Fischer, P. R., Opfer-Gehrking, T. L., Gehrking, J. A., & Low, P. A. (2012). A prospective, 1-year follow-up study of postural tachycardia syndrome. *Mayo Clinic Proceedings*, *87*(8), 746–752. https://doi.org/10.1016/j.mayocp.2012.02.020

Kirbiš, M., Grad, A., Meglič, B., & Bajrović, F. F. (2013). Comparison of active standing test, head-up tilt test and 24-h ambulatory heart rate and blood pressure monitoring in diagnosing postural tachycardia. *Functional Neurology*, *28*(1), 39–45. https://doi.org/10.11138/FNeur/2013.28.1.039

Krause, H., Kraemer, J. F., Penzel, T., Kurths, J., & Wessel, N. (2017). On the difference of cardiorespiratory synchronisation and coordination. *Chaos*, *27*(9). https://doi.org/10.1063/1.4999352

Lambrecht, R., McNeeley, K., Tusing, L., & Chelimsky, T. (2007). Evaluation of a brief cardiovascular autonomic screen. *Autonomic Neuroscience: Basic and Clinical*, *131*(1–2), 102–106. https://doi.org/10.1016/j.autneu.2006.07.001

Lei, L. Y., Chew, D. S., Sheldon, R. S., & Raj, S. R. (2019). Evaluating and managing postural tachycardia syndrome. In *Cleveland Clinic Journal of Medicine* (Vol. 86, Issue 5, pp. 333–344). Cleveland Clinic Educational Foundation. https://doi.org/10.3949/ccjm.86a.18002

Levine, B. D., Pawelczyk, J. A., Ertl, A. C., Cox, J. F., Zuckerman, J. H., Diedrich, A., Biaggioni, I., Ray, C. A., Smith, M. L., Iwase, S., Saito, M., Sugiyama, Y., Mano, T., Zhang, R., Iwasaki, K., Lane, L. D., Buckey, J. C., Cookeh, W. H., Baisch, F. J., … Blomqvist, C. G. (2002). Human muscle sympathetic neural and haemodynamic responses to tilt following spaceflight. *Journal of Physiology*, *538*(1), 331–340. https://doi.org/10.1113/jphysiol.2001.012575

Lopes, O. U., & Palmer, J. F. (1976). Proposed respiratory "gating" mechanism for cardiac slowing. *Nature*, *264*(5585), 454–456. https://doi.org/10.1038/264454a0

Lotrič, M. B., & Stefanovska, A. (2000). Synchronization and modulation in the human cardiorespiratory system. *Physica A: Statistical Mechanics and Its Applications*, *283*(3), 451–461. https://doi.org/10.1016/S0378-4371(00)00204-1

Magagnin, V., Bassani, T., Bari, V., Turiel, M., Maestri, R., Pinna, G. D., & Porta, A. (2011). Non-stationarities significantly distort short-term spectral, symbolic and entropy heart rate variability indices. *Physiological Measurement*, *32*(11), 1775–1786. https://doi.org/10.1088/0967-3334/32/11/S05

Mazzucco, C. E., Marchi, A., Bari, V., de Maria, B., Guzzetti, S., Raimondi, F., Catena, E., Ottolina, D., Amadio, C., Cravero, S., Fossali, T., Colombo, R., & Porta, A. (2017). Mechanical ventilatory modes and cardioventilatory phase synchronization in acute respiratory failure patients. *Physiological Measurement*, *38*(5), 895–911. https://doi.org/10.1088/1361-6579/aa56ae

McGuinness, M., Hong, Y., Galletly, D., & Larsen, P. (2004). Arnold tongues in human cardiorespiratory systems. *Chaos*, *14*(1), 1–6. https://doi.org/10.1063/1.1620990

McIntyre, H. (2013). Admission to hospital could be considered a disease. In *BMJ (Online)* (Vol. 346, Issue 7909). British Medical Journal Publishing Group. https://doi.org/10.1136/bmj.f3242

Mello, P. R., Guerra, G. M., Borile, S., Rondon, M. U., Alves, M. J., Negrão, C. E., Dal Lago, P., Mostarda, C., Irigoyen, M. C., & Consolim-Colombo, F. M. (2012). Inspiratory muscle training reduces sympathetic nervous activity and improves inspiratory muscle weakness and quality of life in patients with chronic heart failure. *Journal of Cardiopulmonary Rehabilitation and Prevention*, *32*(5), 255–261. https://doi.org/10.1097/HCR.0b013e31825828da

Mokri, B., & Low, P. A. (2003). Orthostatic headaches without CSF leak in postural tachycardia syndrome. *Neurology*, *61*(7), 980–982. https://doi.org/10.1212/01.WNL.0000085868.37963.7D

Montano, N., Ruscone, T. G., Porta, A., Lombardi, F., Pagani, M., & Malliani, A. (1994). Power spectrum analysis of heart rate variability to assess the changes in sympathovagal balance during graded orthostatic tilt. *Circulation*, *90*(4 I), 1826–1831. https://doi.org/10.1161/01.CIR.90.4.1826

Moser, M., Voica, M., Kenner, T., Lehofer, M., Egner, S., & Hildebrandt, G. (1995). Phase- and Frequency Coordination of Cardiac and Respiratory Function. *Biological Rhythm Research*, *26*(1), 100–111. https://doi.org/10.1080/09291019509360328

Mrowka, R., Patzak, A., & Rosenblum, M. G. (2000). Quantitative Analysis of Cardiorespiratory Synchronization in Infants. *International Journal of Bifurcation and Chaos*, *10*(11), 2479–2488. https://doi.org/10.1142/S0218127400001754

Niizeki, K., & Saitoh, T. (2012). Incoherent oscillations of respiratory sinus arrhythmia during acute mental stress in humans. *American Journal of Physiology-Heart and Circulatory Physiology*, *302*(1), H359–H367. https://doi.org/10.1152/ajpheart.00746.2011

Ocon, A. J., Messer, Z. R., Medow, M. S., & Stewart, J. M. (2012). Increasing orthostatic stress impairs neurocognitive functioning in chronic fatigue syndrome with postural tachycardia syndrome. *Clinical Science*, *122*(5), 227–238. https://doi.org/10.1042/CS20110241

Okamoto, L. E., RAJ, S. R., Peltier, A., Gamboa, A., Shibao, C., Diedrich, A., Black, B. K., Robertson, D., & Biaggioni, I. (2012). Neurohumoral and haemodynamic profile in postural tachycardia and chronic fatigue syndromes. *Clinical Science*, *122*(4), 183–192. https://doi.org/10.1042/CS20110200

Orjatsalo, M., Alakuijala, A., & Partinen, M. (2020). Heart Rate Variability in Head-Up Tilt Tests in Adolescent Postural Tachycardia Syndrome Patients. *Frontiers in Neuroscience*, *14*, 725. https://doi.org/10.3389/fnins.2020.00725

Pagani, M., Lombardi, F., Guzzetti, S., Rimoldi, O., Furlan, R., Pizzinelli, P., Sandrone, G., Malfatto, G., Dell'Orto, S., & Piccaluga, E. (1986). Power spectral analysis of heart rate and arterial pressure variabilities as a marker of sympatho-vagal interaction in man and conscious dog. *Circulation Research*, *59*(2), 178–193. https://doi.org/10.1161/01.RES.59.2.178

Penzel, T., Kantelhardt, J. W., Bartsch, R. P., Riedl, M., Kraemer, J. F., Wessel, N., Garcia, C., Glos, M., Fietze, I., & Schöbel, C. (2016). Modulations of Heart Rate, ECG, and Cardio-Respiratory Coupling Observed in Polysomnography. *Frontiers in Physiology*, *7*(OCT), 460. https://doi.org/10.3389/fphys.2016.00460

Perhonen, M. A., Franco, F., Lane, L. D., Buckey, J. C., Blomqvist, C. G., Zerwekh, J. E., Peshock, R. M., Weatherall, P. T., & Levine, B. D. (2001). Cardiac atrophy after bed rest and spaceflight. *Journal of Applied Physiology*, *91*(2), 645–653. https://doi.org/10.1152/jappl.2001.91.2.645

Pikovsky, A., Rosenblum, M., & Kurths, J. (2001). Synchronization. In *Synchronization. A universal concept in nonlinear sciences.* Cambridge University Press. https://doi.org/10.1017/cbo9780511755743

Plash, W. B., Diedrich, A., Biaggioni, I., Garland, E. M., Paranjape, S. Y., Black, B. K., Dupont, W. D., & Raj, S. R. (2013). Diagnosing postural tachycardia syndrome: Comparison of tilt testing compared with standing haemodynamics. *Clinical Science*, *124*(2), 109–114. https://doi.org/10.1042/CS20120276

Pomeranz, B., Macaulay, J. B., & Caudill, M. A. (1985). Assessment of autonomic functions in humans by heart rate spectral analysis. *American Journal of Physiology - Heart and Circulatory Physiology*, *17*(1). https://doi.org/10.1152/ajpheart.1985.248.1.h151

Porta, A., Baselli, G., Liberati, D., Montano, N., Cogliati, C., Gnecchi-Ruscone, T., Malliani, A., & Cerutti, S. (1998). Measuring regularity by means of a corrected conditional entropy in sympathetic outflow. *Biological Cybernetics*, *78*(1), 71–78. https://doi.org/10.1007/s004220050414

Porta, A., Baselli, G., Lombardi, F., Montano, N., Malliani, A., & Cerutti, S. (1999). Conditional entropy approach for the evaluation of the coupling strength. *Biological Cybernetics*, *81*(2), 119–129. https://doi.org/10.1007/s004220050549

Porta, A., Faes, L., Nollo, G., Bari, V., Marchi, A., de Maria, B., Takahashi, A. C. M., & Catai, A. M. (2015). Conditional Self-Entropy and Conditional Joint Transfer Entropy in Heart Period Variability during Graded Postural Challenge. *PLOS ONE*, *10*(7), e0132851. https://doi.org/10.1371/journal.pone.0132851

Porta, A., Guzzetti, S., Montano, N., Pagani, M., Somers, V., Malliani, A., Baselli, G., & Cerutti, S. (2000). Information domain analysis of cardiovascular variability signals: Evaluation of regularity, synchronisation and co-ordination. *Medical and Biological Engineering and Computing*, *38*(2), 180–188. https://doi.org/10.1007/BF02344774

Porta, A., Bari, V., Marchi, A., de Maria, B., Takahashi, A. C. M., Guzzetti, S., Colombo, R., Catai, A. M., & Raimondi, F. (2016). Effect of variations of the complexity of the target variable on the assessment of Wiener-Granger causality in cardiovascular control studies. *Physiological Measurement*, *37*(2), 276–290. https://doi.org/10.1088/0967-3334/37/2/276

Porta, A., Bassani, T., Bari, V., Tobaldini, E., Takahashi, A. C. M., Catai, A. M., & Montano, N. (2012). Model-based assessment of baroreflex and cardiopulmonary couplings during graded head-up tilt. *Computers in Biology and Medicine*, *42*(3), 298–305. https://doi.org/10.1016/j.compbiomed.2011.04.019

Porta, A., Maestri, R., Bari, V., de Maria, B., Cairo, B., Vaini, E., la Rovere, M., & Pinna, G. (2018). Paced Breathing Increases the Redundancy of Cardiorespiratory Control in Healthy Individuals and Chronic Heart Failure Patients. *Entropy*, *20*(12), 949. https://doi.org/10.3390/e20120949

Prokhorov, M. D., Ponomarenko, V. I., Gridnev, V. I., Bodrov, M. B., & Bespyatov, A. B. (2003). Synchronization between main rhythmic processes in the human cardiovascular system. *Physical Review E - Statistical Physics, Plasmas, Fluids, and Related Interdisciplinary Topics*, *68*(4), 041913. https://doi.org/10.1103/PhysRevE.68.041913

Raschke, F. (1991). The Respiratory System — Features of Modulation and Coordination. In H. Haken & H. P. Koepchen (Eds.), *Rhythms in Physiological Systems. Springer Series in Synergetics* (pp. 155–164). Springer, Berlin, Heidelberg. https://doi.org/10.1007/978-3-642-76877-4_12

Rehder-Santos, P., Minatel, V., Milan-Mattos, J. C., Signini, É. D. F., de Abreu, R. M., Dato, C. C., & Catai, A. M. (2019). Critical inspiratory pressure - A new methodology for evaluating and training the inspiratory musculature for recreational cyclists: Study protocol for a randomized controlled trial. *Trials*, *20*(1), 1–11. https://doi.org/10.1186/s13063-019-3353-0

Reilly, C. C., Floyd, S. v., Lee, K., Warwick, G., James, S., Gall, N., & Rafferty, G. F. (2020). Breathlessness and dysfunctional breathing in patients with postural orthostatic tachycardia syndrome (POTS): The impact of a physiotherapy intervention. *Autonomic Neuroscience: Basic and Clinical*, *223*. https://doi.org/10.1016/j.autneu.2019.102601

Rosenblum, M., Pikovsky, A., Kurths, J., Schäfer, C., & Tass, P. A. (2001). Phase synchronization: From theory to data analysis. *Handbook of Biological Physics*, *4*(C), 279–321. https://doi.org/10.1016/S1383-8121(01)80012-9

Ruzieh, M., Batizy, L., Dasa, O., Oostra, C., & Grubb, B. (2017). The role of autoantibodies in the syndromes of orthostatic intolerance: a systematic review. In *Scandinavian Cardiovascular Journal* (Vol. 51, Issue 5, pp. 243–247). Taylor and Francis Ltd. https://doi.org/10.1080/14017431.2017.1355068

Saul, J. P., Berger, R. D., Albrecht, P., Stein, S. P., Chen, M. H., & Cohen, R. J. (1991). Transfer function analysis of the circulation: Unique insights into cardiovascular regulation. *American Journal of Physiology - Heart and Circulatory Physiology*, *261*(4 30-4). https://doi.org/10.1152/ajpheart.1991.261.4.h1231

Schäfer, G., Rosenblum, M. G., Kurths, J., & Abel, H. H. (1998). Heartbeat synchronized with ventilation. *Nature*, *392*(6673), 239–240. https://doi.org/10.1038/32567

Scholkmann, F., & Wolf, U. (2019). The pulse-respiration quotient: A powerful but untapped parameter for modern studies about human physiology and pathophysiology. In *Frontiers in Physiology* (Vol. 10, Issue APR, p. 371). Frontiers Media S.A. https://doi.org/10.3389/fphys.2019.00371

Schreiber, T. (2000). Measuring information transfer. *Physical Review Letters*, *85*(2), 461–464. https://doi.org/10.1103/PhysRevLett.85.461

Seals, D. R., Suwarno, N. O., & Dempsey, J. A. (1990). Influence of lung volume on sympathetic nerve discharge in normal humans. *Circulation Research*, *67*(1), 130–141. https://doi.org/10.1161/01.RES.67.1.130

Shaw, B. H., Stiles, L. E., Bourne, K., Green, E. A., Shibao, C. A., Okamoto, L. E., Garland, E. M., Gamboa, A., Diedrich, A., Raj, V., Sheldon, R. S., Biaggioni, I., Robertson, D., & Raj, S. R. (2019). The face of postural tachycardia syndrome – insights from a large cross-sectional online community-based survey. *Journal of Internal Medicine*, *286*(4), 438–448. https://doi.org/10.1111/joim.12895

Sheldon, R. S., Grubb, B. P., Olshansky, B., Shen, W. K., Calkins, H., Brignole, M., Raj, S. R., Krahn, A. D., Morillo, C. A., Stewart, J. M., Sutton, R., Sandroni, P., Friday, K. J., Hachul, D. T., Cohen, M. I., Lau, D. H., Mayuga, K. A., Moak, J. P., Sandhu, R. K., & Kanjwal, K. (2015). 2015 heart rhythm society expert consensus statement on the diagnosis and treatment of postural tachycardia syndrome, inappropriate sinus

tachycardia, and vasovagal syncope. *Heart Rhythm*, *12*(6), e41–e63. https://doi.org/10.1016/j.hrthm.2015.03.029

Shibao, C., Grijalva, C. G., Raj, S. R., Biaggioni, I., & Griffin, M. R. (2007). Orthostatic Hypotension-Related Hospitalizations in the United States. *American Journal of Medicine*, *120*(11), 975–980. https://doi.org/10.1016/j.amjmed.2007.05.009

Staud, R. (2008). Autonomic dysfunction in fibromyalgia syndrome: Postural orthostatic tachycardia. In *Current Rheumatology Reports* (Vol. 10, Issue 6, pp. 463–466). Springer. https://doi.org/10.1007/s11926-008-0076-8

Taha, B. H., Simon, P. M., Dempsey, J. A., Skatrud, J. B., & Iber, C. (1995). Respiratory sinus arrhythmia in humans: An obligatory role for vagal feedback from the lungs. *Journal of Applied Physiology*, *78*(2), 638–645. https://doi.org/10.1152/jappl.1995.78.2.638

Tanaka, H., Sjöberg, B. J., & Thulesius, O. (1996). Cardiac output and blood pressure during active and passive standing. *Clinical Physiology*, *16*(2), 157–170. https://doi.org/10.1111/j.1475-097X.1996.tb00565.x

Tass, P., Rosenblum, M. G., Weule, J., Kurths, J., Pikovsky, A., Volkmann, J., Schnitzler, A., & Freund, H.-J. (1998). Detection of n : m Phase Locking from Noisy Data: Application to Magnetoencephalography. *Physical Review Letters*, *81*(15), 3291–3294. https://doi.org/10.1103/PhysRevLett.81.3291

Taylor, J. A., Myers, C. W., Halliwill, J. R., Seidel, H., & Eckberg, D. L. (2001). Sympathetic restraint of respiratory sinus arrhythmia: Implications for vagal-cardiac tone assessment in humans. *American Journal of Physiology - Heart and Circulatory Physiology*, *280*(6 49-6), 2804–2814. https://doi.org/10.1152/ajpheart.2001.280.6.h2804

Teodorovich, N., & Swissa, M. (2016). Tilt table test today - state of the art. *World Journal of Cardiology*, *8*(3), 277. https://doi.org/10.4330/wjc.v8.i3.277

Thieben, M. J., Sandroni, P., Sletten, D. M., Benrud-Larson, L. M., Fealey, R. D., Vernino, S., Lennon, V. A., Shen, W. K., & Low, P. A. (2007). Postural orthostatic tachycardia syndrome: The Mayo Clinic experience. *Mayo Clinic Proceedings*, *82*(3), 308–313. https://doi.org/10.4065/82.3.308

Toledo, E., Akselrod, S., Pinhas, I., & Aravot, D. (2002). Does synchronization reflect a true interaction in the cardiorespiratory system? *Medical Engineering and Physics*, *24*(1), 45–52. https://doi.org/10.1016/S1350-4533(01)00114-X

Toledo, E., Rosenblum, M. G., Kurths, J., & Akselrod, S. (1999). Cardiorespiratory synchronization: Is it a real phenomenon? *Computers in Cardiology*, 237–240. https://doi.org/10.1109/cic.1999.825950

Tzeng, Y. C., Larsen, P. D., & Galletly, D. C. (2003). Cardioventilatory coupling in resting human subjects. *Experimental Physiology*, *88*(6), 775–782. https://doi.org/10.1113/eph8802606

Vejmelka, M., Paluš, M., & Lee, W. T. (2009). Phase synchronization analysis by assessment of the phase difference gradient. *Chaos*, *19*(2), 023120. https://doi.org/10.1063/1.3143903

Wang, L. B., Culbertson, C. J., Deb, A., Morgenshtern, K., Huang, H., & Hohler, A. D. (2015). Gastrointestinal dysfunction in postural tachycardia syndrome. *Journal of the Neurological Sciences*, *359*(1–2), 193–196. https://doi.org/10.1016/j.jns.2015.10.052

Watano, C., Shiota, Y., Onoda, K., Sheikh, A. M., Mishima, S., Nitta, E., Yano, S., Yamaguchi, S., & Nagai, A. (2018). Evaluation of autonomic functions of patients with multiple system atrophy and Parkinson's disease by head-up tilt test. *Journal of Neural Transmission*, *125*(2), 153–162. https://doi.org/10.1007/s00702-017-1816-6

Wu, S. da, & Lo, P. C. (2010). Cardiorespiratory phase synchronization during normal rest and inward-attention meditation. *International Journal of Cardiology*, *141*(3), 325–328. https://doi.org/10.1016/j.ijcard.2008.11.137

Zhang, J., Yu, X., & Xie, D. (2010). Effects of mental tasks on the cardiorespiratory synchronization. *Respiratory Physiology and Neurobiology*, *170*(1), 91–95. https://doi.org/10.1016/j.resp.2009.11.003

Zhang, Q., Patwardhan, A. R., Knapp, C. F., & Evans, J. M. (2015). Cardiovascular and cardiorespiratory phase synchronization in normovolemic and hypovolemic humans. *European Journal of Applied Physiology*, *115*(2), 417–427. https://doi.org/10.1007/s00421-014-3017-4